

A Biologically Inspired Model of Bat Echolocation In A Cluttered Environment With Inputs Designed From Field Recordings

Author: Kristen Teczar Loncich

Persistent link: <http://hdl.handle.net/2345/bc-ir:103738>

This work is posted on [eScholarship@BC](#),
Boston College University Libraries.

Boston College Electronic Thesis or Dissertation, 2014

Copyright is held by the author, with all rights reserved, unless otherwise noted.

Boston College
The Graduate School of Arts and Sciences
Department of Physics

A BIOLOGICALLY INSPIRED MODEL OF BAT ECHOLOCATION IN A
CLUTTERED ENVIRONMENT WITH INPUTS DESIGNED FROM FIELD
RECORDINGS

A dissertation

By

KRISTEN TECZAR LONCICH

submitted in partial fulfillment of the requirements

for the degree of

Doctor of Philosophy

November 2014

A biologically inspired model of bat echolocation in a cluttered environment with inputs designed from field recordings.

Kristen Teczar Loncich

Advisor: Dr. Willie Padilla, Boston College
Dr. David Mountain, Boston University

Bat echolocation strategies and neural processing of acoustic information, with a focus on cluttered environments, is investigated in this study. How a bat processes the dense field of echoes received while navigating and foraging in the dark is not well understood. While several models have been developed to describe the mechanisms behind bat echolocation, most are based in mathematics rather than biology, and focus on either peripheral or neural processing—not exploring how these two levels of processing are vitally connected. Current echolocation models also do not use habitat specific acoustic input, or account for field observations of echolocation strategies. Here, a new approach to echolocation modeling is described capturing the full picture of echolocation from signal generation to a neural picture of the acoustic scene. A biologically inspired echolocation model is developed using field research measurements of the interpulse interval timing used by a frequency modulating (FM) bat in the wild, with a whole method approach to modeling echolocation including habitat specific acoustic inputs, a biologically accurate peripheral model of sound processing by the outer, middle, and inner ear,

and finally a neural model incorporating established auditory pathways and neuron types with echolocation adaptations. Field recordings analyzed underscore bat sonar design differences observed in the laboratory and wild, and suggest a correlation between interpulse interval groupings and increased clutter. The scenario model provides habitat and behavior specific echoes and is a useful tool for both modeling and behavioral studies, and the peripheral and neural model show that spike-time information and echolocation specific neuron types can produce target localization in the midbrain.

1	Contents	
2	Introduction	1
	2.1 Research Goal	1
	2.2 Bat Biology	5
	2.3 Echolocation Strategies	6
	2.4 Echolocation Models	9
	2.5 Field Research Studies	14
	2.6 Proposed Echolocation Model and Field Work	19
3	Field Research	20
	3.1 Introduction	20
	3.2 Field Recording Sites	25
	3.3 Methods	32
	3.4 Results	38
	3.5 Discussion	47
4	Scenario Model	50
	4.1 Introduction	50
	4.2 Target Model	51
	4.3 Flight Path	53
	4.4 Echo Model	55
	4.4.1 Pulse Generation	55
	4.4.2 Echo Generation	59
	4.5 Pulse Timing	64

4.6 Results	64
4.7 Discussion	71
5 Peripheral Model	74
5.1 Introduction	74
5.2 Head Related Transfer Function	75
5.3 <i>Eptesicus fuscus</i> HRTF Measurements	79
5.4 HRTF Measurement Implementation	86
5.5 Middle and Inner Ear Model	93
5.6 Auditory Nerve Response	97
5.7 Discussion	104
6 Neural Model	105
6.1 Introduction	105
6.2 Auditory Pathways	105
6.3 MSO Function	108
6.4 Delay Tuned Neurons	111
6.5 Delay Tuned Neuron Model	112
6.6 Range Detection Pathway	118
6.7 Discussion	120
7 Conclusions	122
8 Acknowledgements	124
9 Works Cited	126

2 Introduction

2.1 Research Goal

Echolocating bats navigate and forage in the dark by emitting high frequency vocalizations and listening to returning echoes. Understanding the strategies bats and other echolocating mammals use for navigation and localization, and how neural networks can process the acoustic information that is generated and received is important for developing improved man made sonar systems. From detecting targets under sediment in the ocean, to understanding how active sonar may effect marine life, or developing sonar use for the visibly impaired, echolocation studies have broad and valuable applications (62, 58, 79). Developing models for echolocation can help improve our understanding of biological sonar, and how it can be applied to man made systems.

In this thesis, a biologically inspired model for echolocation is developed and discussed. Although there have been many models developed in the past, in this study a new modeling approach is taken. The goal of this study is to model the echolocation of an *Eptesicus fuscus* starting from signal generation and ending at an acoustic picture of the environment. This study fully incorporates the biology behind echolocation at every stage, including signal generation strategies, what a bat *hears* in a natural environment, localization cues arising from head and body effects on echoes, middle and inner ear sound processing, and neural network design using observed auditory pathways and neuron types. While other studies may focus on any one aspect of this process, modeling the different stages of

echolocation together highlights how they build upon each other to create a robust bio sonar system. Additionally, focusing on a biologically relevant model, rather than a mathematical model, is a better approach to modeling if understanding bio sonar is the goal.

In order to better provide the echolocation model in this study with accurate acoustic information, a field study was conducted to investigate signal generation strategies in cluttered and open environments. Echolocation in cluttered environments is of particular interest due to the increased challenge that the large magnitude of acoustic information presents in that environment. Three main stages of echolocation were then modeled. First, a scenario model simulates what a bat hears as it navigates. Next, a peripheral model incorporates head related transfer function measurements as well as middle and inner ear sound processing to arrive at a firing rate estimate at the auditory nerve. Finally, a neural model was developed that uses several layers of neurons and well-established neuron types to model possible pathways for sound localization. This biologically inspired model demonstrates how the different stages of echolocation build upon each other, highlights advantages and disadvantages of signal generation observed in field recordings, and can be used to further investigate both echolocation strategies, and neural network localization efficacy.

In the next chapter, field recordings that were made for the purpose of this work are presented. Recordings were made at field locations with differing levels of clutter in

order to better understand how increasing levels of obstacles such as tree branches and leaves affect the timing of pulses generated by an echolocating bat. In that chapter, analysis of recordings will demonstrate three main insights into echolocation in cluttered environments: one, bats emit pulses in sonar sound groups, two, the number of sonar sound groups increases with increasing levels of clutter, and three, recordings of bats in the field reveal more variability in pulse timings and less use of sonar sound groups.

In the fourth chapter, the scenario model developed for this study will be described. The scenario model simulates what a bat hears as it navigates through a virtual two dimensional flight arena. This is a valuable model simulating the acoustics of echolocation and can be used as a tool for creating model inputs and also to better understanding field research recordings. Basic principles of sonar, established theories of acoustic propagation loss, and a model of an *Eptesicus fuscus* call were combined to build this scenario model. Simulations of bat calls, timings, and target density are based on observations made during the field recordings presented in this study as well as other published studies (55, 10, 76). This scenario model not only acts as a tool for studying echolocation, but also demonstrates the effects of clutter on returning echoes and demonstrates acoustic challenges and limitations for bio sonar when calls are emitted in sonar sound groups. The scenario model also demonstrates the possibility of target “avoidance or capture” confusion. Spatially separate targets to be avoided can create overlap echoes with spectral

notches that could be confused with spectral notches created by flying insects that are to be captured.

In order to develop a neural model to analyze bat calls and echoes that create an acoustic “picture” of the target field, a peripheral model must first be used to simulate the effects of the head, middle, and inner ear on neural inputs. This model is described in chapter 5. First, the head related transfer function (HRTF) must be considered. Although there are established models of HRTFs, measured data on the HRTF for the *Eptesicus fuscus* had been collected and published by another research lab (2). These measurements were shared by Dr. Cynthia Moss and are incorporated into this model. The theory behind HRTFs and the effect of this measured HTRF on the simulated acoustics is presented in the peripheral model chapter. Also included in the peripheral model chapter are the effects of the middle and inner ear on the signal input to a neural network. Again, models of the inner and middle ear have been previously established. For this study, the model created by Dr. David Mountain (Earlab Desktop Modeling Environment) is used to model the middle and inner ear. In chapter 4, theory behind middle and inner ear modeling is presented, as well as details of species specific inputs, and the effects of the middle and inner ear on simulated echolocation acoustics.

Finally, a neural model is presented in chapter 6. First, known auditory pathways and proposed neural mechanism for target localization are discussed. A proposal for a range detecting neural model is the presented. MacGregor style neurons were

modified to model the firing behavior delay tuned neurons, and a neural network of these neurons demonstrates how such a network can identify target range. Further work must be done to create an additional neural network for detecting azimuth to fully realize the potential of a biologically relevant neural network for target localization.

2.2 Bat Biology

There are many species of bats (*Chiroptera*), both echolocating (*Microchiroptera*) and non-echolocating (*Megachiroptera*). Bats are a very diverse animal; over 1,000 bat species (nearly a quarter of all mammal species) have been identified (73). Non-echolocating megabats are generally fruit eating, while most echolocating microbats eat insects. In New England, common bat species include the *Myotis lucifigus*, *M. sodailis*, *M. keenii septentrionalis*, *Pipistrellus subfavius*, and *Eptesicus fuscus*. These species were all identified during an extensive bat-banding project conducted by Donald Griffin from 1933-1938, in which thousands of bats in caves throughout New England were banded (29). Since that time, the species diversity of New England bats has changed for several reasons, most notably due to a fungus known as White Nose Syndrome (WNS), which has greatly affected bats that hibernate in caves (21). *Myotis lucifigus* populations, once one of the most abundant species in New England has been severely affected. The *Eptesicus fuscus* has been less affected by WNS because many bats of that species hibernate in buildings rather than caves where the fungus has spread. This study focuses on the *Eptesicus fuscus* due to the ability

to conduct local field work, and the wide variety of available literature on the species.

The common name of the *Eptesicus fuscus* is the big brown bat. They are frequently studied in laboratory experiments. The big brown bat habitat is spread throughout North America. They are relatively large in size (14-30 g), have comparatively smaller ears, and long blackish brown fur (1). The *Eptesicus fuscus* have strong jaws and teeth as they primarily feed on hard-shelled beetles, but also eat a variety of other flying insects including moths. *Eptesicus fuscus* are active from spring till early fall. Females roost in large nursery colonies and give birth to one or two pups, while males roost alone or in small groups (15). Unlike other New England species, the big brown bat often hibernates in buildings rather than caves (85). They have a long life span of about 19 years. Although *Eptesicus fuscus* have a long life span, it is shorter than other bats, including the common *Myotis lucifigus* that has a life span of 34 years. The shorter life span of the big brown bat may be due to its larger size (11).

2.3 Echolocation Strategies

The term “echolocation” was coined by Donald R. Griffin, after his discovery, with Robert Galambos, that bats use high frequency vocalizations for navigation in the dark. Griffin and Galambos were students at Harvard at the time of the discovery in 1940. Griffin’s work on bird migration had lead to an extensive bat-banding project and subsequent studies of echolocation. Harvard Physics Professor George

Washington Pierce had built a device that could record high frequency sounds, which had previously not been possible. Through a series of experiments using the high frequency device and systematically blocking the bat's senses, Griffin and Galambos were able to show that bats emitted high frequency vocalization used for navigation (30). The discovery of echolocation has opened the door to a rich history of echolocation studies and applications.

Echolocating bats can generally be divided into three groups, constant frequency (CF), frequency modulated (FM), and combination constant and frequency modulated (CF-FM), based on the structure of their high frequency calls. CF bats emit long calls at a constant frequency. Like other species, these bats use pulse-echo matching for target localization, but are also believed to rely on information arising from the Doppler shift of returning calls to determine the speed and direction of prey. The rate of prey wing beat can be gathered from the changing shifts in frequency and may also provide CF bats with information about not only *where* prey is, but also *what* the prey is (6). FM bats emit frequency-modulated calls. These calls sweep through a broad range of frequencies, making the Doppler shifts in frequency less prominent. While the entire echo from a CF bat will produce a spectral mismatch when compared to the call due to the Doppler shift, only a small portion of an echo received by an FM bat will have a spectral mismatch from the Doppler shift. FM bats instead rely on spectral notches for prey information (71). Bat species using FM calls for echolocation include the *Myotis lucifigus*, and the *Eptesicus fuscus*. Many CF bats are more accurately classified as CF-FM. These bats

generally produce calls with a long constant frequency followed by a short downward frequency sweep. The *Pteronotus parnelli*, or the mustache bat is a commonly studied CF-FM bat, as well as the *Rhinolophidae*, or horseshoe bat (75, 74, 51).

Donald Griffin categorized echolocation of bats by dividing their behavior into three stages. At each stage, echolocation calls are emitted with a particular interpulse interval (IPI). Calls emitted during the “search” phase have an interpulse interval ranging from 100-1000ms. In the “approach” phase the IPI was measured to be 12.5ms, and in the “terminal” phase, also known as the “buzz”, calls were emitted with IPIs as small as 5ms (31). The echolocation calls of an *Eptesicus fuscus* in particular have been widely studied (9, 24, 38, 39, 45, 46). Calls emitted during the three phases of echolocation can also be classified by duration, spectral content, and amplitude. As the bat transitions from search, to approach, and finally terminal phase, the calls emitted decrease in duration, spectral content, and amplitude. The duration a call emitted in the search phase is 5-10ms long, while a call emitted in the terminal phase can be as short as 0.5ms (68). The spectral content of *Eptesicus fuscus* calls is from 120kHz to 20kHz, and is comprised of a fundamental frequency sweep, second, and often third harmonic. The strongest frequency is around 35kHz for the *Eptesicus fuscus* (24).

2.4 Echolocation Models

Several approaches to computational modeling of echolocation have been explored and reported on. One model perhaps receiving the most attention was the spectrogram correlation and transformation (SCAT) model. This model focused on assessing performance of glint recognition. A glint is an echo arising from a combination of multiple reflections off different parts of one insect, such as the body and wing. This model converged spectral and temporal information to construct target image information from two-glint echoes (64). While the SCAT model succeeded in reproducing images perceived by the *Eptesicus fuscus* in behavioral experiments on two-glint resolution, and provided insight as to predicting neural organization, the SCAT model uses a functional mathematical approach to rather than a biological one, and is limited in focusing on small spectral and temporal glint features. The cochlear block of the SCAT model can be improved on, and in the model described in this thesis, is replaced with the EarLab model, developed by David Mountain at Boston University, which is more biologically accurate. The SCAT model also does not include a neural network based on the connectivity of the auditory pathway. The SCAT model also does not place an emphasis on localization, nor does it incorporate head related effects on echoes. While the SCAT model did receive much attention, a more complete and biologically based model is necessary.

An even less biologically based model by Dror, Zagaeski, and Moss trained a feedforward, fully connected three-layer neural network with a back-propagation learning algorithm to recognize three-dimensional shapes based on the echoes

received (20). One interesting aspect of this model was that the echoes from two different shapes were analyzed, a tetrahedron and a cube. These two objects were ensonified and echoes were recorded that arose from different planes of the objects. The study used a FM signal designed to mimic an *Eptesicus fuscus* call. They analyzed which pieces of an echo (high or low frequency) carried information about shape and demonstrated the importance of the frequency domain rather than time domain for recognizing targets. While their work analyzing how different domains of the call spectrum may aid in identification, their modeling approach used a feedforward neural network rather than a biologically inspired neural network where the neuron behavior and connectivity is modeled. Their work did not emphasize building a neural network based on knowledge of the auditory pathways; rather they taught a generic neural network to recognize targets. Again, while the results of this model had interesting implications for target recognition and frequency analysis, it was fairly narrow in scope.

Ikuo Matsuo has published a series of papers modeling echolocation for 3d target recognition (47-49). His models use a similar approach to modeling the cochlear output as was used in the cochlear block of the SCAT model. These models focused on the spectral content of calls, and used a computational model to de-convolve the spectrum and extract information about cues from the external ears, as well as identify targets that produce echoes closely spaced in time such that they overlap. Matsuo uses a more mathematical approach to modeling echolocation. While his models do suggest the ability of a bat to discriminate and identify very fine structure

in calls, these models are not biologically based, nor does they include a neural network.

Another study focused on a very-large-scale integration (VLSI) model for range detection. In this study neurons were designed that would fire if they received an inhibitory input from a call and an excitatory input from an echo at a specific delay. This model relied on postinhibitory rebound (PIR) as a mechanism for delay tuning. Although the delay-tuned neurons described in this thesis do not directly use PIR to achieve delay-tuned response, they are also inspired by that mechanism. In the VLSI model, traditional neuron models are not used, rather transistors that capture the fundamental biological aspects of the neuron membrane and current-voltage relationship. This model takes a unique approach at neuronal modeling with a biologically inspired VLSI model, and does show how delay-tuned neurons can be used for range detection. It does not, however, incorporate the actual spectral content of a bat call or returning echo. The model also does not incorporate a peripheral model, nor does it aim at target localization (14).

An autocorrelation model for bat sonar was proposed by Ziegrebe in 2008, which aimed at obtaining target distance and shape information. In this study peripheral auditory processing was modeled, however the model was monaural so many cues arising from binaural processing were not captured. While this model did incorporate actual HRTF measurements (25), those measurements were made using a *Phyllostomus discolor*, not an *Eptesicus fuscus*. The *Phyllostomus discolor* will

have a different HRTF due to size and ear shape differences; it is also a spear nosed bat, which would affect echoes significantly. The *P. discolor* is not native to New England and can be found in Central and South America. Its calls contain a large spectral range of 5-142kHz, and most of the energy is contained in the third and fifth harmonic. Although the *P. discolor* is an echolocating bat, unlike most echolocating bats, it is a fruit eater. This bat has likely evolved different echolocation strategies and neural processing than an insect-eating bat that needs to capture moving prey (94). In addition to species specific differences arising, this model also does not incorporate modeled habitat specific echoes, nor does it include a neural network.

Fontaine and Peremans's work on first-spike latency coding utilizes a modeling approach most similar to the one presented in this thesis (26). This model consists of the peripheral auditory system and central auditory system. The peripheral auditory system includes HRTF measurement obtained from Cynthia Moss. These same measurements were included in the model described in this thesis. The peripheral model in the Fontaine and Peremans study then uses a bank of gammatone bandpass filters followed by half wave rectifiers and low pass filters to simulate middle and inner ear processing. The peripheral auditory system is improved on in my study by the utilization of the EarLab model, which is more biologically accurate. The central auditory system is built with leaky integrate and fire neurons and polarity inverters (for inhibitory input), and contains both monaural and binaural pathways. Auditory pathways from the dorsal and anterior ventral cochlear nucleus to the inferior colliculus were incorporated to this model.

Coincidence detection was used to improve signal detection. The model demonstrates that First Spike Latency (FLS) code can represent monaural and binaural intensity cues resulting from the head related transfer function (HRTF). The efficacy of FPL coding for localization rather than traditional rate coding is highlighted. This is important because the short duration of echolocation calls suggests rate coding would not be useful. While there are similarities between the Fontaine Peremans model and the one presented in this thesis, there are also several important differences. One, the input to the peripheral model discussed in this thesis uses modeled *Eptesicus fuscus* signals and echoes arising from a simulated habitat. The peripheral model is also improved on by using Earlab for modeling middle and inner ear sound processing. The Fontaine Peremans model uses Support Vector Machine algorithms for azimuth and elevation detection, while the neural model presented in this thesis codes for range.

While several models of echolocation have been studied, currently there are no biologically influenced models that use this whole method approach. The model presented in this thesis describes echolocation from modeling signal generation and returning echoes in a natural environment, to processing sound at the peripheral level, and then finally coding a neural network that includes known auditory pathways and neuron types identified in echolocating bats for range detection. None of the models I have described here include an acoustic model in which the returning echoes from obstacles are simulated.

2.5 Field Research Studies

The motivation behind the model described in this thesis was, in part, to arrive at a better understanding of how bats echolocate in cluttered environments. In this thesis, field research was conducted to investigate what temporal strategies a bat uses in cluttered environments. The research also sought to compare results reported on in laboratory settings to those in the field. In conducting this field research, more accurate inputs were created for the echolocation model. Although there are many studies reporting on echolocation of *Eptesicus fuscus* and other species in laboratory settings, recording challenges in the field result in fewer field studies. It is important that field recording be made in conjunction with laboratory recordings, as it has been shown that bats do not emit the same signals in confined spaces as they do in the wild (31). Some of the field studies published in literature, as related to this thesis, are reported on here.

Published field studies have investigated a number of echolocation features, including sonar beam, spectral content, duration, and repetition rate of calls, social calls, and the effects of clutter on echolocation behavior. A 2009 study of the *Myotis duabentonii*, an FM bat, compared the recorded sonar beam of a flying *M. daunetonii* in the lab with recordings made over a pond in Odense, Denmark (78). Field recordings of the bats were made in 2003 and 2005. Bats were attracted to the field recording location by throwing mealworms onto the surface of the water in front of the microphones. This study found two distinct differences between the laboratory beam and field beam. One, the sonar beam was highly directional and increase

directionality with frequency. The half-amplitude angle of the beam at 55kHz was measured as 40° in the lab, while it was measured at only 20° in field recordings. A second observation was that the intensity of calls was also greater in field recordings. Search phase calls recorded in the field were approximately 8dB greater than calls in the laboratory. The authors suggested that a more intense call was needed in the wild, causing the bat to open its mouth wider during vocalizations, which also increased the directionality of the call. The piston model often used to model sonar beams correlates directionality with intensity, because more directional beams have more on axis energy, increasing the intensity. It was suggested that this phenomenon might be true for other species of bats, which also used broad calls in laboratory settings.

A field study was conducted to investigate sonar signal design when bats flew alone and in groups in the wild (55). In this study, four species of bats were studied, the *Euderma maculatum*, *Eptesicus fuscus*, *Lasiurus borealis*, and *L. cinereus*. For this study, bats were captured in British Columbia and Ontario, tagged with reflective bands for identification, and released back into open areas. The goal of the recordings was to examine the difference between calls made as bats flew in groups or individually, with an emphasis on calls made during the search phase. For all four species, the duration of the calls decreased when bats flew in groups, and the IPIs increased. Spectral differences were less pronounced. Bat encounter acoustic clutter when they fly in groups or individually in areas with many closely spaced targets. They may employ similar echolocation strategies in both environments.

A question often asked in echolocation studies, is how clutter may affect bat behavior. A 2004 study reported on the effect of clutter on echolocation call structure of two different FM bat species, the *Myotis septentrionalis*, and the *M. lucifigus* in New Brunswick, Canada (10). In this study, bats were captured, tagged with small glow sticks, released back into the field, and vocalizations were recorded. The bats were released at one of three sites categorized by the amount of clutter. The sites were categorized as low, medium, and high clutter based on the horizontal distance to the nearest trees. Low clutter sites, such as a forest clearing, had a nearest tree distance of 10 meters or greater. Medium clutter sites, like the edge of the forest or a small gap in the forest, had trees within 3-10 meters. High clutter sites had trees at distances of 3 meters or less. The bats in this study flew 2-7 meters above the ground. Both the frequency content of calls and the duration of calls varied with the amount of clutter. As with the previous study described, signal duration shortened in more acoustically cluttered environments. The duration of calls nearly doubled from approximately 2ms in high clutter locations to 4ms in low clutter. The shorter call durations in clutter may help the bat to focus the acoustic picture in a cluttered environment. The characteristic frequency, maximum frequency, and minimum frequency all decreased with decreasing clutter. Reduced spectral content of calls in cluttered environments may reduce acoustic information helpful for navigating in a cluttered environment, but may be a side effect of the shorter call duration. This study highlighted the effects of clutter on call structure, but did not address temporal issues of call rate.

Dr. Cynthia Moss has conducted extensive experiments on bats in the laboratory, and also sometimes in field settings. Most of her studies focus on the *Eptesicus fuscus*, and two studies of note explore differences in echolocation in field and laboratory settings. A 2000 study focused on the differences in call structure and IPI in the field and laboratory setting (76). Field recordings were made in open fields and wooded areas. Open field recording calls were longer in duration, narrower in bandwidth, and had longer IPIs than calls made in wooded areas. As compared to field recordings, laboratory recordings were shorter still, had lower IPIs, and less variability in bandwidth. The calls made in laboratory setting more closely resembled calls made in the approach phase when compared to calls made in the field. The IPI recorded in wooded areas was 122ms, while laboratory IPIs averaged 88ms. The duration of wooded area calls was 6-11ms, and laboratory calls measured 3-5ms in duration. This study suggested that behavior recorded in laboratory differs from field recordings.

A recent study from the Moss lab investigated specifically the difference between temporal features of IPIs in the field and laboratory (41). Studies conducted in laboratory environments have suggested that bats emit pulses in “strobe” groups, where a group of shorter IPIs are followed by a longer IPI (53, 34). This study sought to investigate whether “strobe” groups identified in the lab would occur in cluttered field settings. Sonar sound groups were identified in both a variety of “cluttered” laboratory flight rooms, as well as at a “cluttered” field recording location. The sonar sound groups differed significantly at the field sight than

laboratory site, with much greater sonar groups that had much longer average IPIs. This suggests a different temporal echolocation strategy in field settings, however, the site specific features of the field recording site may have greatly influenced the results of this study.

In the field study presented in this thesis, previous studies on sonar structure in the wild and “strobe” groups in cluttered environments were built upon to provide further insight into how clutter effects the behavior of bats and how this behavior compares to laboratory studies. The field study reported on in this thesis again confirms that bats do emit calls in sonar sound groups, or “strobe” groups, but identifies these groups in a variety of “cluttered” environments, a suggesting a correlation between the amount of clutter and number of sonar sound groups. The structure of the sonar groups, or the IPI within groups, was much less than that identified in Kothari et al 2014, and was closer to those produced in laboratory settings. The overall percentage of sonar sound groups identified was significantly less in this field study, and the variability of calls in general was much greater, suggesting that while sonar groups may be a valuable tool used by bats in cluttered environments, it is not as highly used as previous laboratory studies suggested.

2.6 Proposed Echolocation Model and Field work

In this thesis, a model of echolocation is put forward that is highly biologically inspired. The following chapters describe in detail the field work conducted as well as the echolocation model. A field study was conducted to provide the model with inputs that were based on actual recordings of bat behavior in the wild, in a variety of environments, classified by the level of “clutter”. The echolocation model is divided into a scenario model, peripheral model, and neural model. Field recordings and field clutter density measurements were used to set the parameters of the scenario model flight arena and signal generation. The scenario model simulates what the bat “hears” as it navigates through a target field. The output of the scenario model is used as the input for the peripheral model, in which HRTF measurements and biologically accurate modeling of the middle and inner ear result in an average firing rate at the auditory nerve. This firing rate is then used for input to the neural model, where known auditory pathways and neuron types are modeled to produce an acoustic picture of what the bat “sees” with its hears. The work in this thesis represents a new and whole approach to echolocation modeling that is highly biologically based and results in 2D target localization.

3 Field Research

3.1 Introduction

Many studies have been conducted to better understand biosonar. Echolocating bats outperform current man-made sonar systems and a more detailed understanding of biosonar could serve to improve man-made sonar. An *Eptesicus fuscus* emits a high frequency modulated call and uses the returning echoes from surrounding objects to navigate, feed, and create an acoustic picture in the dark. It is important to understand what strategies are used to create this acoustic picture and how those strategies enhance neural coding to improve the acoustic picture. With a greater knowledge of echolocation by bats, models for target localization and identification can be more accurately informed and improved on.

One question that is not well understood is how an echolocating bat interprets the multitude of echoes received when navigating cluttered environments of closely spaced targets, such as a wooded area. These environments produce dense acoustic information for interpretation. Several studies have considered this question using echolocating bats in laboratory settings. In particular, studies by Dr. Cynthia Moss, and Dr. James Simmons' labs have each probed this question and revealed new information about strategies bats may be employing while flying in cluttered environments. Both studies suggested that bats emitted their calls in pulse pairs or groups, generally referred to as "strobe" pairs or groups, with short interpulse intervals (IPI) being preceded and followed by a longer IPI. The goal of this field

research was to investigate whether strategies employed in laboratory settings are utilized in the field.

In Simmons' study (59), a flight room where closely spaced chains had been hung was used to simulate a cluttered environment. The chains are hung close enough that a bat will not fly through the chain field, and a wider flight path through the field is cleared. An *Eptesicus fuscus* is tasked with flying from one end of the flight room to a landing pad at the opposite end via the predetermined path. A microphone was mounted to the head of the bat, and others were set up throughout the room to record both the call of the bat and returning echoes. Two significant observations were made. One, the bats were found to emit signals in "strobe" groups, with shorter IPIs followed by longer IPIs. This is significant because it suggests that the bats may be comparing echoes within strobe groups for better target localization, but it also can present an echolocating bat with a new challenge. One task of an echolocating bat is to match its pulses with the returning echoes. If pulses are emitted close together in time in a dense target field, echoes from a second pulse may arrive within the same window of time as echoes arriving from the first pulse. This presents the bat with a pulse-echo matching challenge, referred to as "pulse-echo ambiguity". Despite this added challenge, Simmons' experiment showed that bats did emit pulses almost exclusively in "strobe" groups and with regularity.

A second significant observation was that the pulses made within a “strobe” group were not identical. Pulses within groups were shifted in frequency content by 3-6kHz. This frequency shift accounts for only 4-8% of the bandwidth of broadcasted call. Despite the small percentage of the bandwidth that changes, flight performance was good and the presumed challenges of navigating in cluttered settings must have been overcome. Perhaps these small shifts in frequency serve to disambiguate pulse echo matching. It was noted that shifts in frequencies more greatly affected the higher harmonics of the frequency modulated call, suggesting that the higher harmonics, which are attenuated greatly may play a more important role than previously thought.

Another experiment conducted by the Moss lab (53) also looked at the question of navigation and target pursuit in cluttered environments. In her experiments, a worm is tethered in a flight room in front of artificial vegetation. The calls of an *Eptesicus fuscus* are recorded as the bat maneuvers to catch the insect. As the bat approaches its prey, echoes from calls hitting the insect target combine with a large number of echoes from the artificial foliage just behind the prey. In this experiment, the bat also emitted pulses in groupings before emitting the rapid, shorter, and quieter string of pulses, or “buzz”, usually produced right before a capture. These groupings were again identified as “strobe” groups with two to four pulses emitted closely in time, preceded and followed by a longer IPI. Unlike the Simmons experiments, there was less regularity to IPIs. This is likely due to the difference in the experimental set-ups. In the Simmons experiment the bat is confined to a single

flight path and the clutter targets, hanging chains, are hung in a regular order.

Moss's work more closely simulates the irregular clutter encountered in a natural habitat with artificial foliage, and the bat has more freedom to choose its flight path.

Results of laboratory experiments suggested interesting strategies for echolocating in cluttered environments. However, it is possible that the behavior of trained laboratory animals differs significantly from wild echolocating bats, and it is important to understand the behavior of bats in both environments. In fact, an additional study was done by Moss that again examined IPI temporal patterning in several different laboratory settings, as well as at two field sites (41). Three sonar sound groups were identified where calls occurred in groups of 2, 3, or more than 3 ($n=2$, $n=3$, $n>3$). Calls made in a field setting were produced in sonar groups with much longer IPIs than the laboratory settings. Sonar groups were only identified at one field location, and the mean IPI was 118.2 ms. The four laboratory settings resulted in sonar groups with mean IPIs of 35.4, 25.1, 29.8, and 33.6 ms. While sonar groups were identified in both the field and laboratory recordings, the much longer group IPIs in the field recordings, suggest significant differences between sonar behavior in the field versus the lab. Also, a greater proportion of calls occurred in sound groups in the field recordings than in laboratory recordings.

Recording an echolocating bat in a cluttered field environment is a difficult task.

While catching prey, bats generally hunt in open areas, where echoes from non-insects are unlikely to interfere. Bats are often observed flying in the same general

area every evening, sometimes in a repeated flight path while feeding. Due to these regular nightly feedings, recording bats hunting in a known feeding area is a good strategy for reliably recording bats in the field. However, these recordings reveal little about the call rate behavior in cluttered environments a bat may pass through on its way to open fields and water. Many feeding sights of bats are located at ponds and lakes that are surrounded by forest, which must be first passed through. While some bats have been recorded as flying at very high altitudes (87), it is not necessarily the case that bats simply *avoid* the clutter of forests. In fact, bats can be observed flying in forested areas. Not only do they fly through forested areas, they also can be recorded feeding in much less open areas than large ponds and fields, such as over small streams and footpaths. In those settings, although there are smaller open areas of up to a few meters, the bat certainly encounters many returning echoes from surrounding foliage, especially when a flight path approaches the perimeter.

In this study, field recordings were made in three feeding locations, each with a unique level of clutter. Although each location provided some level of clutter from foliage at the perimeter, the available open space varied significantly. The main focus was to identify “strobe” groups, if any, and to identify potential differences in echolocation strategies employed in varying levels of clutter. Results showed that the median IPI related to the amount of clutter, with lower IPIs in areas with greater clutter as might be expected where more processing of echoes is required. Highly regular temporal patterns sometimes seen in laboratory recordings were not

observed. However, “strobe” groups of two or three calls were identified. While “strobe” groups were identified in both open and cluttered field environments, a higher percentage of calls in cluttered environments occurred in “strobe” groups than in open environments. The goal of this work is to better understand echolocation in the field in order to supply models with accurate inputs, and develop models that exploit strategies used by bats. It is important to understand field behavior as well as laboratory behavior in order to improve models. Current man-made sonar systems underperform biosonar, and modeling approaches do not fully take advantage of long evolved biosonar strategies. Attaining further understanding of biosonar can improve computational models.

3.2 Field Recording Sites

Field recordings were made at three known feeding areas of bats on Cape Cod, MA. Two field recording sites were located in the Mass Audubon Skunknet River Wildlife Sanctuary, a 147 acre refuge in Osterville, MA. Recordings were made at a small clearing at the edge of West Pond, a large pond with regular bat activity. Recordings were made from a bat that flew over the open space of the pond, but also a regularly at the wooded edge of the pond. The second location was over Skunknet River, which feeds into West Pond. Recordings were made at a section of the river approximately 50 meters from West Pond where the trees open up to a small clearing. The sites are centrally located in the reservation, approximately a quarter mile from roads and are quiet with the exception of insect noise.

The third field recording site is located in The Trustees of Reservations Mashpee River Reservation, in Mashpee, MA. The site is located at the edge of the reservation, abutting a large plot of private land. The 248 acre reservation also abuts town reservation land. A large path bisects a stream leading from Trout Pond into Mashpee River. The path has been washed out by water that rushes into a small wooded “glade” where regular bat activity occurs. There is noise heard from both the rushing water and traffic from nearby Rt. 28.

These recording sites were chosen due to known regular bat activity, and the variety in clutter from surrounding forest. The sites ranked in order of clutter least to greatest: West Pond, Skunknet River, Mashpee Glade. The Mashpee Glade is a particularly unusual site for bat feeding activity. Together, Kristen Loncich, Donald Griffin, and Greg Auger had previously made recordings of bat activity in all three locations during 2000-2002. During that time, a significant number of recordings were made at the Mashpee Glade. It is a particularly unusual site for recording due to it being small, enclosed, and wooded. What also makes the site unusual is that Trout Pond is adjacent, where it would be presumably easier to navigate and feed over open water. There is a small opening of trees in the Glade, but the bat routinely flies a flight pattern that takes it from one edge of the glade to the other, directly into the wooded edge.

To approximate the density of wooded areas on Cape Cod, the density of tree trunks at two locations in Skunknet Reservation was measured. Each location was marked

15 by 15 feet, and the positions of the trunks as measured 1 meter from the ground was recorded. The first density measurement site contained 6 trunks ranging from 3-12 inches in diameter. The second site contained 12 trunks of similar varying size as the first site, but with mostly smaller trunks around 4 inches in diameter. As you move up into the tree canopy, the density of clutter that a bat encounters increases greatly with many branches and foliage to avoid. Figures 3.1 and 3.2 are maps of the recording locations with the specific sites numbered. Figures 3.3-3.6 are photos of the three recording locations. Figure 3.3 shows the clearing at the edge of West Pond with foliage at the water's edge. Figure 3.4 is a photo Skunknet River as it leads into West Pond. Figure 3.5 is a photo of the Mashpee Glade taken from the path that bisects the river from the pond. This photo is of the wooded end of the glade where recordings were made. The photo in figure 3.6 is of the small open area in the center of the Glade.



Figure 3.1. Skunknet River Wildlife Sanctuary. Field recording site at West Pond is site 1 and the Skunknet River is recording site 2.



Figure 3.2. Mashpee River Reservation. Field recording site 3, indicated with red arrow.

**Figure 3.3. West Pond
Recording Location.**



**Figure 3.4. Skunknet River
Recording Location.**





Figure 3.5. Glade recording site from path edge. Recording microphone located in wooded area.



Figure 3.6. Small opening in Glade.

3.3 Methods

Acoustic recordings of bat activity were made in order to determine the IPIs used during navigation and feeding at the three recording sites on evenings from August until October in 2012 and 2013. At the beginning of October, bat activity reduces and eventually ceases. Call time recordings were made using a Pettersson D100 heterodyning bat detector, figure 3.7. The detector can be tuned to a best center frequency of the bat call. A heterodyning detector does not retain frequency content of recorded calls, only onset timing information and amplitude. The detector plays in real time the ultrasound within 4kHz of the tuned frequency, using a method of frequency subtraction. It has a frequency range of 10-120kHz. The output of the Pettersson detector is recorded with a digital recorder for computational analysis. The bat detector is mounted on a 10 foot pole that is extended into each field site. The location of the detector was fixed in the same position for each recording night. Recordings from eight evenings at Skunknet Reservation and eight evenings at the Mashpee Reservation were included in this analysis of temporal IPI patterning.



Figure 3.7. Pettersson D100 heterodyne bat detector.

A peak-detection algorithm is used to retrieve timing information from the Pettersson D100 bat detector. Peaks times are saved and continuous stretches of ten peaks or more are used in the analysis. Due to the directionality of the microphone as well as the position of the bat at the time each call is produced, generally, sweeps of bat calls were recorded. "Missed spikes" in the recordings can occur if the bat moves its body or head position during a sweep such that the amplitude of recorded call falls within the region of noise. Figure 3.8 shows a sweep of bat calls recorded by the bat detector with peaks picked out with red markers.

In order to capture the frequency content of calls to better characterize echolocation calls, a microphone capable of recording high frequencies was used to record calls at the Mashpee Glade in the fall of 2013. Figure 3.9 shows an example waveform of a recorded call and figure 3.10 is the corresponding spectrogram. The call is approximately 6 ms in duration. A first harmonic sweeps from 60-20kHz. Part of a second harmonic sweeps from 90-40kHz, and has a notch around 60kHz.

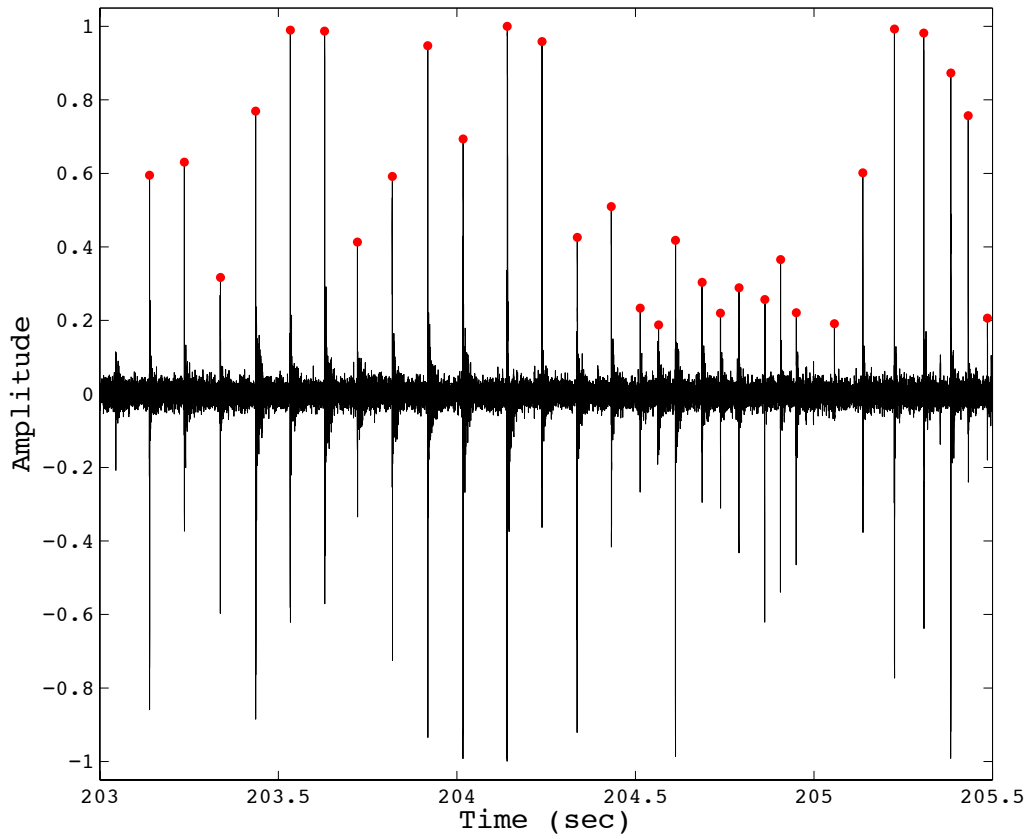


Figure 3.8. Petterson bat detector recording of bat pass with peaks of bat pulses detected and noted with red markers.

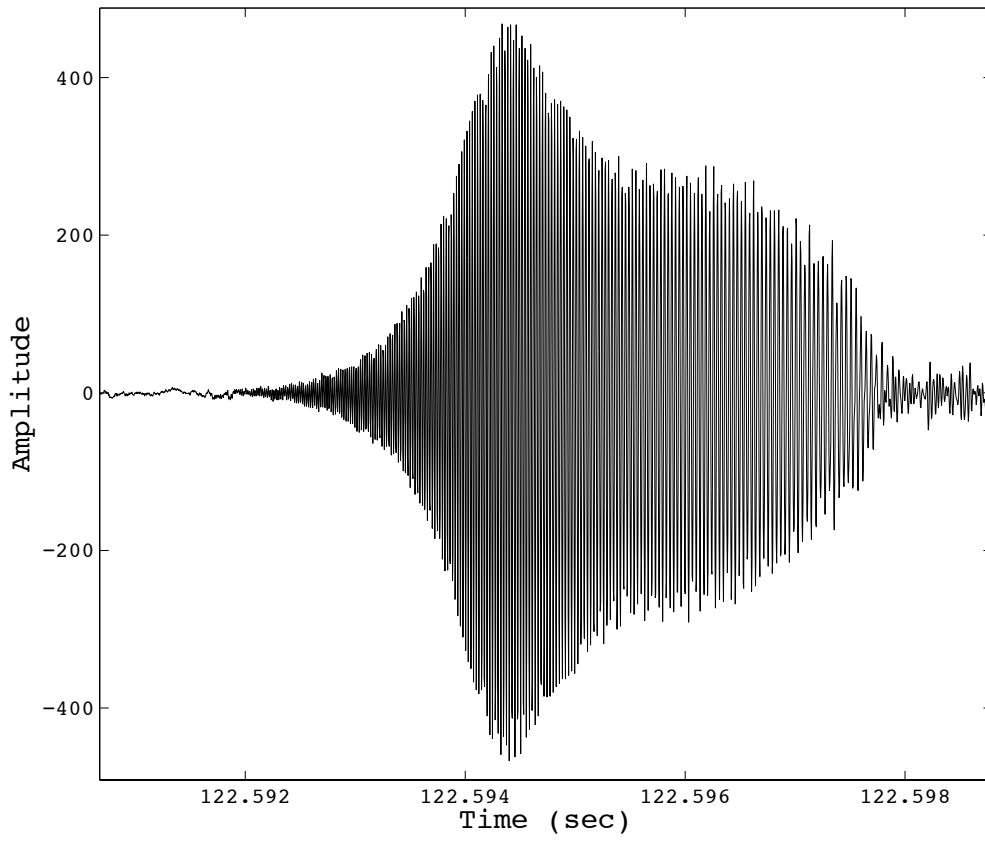


Figure 3.9. Recorded bat call waveform.

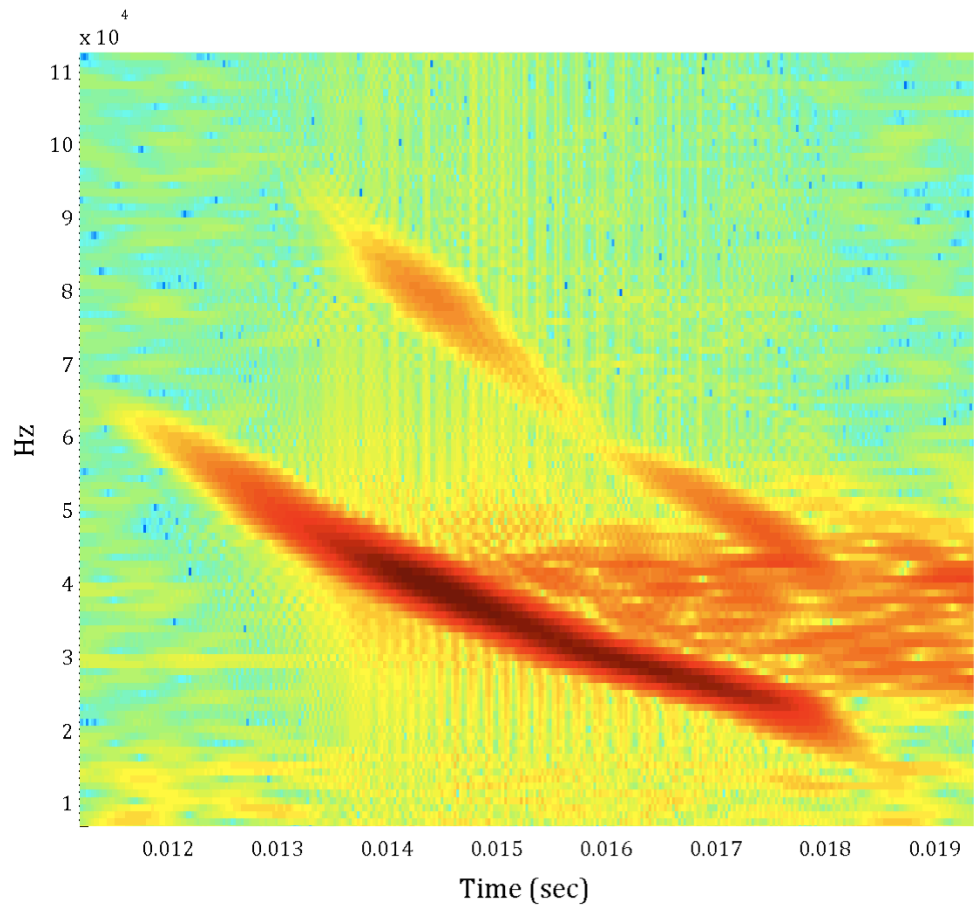


Figure 3.10. Recorded bat call spectrogram.

3.4 Results

Interpulse intervals calculated from bat passes at the three field recording sites revealed that the mean and median IPI correlated with the “clutter” of each site, with the Mashpee Glade providing the most clutter and the lowest IPIs (mean=77.05ms, median=76.21ms), and the most open location having the highest IPIs (mean=87.80ms, median=90.88ms). IPIs ranged across all three locations from 45-120ms. Detailed statistics from each of the three recording sites are listed in Table 3.1.

Location	Number of IPIs	Mean (ms)	Median (ms)	Standard Deviation (ms)	Skewness	Kurtosis
Mashpee Glade	6959	77.05	76.21	16.78	0.2275	2.2130
West Pond	6189	87.80	90.88	16.67	-0.5429	2.5504
Skunknet River	590	78.94	80.81	16.87	-0.0482	2.0609

Table 3.1. IPI statistics at three field recording sites.

Histograms for all IPIs at each location are shown in figure 3.12. Note that the histogram from the Glade is skewed to the left, while the histogram from West Pond is skewed to the right. Further analysis of the Glade histogram, suggests that the data is slightly bimodal, with a secondary peak around 90ms. If the bat were emitting calls in “strobe” groups or pairs, some bimodality in the histogram would be expected. In order to further analyze the potential for “strobing”, return maps of the IPIs over West Pond and at the Mashpee glade are shown in figures 3.13 and 3.14. As expected, the West Pond return map contains a cluster of points around the

median IPI. The Glade return map contains a primary cluster of points around the median IPI, and another cluster about the secondary peak IPI in the histogram. If the pulses were emitted in “strobe” groups or pairs, a distinct clustering off of the $n=n+1$ axis would be expected. No such cluster is prominent on the map, suggesting that two different modes of IPIs exist in the Glade data.

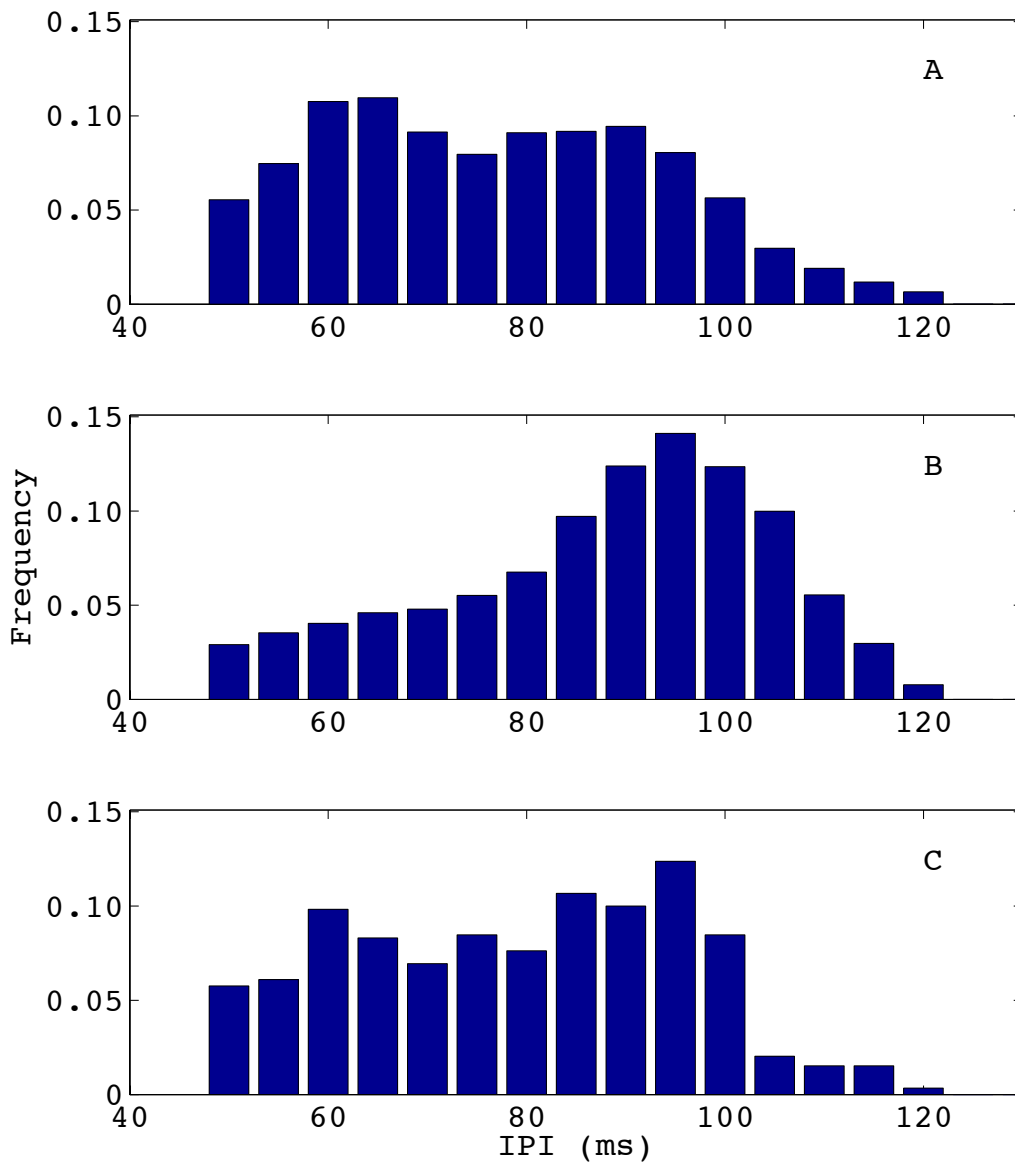


Figure 3.12. Histograms of IPIs for three recording sites. Panel A is at the Mashpee Glade, Panel B is over West Pond, and Panel C is over Skunknet River.

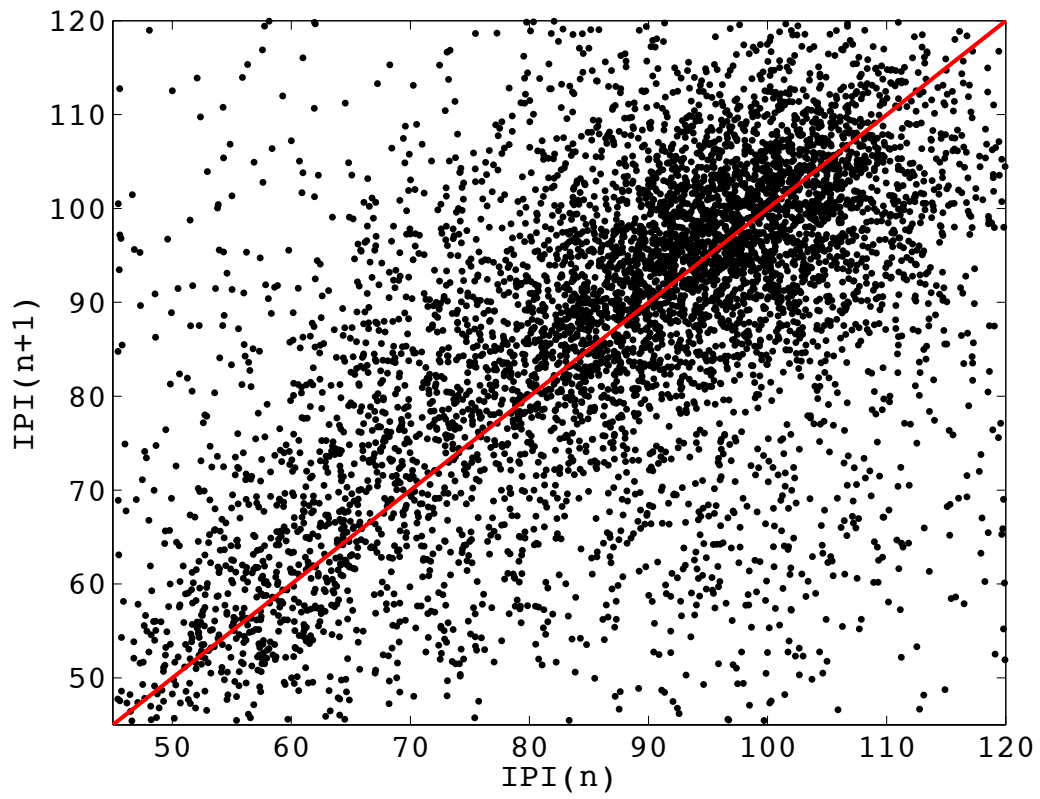


Figure 3.13. Return map of IPIs from all nights recorded at West Pond.

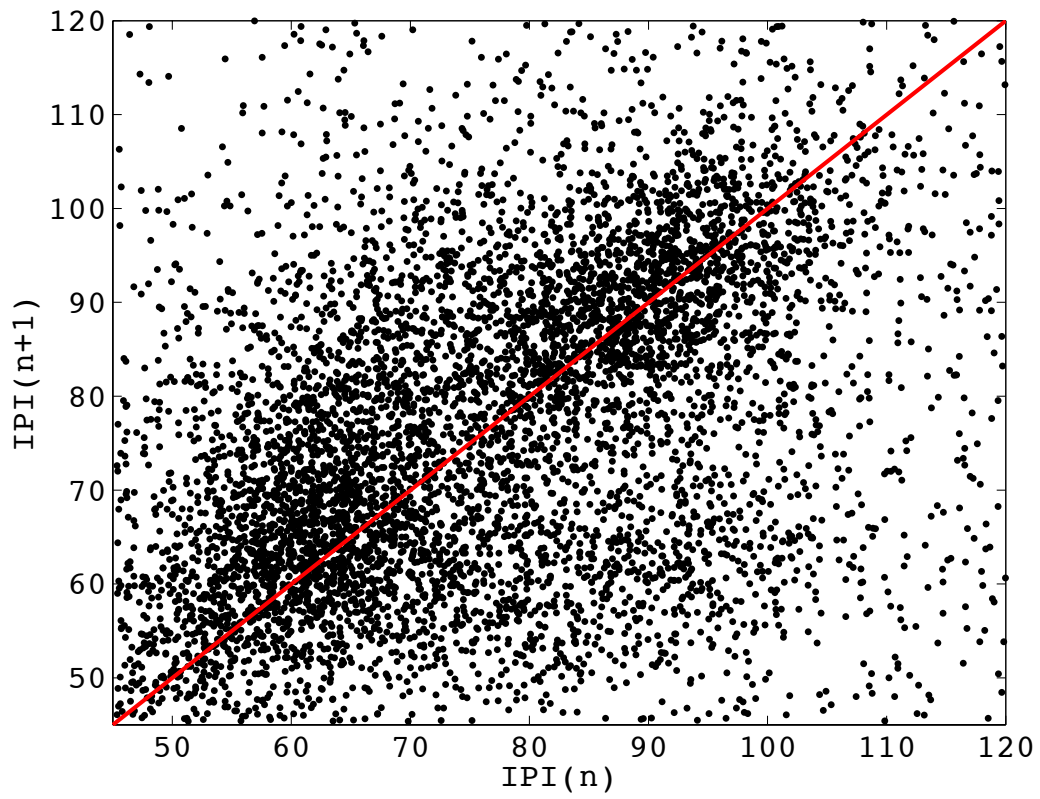


Figure 3.14. Return map of IPIs from all recordings at Mashpee Glade.

Considering the potential presence of two IPI modes in the Glade data, IPIs were divided among the 8 different evenings of recordings. Table 3.2 contains the statistics for IPIs on each night of recordings at the Mashpee Glade. The mean and median IPI ranged from 69.75-83.32 ms and 66.17-85.84 ms. The IPI skew shifted from the left to the right as the IPI median increased. IPIs from night to night at West Pond were higher than at the Mashpee Glade, but the median IPI in both locations varied by about 20 ms over all the nights recordings were made. The mean and median IPI ranged 77.30-94.92 ms and 77.05-97.09 ms at West Pond.

Date	Number of IPIs	Mean (ms)	Median (ms)	Standard Deviation (ms)	Skewness	Kurtosis
9/16/12	776	69.75	66.17	15.50	0.6593	2.7350
9/17/12	195	73.73	69.98	16.77	0.5071	2.2653
9/18/12	2042	73.77	71.08	15.66	0.4974	2.6499
9/19/12	927	76.91	76.67	16.63	0.2458	2.2994
9/20/12	264	75.81	74.41	16.06	0.2332	2.1553
9/23/12	1028	80.57	81.19	16.70	0.0637	2.1649
9/24/12	153	75.97	75.64	15.43	0.0745	2.0717
9/25/12	1584	83.32	85.84	16.57	-0.2346	2.3395

Table 3.2. Detail of IPIs each night of recording at Mashpee Glade.

Examining whether or not IPI temporal strategy varied between the Glade and West Pond locations, and not simply the mean and median IPI, call passes were tested for calls occurring in “strobe” doublets or triplets. The same criteria used in Kothari et

al. for identifying calls occurring in sound groups were used here for ease of comparison. A doublet was identified if the following two criteria were met (41),

$$IPI_n * 1.2 \leq IPI_{n-1}$$

$$IPI_n * 1.2 \leq IPI_{n+1}$$

For triplets the following two criteria must be met,

$$u * 1.2 \leq IPI_{n-1}$$

$$u * 1.2 \leq IPI_{n+1}$$

where u was the mean of IPI_n and IPI_{n+1} .

A stability criteria was also used,

$$\left[\frac{abs(u - IPI_n)}{u} \right] \text{ and } \left[\frac{abs(u - IPI_{n+1})}{u} \right] < T$$

where $T=0.05$ tolerance.

A summary of the sound groups identified is in table 3.3. More calls occurred in doublets (11.73%) than triplets (7.07%) at the Mashpee Glade, while over West Pond, roughly the same percentage of calls occurred in doublets and triplets. At the Mashpee Glade, nearly twice as many calls overall occurred in a sound groups than over West Pond (18.8% vs. 9.79%). This suggests that more calls were made in “strobe” groups in the more cluttered environment of the Glade, than over the open space at West Pond. Overall median IPI within “strobe” groups at Mashpee Glade were lower than at West Pond, and at both locations, the median IPI of triplets was greater than of doublets. An example of a bat pass with clear “strobe” groups is shown in figure 3.15.

	Number of Sound Groups	Percentage of Calls Occurring in a Sound Group	Mean IPI (ms)	Median IPI (ms)	Standard Deviation (ms)
Glade Doublets	408	11.73	58.56	57.17	9.4281
Glade Triplets	164	7.07	60.49	60.59	7.0055
West Doublets	152	4.90	63.57	61.41	12.1583
West Triplets	101	4.89	65.03	64.34	10.7341

Table 3.3 Sound Group Summaries at Mashpee Glade and West Pond.

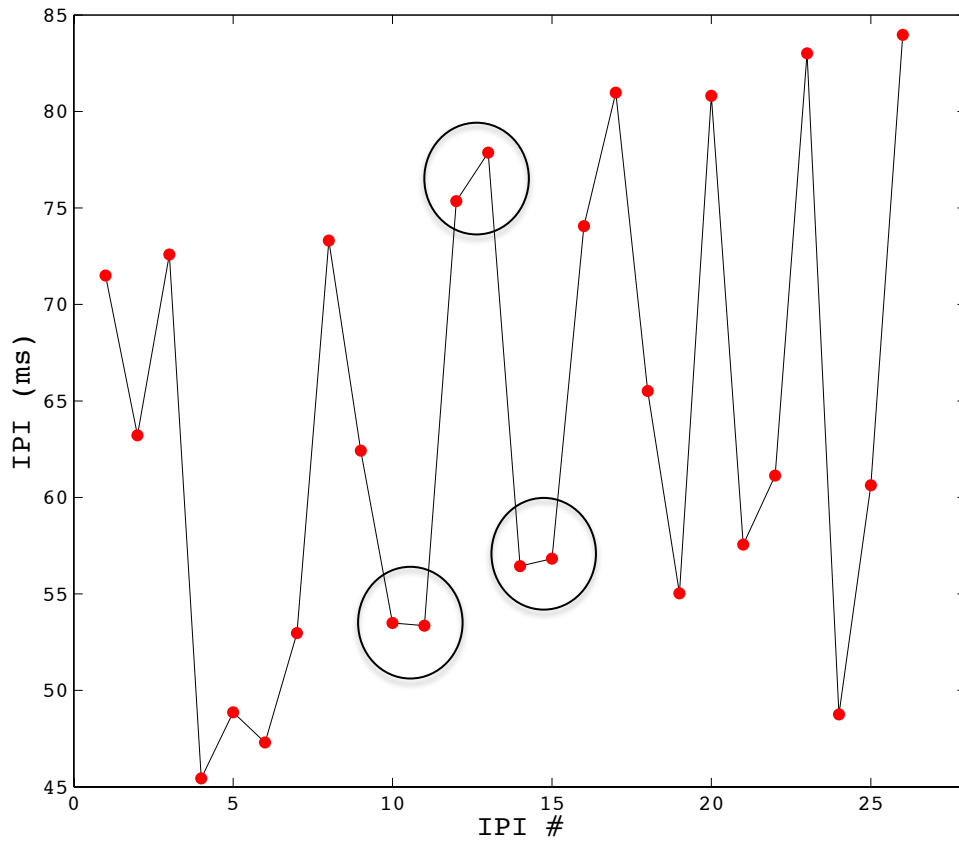


Figure 3.15. Pass of bat at Mashpee Glade with IPI plotted showing pulses being emitted in strobe groups, where two or more short IPIs are followed by a longer IPI. Three strobe groups are circled.

3.5 Discussion

Three key observations were made in this study. One, IPIs vary with the amount clutter. Over West Pond where more space was available for feeding and navigation, the median IPI was 90.88ms. At the field location with the most clutter, Mashpee Glade, the median IPI was 76.21ms. IPIs fell within the same range in both locations, such that IPIs at the Glade skewed to the left while IPIs at West Pond skewed to the right. This general observation reinforces the idea that more calls are required to resolve an acoustic picture in a cluttered environment.

A second observation was the existence of sonar “strobe” groups at both the cluttered and open environment. While these sonar groups did not occur with the same frequency observed in laboratory settings or with the same regularity, sonar “strobe” groups did in fact occur. “Strobe” groups were twice as likely in the cluttered environment than over the open pond, with call doublets and triplets making up 18.8% of the calls at the Glade, and 9.79% of calls at West Pond. Even within “strobe” groups, IPIs were found to be lower in the cluttered environment than the open environment, consistent with the general observations of median IPI noted. The observation of “strobe” groups in field recordings and the increased number of “strobe” groups in cluttered environments, suggests this type of temporal patterning may be an important tool particularly when clutter increases the difficulty in echolocation.

Finally, differences in temporal patterns of calls in these field recordings as compared with laboratory recordings were noted. Simmons (59) also showed an increasing number of “strobe” groups with increasing clutter, but strobe groups were more consistent and frequent than in field recordings. While “strobe” groups do appear to be used, there appears to be a more random approach to temporal patterning of calls. It should also be noted that there were significant differences between these field recordings and those presented in Moss (41). The percentage of calls occurring in sonar groups was lower and the median IPI was also significantly lower. This difference could be due to a variety of factors including the spatial make up of the field sites and clutter density, location of bat with respect to clutter, species of bat, or individual echolocation preferences of the particular bat.

It should be noted that the species of bat recorded in this study is not known. *Eptesicus fuscus* and *Myotis lucifigus* are common bats on Cape Cod. Further call analysis and visual markers would be needed to accurately identify which species was recorded. While it is likely that the same bat was recorded at each field site over the recording periods, this cannot be confirmed. Regularity in feeding times, and flight paths (visually observed at dusk), suggest the same bat flew at a given field site on all nights of recordings. Additional recordings made with multiple microphones for triangulation of the bat would improve understanding of temporal patterns. The position of the bat with reference to clutter may be important in determining whether or calls are emitted in “strobe” groups. This information would be particularly useful when recordings are made over West Pond. The bat at

that location does fly a path that brings it near the edge of the water (and close to foliage) at times. Knowing whether “strobe” groups are produced only when the bat approaches the perimeter of an open area or also produced in large open areas would help to better understand IPI patterning. This study confirmed previous studies of call rates, identified call “strobe” groups in both cluttered and open spaces, and showed how those “strobe” groups may correlate with clutter levels. Further investigation of IPI timing among a variety of cluttered field recordings sites would continue to improve understanding of the temporal patterning of IPIs, and how that information may be used to improve echolocation models.

4 Scenario Model

4.1 Introduction

Echolocating bats navigate and feed in environments with targets in a variety of numbers, shapes, and textures. The calls made by many different bat species are well defined in spectral content and three phases of echolocation, 'search', 'approach', and 'terminal', have been characterized based on the spectral content, duration, and interpulse intervals of the calls emitted (32, 68, 76). While these three general phases have been defined for many years, field and laboratory studies have shown that the activity of a bat does not always fit into a specific category, and any one phase of echolocation may not be sustained for a long period during flight, resulting in streams of calls that more closely resemble a combination of phases rather than fitting into one specific phase (53, 34, 3).

An echolocating bat is tasked with matching calls with returning echoes to create an acoustic picture of its surroundings. It is important to understand not only what call the bat is making and when the call is made, but also what the returning echoes sound like. Studies have examined the spectral content of echoes from several target shapes (20, 72, 92). In order to get a full picture of what an echolocating bat hears, not only does the spectral content of echoes from targets need to be understood, but also how the timing of bat calls and the position of targets combine to create a stream of echoes for any given emitted call. The goal of the scenario model created in this study is to provide a stream of echoes for a given target arrangement. The target arrangement, target type, bat call, and bat call timing, can

all be varied to better understand what a bat hears when it echolocates under a variety of circumstances. In particular, this study uses the scenario model to build a picture of echoes from point reflector targets in a “cluttered” environment. This is aimed at better understanding what a bat hears when it navigates and feeds in a “cluttered” environment such as those previously discussed in the field research section of this study. This model can aid in developing a stream of echoes that would result from a particular field location. While recordings of bat calls can be made in field settings, capturing the echoes as heard by bats has not been done, as that task involves many obstacles. A microphone would need to be located at the position of the bat when the echo is received and in the orientation of the bat’s head. This model can provide an approximation of what the bat hears without making such recordings.

4.2 Target Model

In this model, a virtual bat (animat) must fly through a two-dimensional virtual cluttered environment. The target field consists of an arena 14 meters wide by 14 meters deep. A grid of potential target locations 10 meters wide by 10 meters deep is centered in the arena. The minimum separation of potential targets is 0.25 meters, resulting in 1681 potential target locations on the grid. The number of desired target locations is input to the model, and the coordinates of targets are randomly selected from the 1681 potential locations. Tree density measurements made at Skunknet River Wildlife Sanctuary were considered when setting target

location parameters. In figure 4.1, an arena is plotted with all potential target locations shown as well as forty randomly selected target locations.

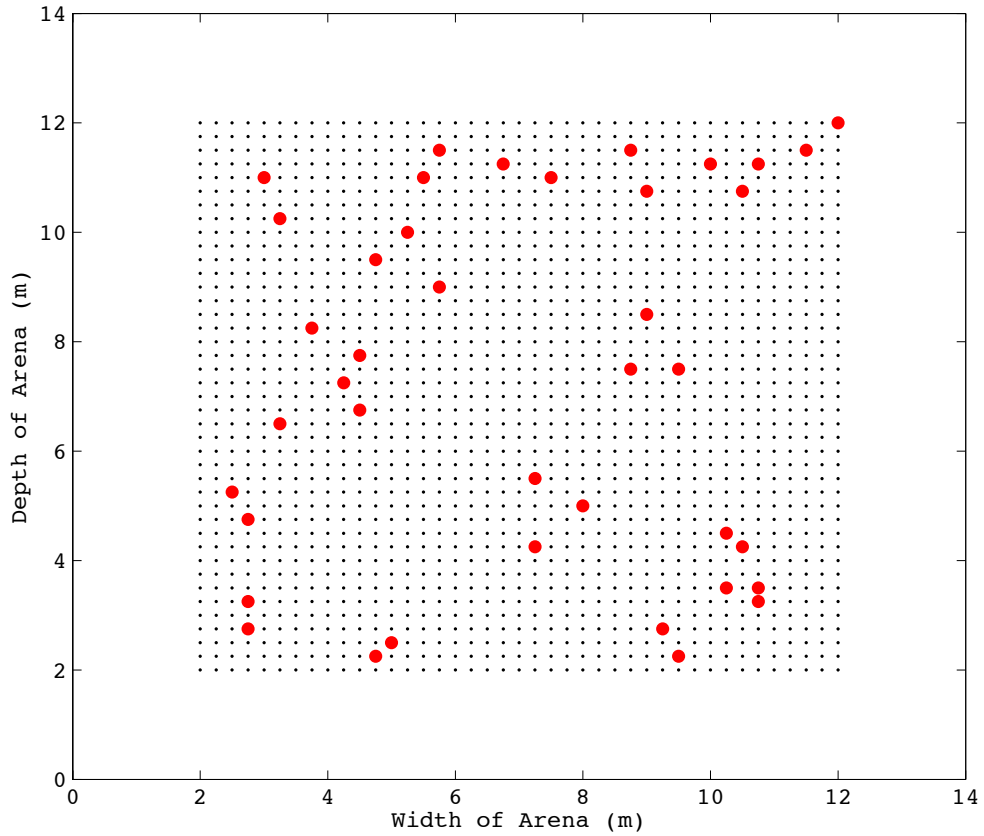


Figure 4.1 Target Field. Black dots mark potential target locations. Forty targets, randomly selected from the potential locations are indicated by red circles.

4.3 Flight Path

The animat flies a straight path through the target field in this model. The flight path is set before flight begins. Real-time decision making does not occur, although field observations of bats flying in cluttered environments do often include rapid changes to flight orientation (3). The goal of this model is not to optimize the flight path based on target locations, but rather to explore how call patterning can improve a bat's audio picture of the target field. The head direction of the bat is also fixed in the direction of the flight.

For each target field used in the model, a random starting position located on the far left side of the field is selected as well as a random ending position on the far right side of the field. A straight flight path from the start to the end point is calculated and tested for target avoidance. The animat must avoid targets in the flight arena by a minimum of 20 centimeters. This avoidance parameter was set based on field observations, and considerations of the average wing span of an *Eptesicus fuscus* of approximately 30 centimeters (22). Flight paths that do not meet minimum target avoidance are not used. Multiple flight paths that meet avoidance parameters are created for each target field used this model so that different paths through the same target fields can be compared. Figure 4.2 shows a flight path of an animat through a target field.

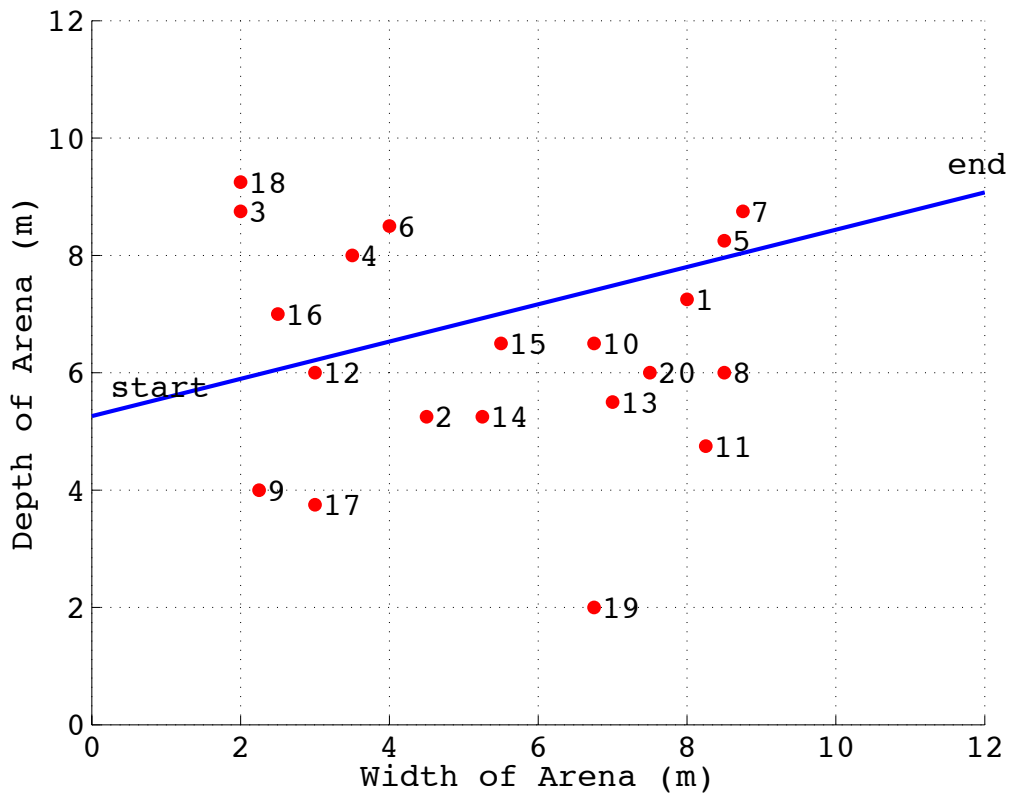


Figure 4.2 Flight Path. The blue line shows the path of the animat through field of 20 randomly selected targets. The minimum target avoidance distance is 20 centimeters.

4.4 Echo Model

4.4.1 Pulse generation

An *Eptesicus fuscus* call varies depending on the activity of the bat. In the field and laboratory recordings, the calls sweep downward in frequency from as much as 120kHz to approximately 20kHz. The signal duration varies from 20ms to less than 1 ms in both field and laboratory recordings. The signal duration is longer during the bats' 'search' phase and decreases as it transitions to the 'approach' and 'terminal' phase. The call is often comprised of a fundamental frequency sweep as well as a second and sometimes third harmonic sweep. During general navigation, bat calls sweep downward from approximately 100 to 20 kHz, and are several milliseconds in duration. Additionally, the minimum frequency of the calls varies depending on if the bat is in search, approach, and terminal phase (60, 31).

In this study, the bat call is approximated with a logarithmic swept-frequency cosine signal comprised of a fundamental frequency sweep from 50 to 20 kHz, and a second harmonic from 100 to 50 kHz. The signal is modulated with a hyperbolic tangent function to account for the signal quickly ramping up and down at the start and finish of call. The waveform and spectrogram of the signal are shown in figure 4.3.

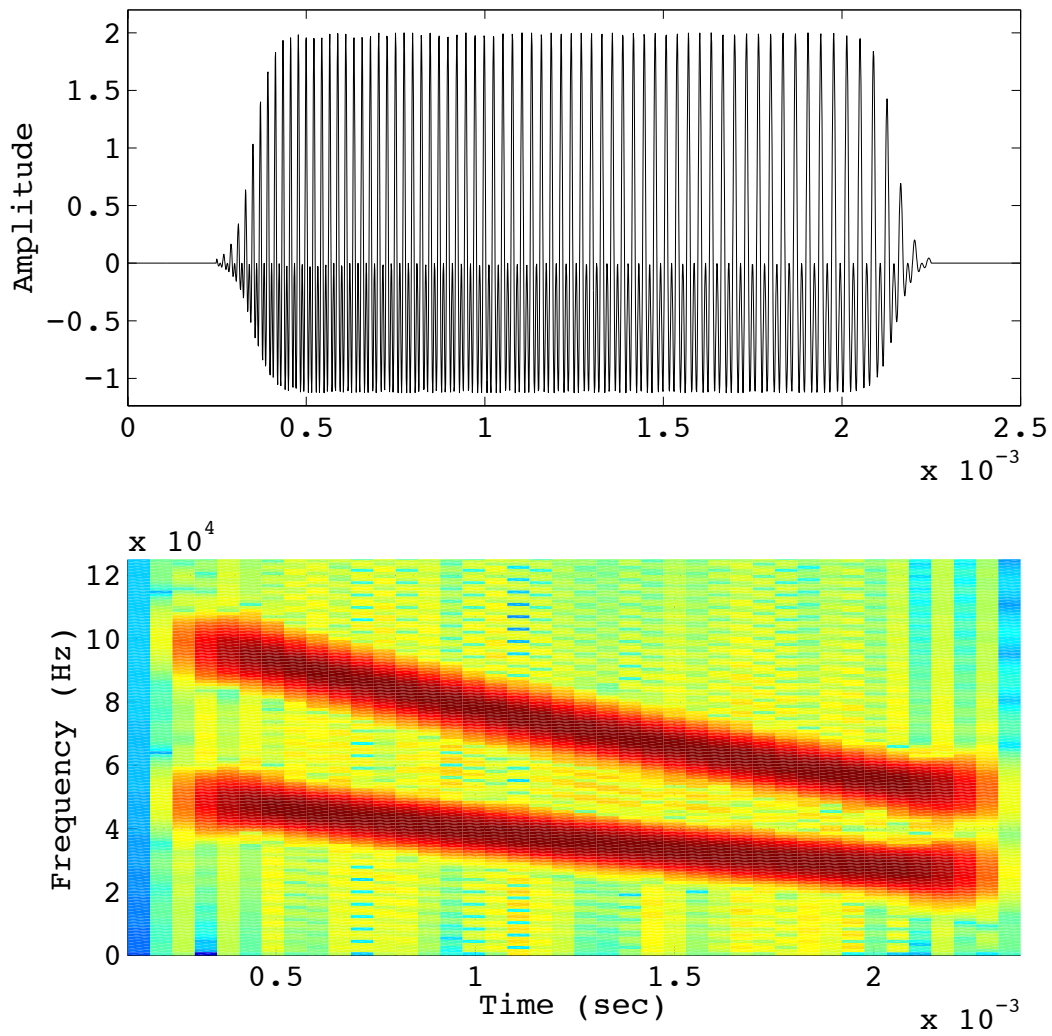


Figure 4.3. Waveform and spectrogram of modeled bat call.

The beam shape of the *Eptesicus fuscus* signal is highly directional and varies with frequency content of the call (78, 27). It has been reported that the beam shape of the signal in the horizontal plane consists of one large lobe and two equally sized lobes in the vertical plane oriented dorso-ventrally (28). In the horizontal plane the signal can be modeled as a piston sound source. In Barshan and Kuc 1992, an approximation of the pressure amplitude is given:

$$p(r, \theta) = \frac{p_0 r_0}{r} e^{-\theta^2 / 2\sigma_T^2} \quad (4.1)$$

For $r > r_0$ where r is the radial distance, θ is the azimuth, p_0 is the propagating pressure amplitude at range r_0 and $\theta = 0^\circ$, and σ_T is the beam width. The mean value of the -3dB beam width (the half power point of the beam width) was measured to be 70 degrees, or $\sigma_T = 35$. (17). The pressure amplitude for an *Eptesicus fuscus* has not been reported in literature, however Surlykke and Moss 2000 stated that the source level for the *Eptesicus fuscus* was similar to that of the European bat, *Eptesicus serotinus* that emits source levels as high as 125 dB sound pressure level (SPL) at 10 cm. For the purpose of this study, the source level of the *Eptesicus fuscus* was approximated to be 120dB SPL at 1 meter. The beam pattern and Gaussian spreading of the signal in the horizontal plane are shown in figure 4.4.

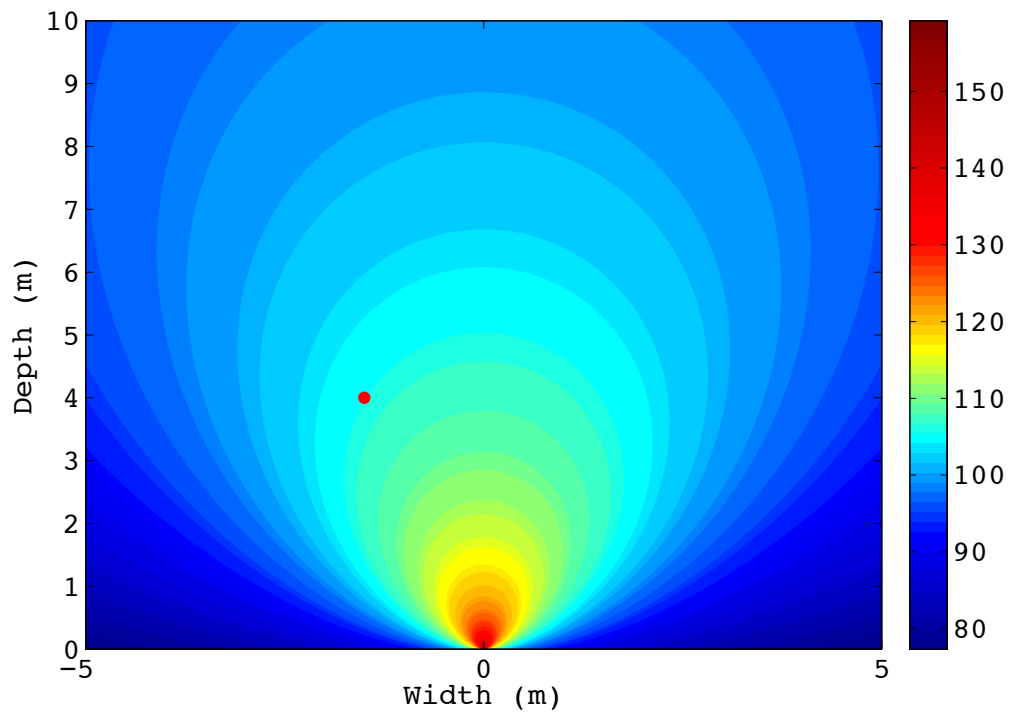


Figure 4.4 Gaussian spreading of the bat call. The bat is located at position (0,0) and the red dot indicates the location of a potential obstacle. The maximum intensity of the call is 120dB at a 1m distance from bat. At the position of the obstacle, the intensity has dropped to approximately 107dB.

4.4.2 Echo Generation

The basic active sonar equation is used to develop an acoustic model of returning echoes:

$$SE = (SL + TS - 2PL) - N - DT \quad (4.2)$$

where SE denotes the signal excess, SL is the source level, TS is the target strength, PL is propagation loss, N is noise, and DT is detection threshold. The source level was defined in the previous section as 120 dB at 1 meter. All of the targets were modeled as point reflectors. The target strength is defined as:

$$TS = 10 \log \left(\frac{\text{reflected intensity}}{\text{incident intensity}} \right) \quad (4.3)$$

and so, for a point reflector TS=0dB. While point targets are modeled as point reflectors in this study, the model may be used to study other shape targets as well.

The propagation loss combines the losses from both atmospheric absorption and spreading. Both the pulse emitted by the bat and the returning echoes are subject to atmospheric absorption. The attenuation of the amplitude of the pulse and echo is $\alpha * z$, where z is the radial distance, and α is the atmospheric absorption coefficient.

In order to calculate the atmospheric absorption coefficient, the absolute temperature in K, relative humidity r_h as a percentage, and the atmospheric pressure p_a in Pa must all be known. The absorption coefficient was taken from Computational Atmospheric Acoustics, by Erik M. Salomons, which provides the formulas from the International Standard ISO 9613-1:1993(E) as follows (66):

$$\alpha = 8.686 f^2 \tau_r^{\frac{1}{2}} (1.84 \times 10^{-11} \rho_r^{-1} + \tau_r^{-3} [b_1 + b_2]) \quad (4.4)$$

Where $\tau_r = T/T_{20}$ and $\rho_r = p_a/p_r$ are dimensionless quantities with $T_{20}=293.15K$ and $p_r=103.325$ Pa, and b_1 and b_2 are given as:

$$b_1 = 0.1068 \exp\left(-\frac{3352}{T}\right)/(f_{r,N} + f^2/f_{r,N}) \quad (4.5)$$

$$b_2 = 0.01275 \exp(-2239.1/T)/(f_{r,O} + f^2/f_{r,O}) \quad (4.6)$$

Where $f_{r,O}$ and $f_{r,N}$ are the relaxation coefficients of nitrogen and oxygen, given as:

$$f_{r,N} = \rho_r \tau_r^{-\frac{1}{2}} \left(9 + 280h \exp\left(-4.17 \left[\tau_r^{-\frac{1}{3}} - 1 \right] \right) \right) \quad (4.7)$$

$$f_{r,O} = \rho_r \left[24 + \frac{40400h(0.02 + h)}{0.391 + h} \right] \quad (4.8)$$

where h is the percentage molar concentration of water vapor in the atmosphere

given as $h = \frac{r h \rho_{sat}}{\rho_r}$, where $\rho_{sat} = 10^{C_{sat}}$ and $C_{sat} = -6.8346 \left(\frac{T_{01}}{T}\right)^{1.261} + 4.6151$, and

$T_{01} = 273.16K$ is the triple point temperature of water. The temperature used is

293.15K, 70% humidity, and an atmospheric pressure of 101.325 Pa. Figure 4.5

shows the attenuation coefficient for the frequencies contained in the bat call.

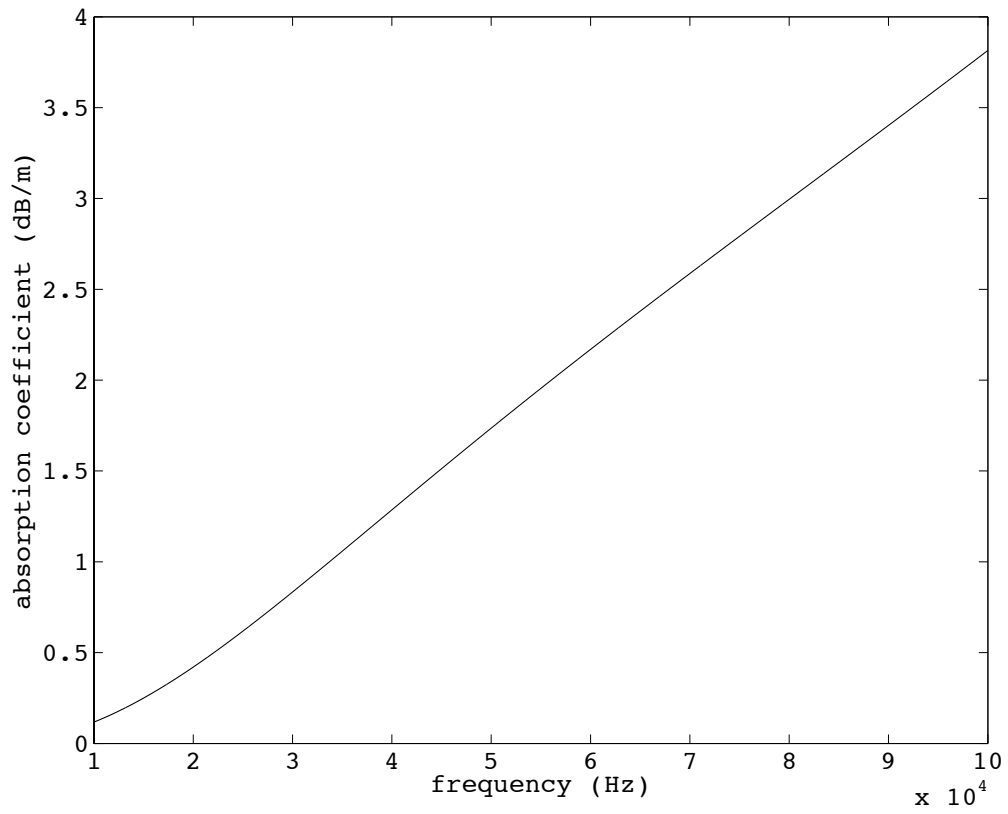


Figure 4.5 Atmospheric attenuation coefficient. Temperature is 293.15K, relative humidity is 70%, and atmospheric pressure is 101.325 Pa.

Noise, N , is set to zero in this model. Possible sources for noise in field recordings include road traffic, rushing water, and other insects. Only noise in the frequency range of the bat call will affect echo detection due to the frequency selectivity of the basilar membrane in the inner ear. In field recordings made for the purpose of informing this model, noise levels did not interfere with the call significantly. If a different study needed to include a significant noise level, this may be included in the model.

The detection threshold (DT), is the level at which an animal can detect a sound. Detection thresholds vary with frequency. The *Eptesicus fuscus* have good high frequency hearing abilities. Although the bat call sweeps over a large range of frequencies, many bats have a 'best' frequency at which they can detect sounds with a minimum dB threshold. The DT for this model was set using results from a study by Koay, Heffner, and Heffner, 1997. They reported on the audiogram of the *Eptesicus fuscus* for three animals. Figure 4.6 is the published audiogram. The best threshold average was 7dB at 20kHz. Echoes must be 7dB or louder at 20kHz in order for echo detection to occur.

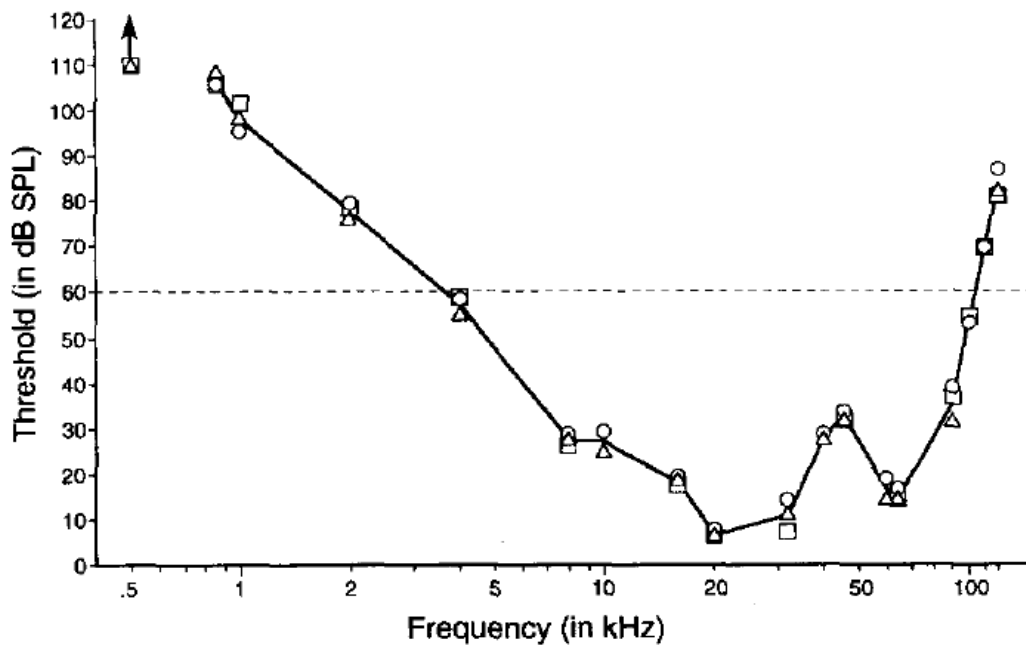


Figure 4.6. Audiogram of *Eptesiscus fuscus* from Koay, Heffner, and Heffner 1997.

4.5 Pulse Timing

In this model, the timing between animat signal generations can be selected such that signals are generated at regular intervals, or in “strobe pairs”. Two interpulse intervals (IPIs) are set such that $IPI1=IPI2$, or $IPI1>IPI2$. In the model, the animat’s location is updated at the time of each signal generation and all echoes are received while the animat is at that position. The maximum distance the animat could be from a target is $10\sqrt{2}$ meters. An echo would return from that maximum distance in 0.083 seconds. The flight speed of the animat is based on the typical flight speed of the *Eptesiscus fuscus*, reported to be 3m/s (43). At that reported speed, the animat would fly approximately 0.25 meters before the final echo arrived, resulting in a small arrival time error for the echoes. The maximum error in arrival time for echoes with this approximation is 0.73 milliseconds, significantly less than the signal duration time.

4.6 Results

When the animat flies through the arena emitting pulses, it receives echoes from the various targets located in the arena. Targets with animat-target angles greater than 90° (i.e, behind the bat) are not detected. The distance between the animat and targets may result in echoes returning from distinct targets that arrive separated in time or overlapping in time if located at similar ranges. The animat is limited in its ability to localize targets from the information given by echoes. Range can be detected from signal-echo time delay. Once the range of the target is acquired, the azimuth can be determined by solving equation 4.1 for the angle θ :

$$\theta = \sigma_T \left(-2 \ln \left(\frac{pr}{p_0 r_0} \right) \right)^{1/2} \quad (4.8)$$

This calculation must be completed for individual frequencies to account for the frequency dependent attenuation of the signal, and must be corrected for spherical spreading loss of the echo.

Echoes that increase in amplitude with subsequent signals indicate that the animate is approaching a target. Since all the targets are modeled as point reflectors, echoes arriving separately in time will have the same frequency content, but vary in amplitude. Targets at similar ranges produce “overlapping echoes” and the frequency content is altered, resulting in regular or irregular beats seen in the waveform, and notches in the spectrogram. In figure 4.7 a full flight arena with targets and the animat flight path are shown. The green markers indicate the animat location at signal generation. For illustration purposes, interpulse intervals 1 and 2 are set such that $IPI1=0.08s$ and $IPI2=0.5s$, although shorter interpulse intervals are tested in the model.

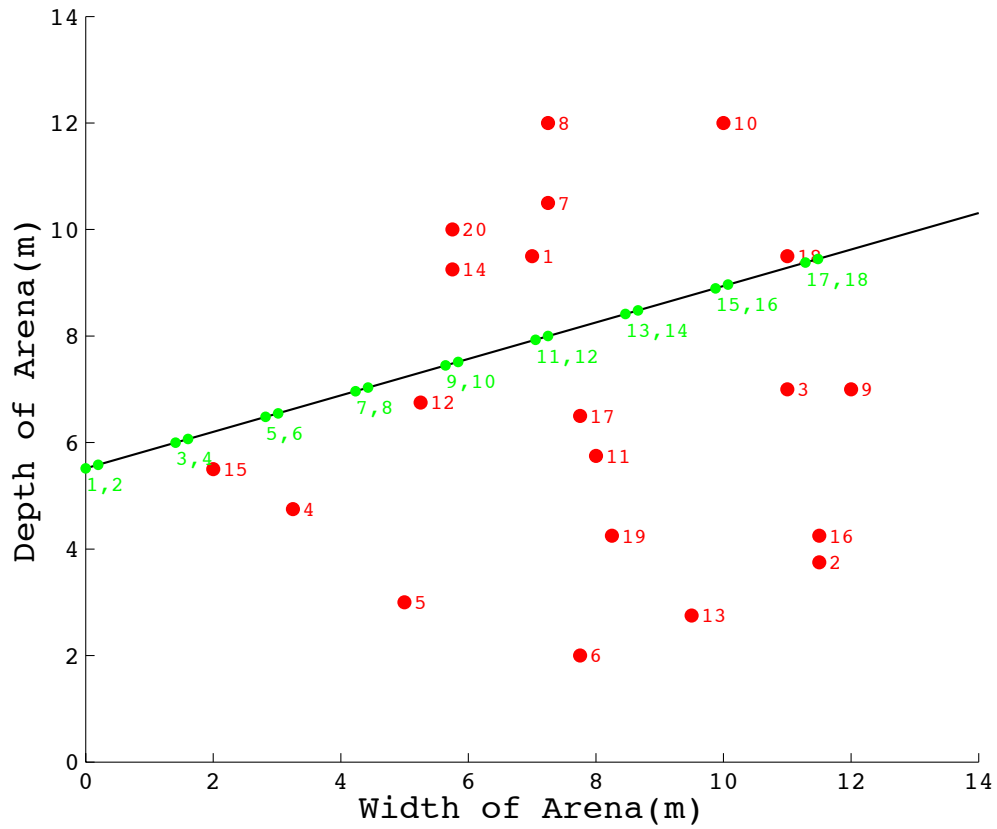


Figure 4.7. Flight Arena with animat flight path indicated by black line. Green marker indicate location of animat at the time of signal generation and are numbered in green. Targets located at red markers and are numbered in red.

Figure 4.8 shows a flight path and targets, with echoes returning from signal generated at position 13. In the upper panel, the path and targets are shown. Targets with an animat-target angle exceeding 90° (as measured from the flight path direction) fall behind the yellow line and are not detected. These targets are marked with a black 'x'. In the lower panel, echoes returning from targets 7, 14, 12, 6, 20, and 13 are shown. The echo from target 7 arrives independently in time. Targets 14 and 12 are located radially within 2.6 cm of each other, resulting in an "overlap" echo. Figures 4.9 and 4.10 show the waveform and spectrogram of the echo from target 7 and the 'overlap' echo from targets 14 and 12. In figure 4.10 beating can be seen in the waveform, and spectral notches occur.

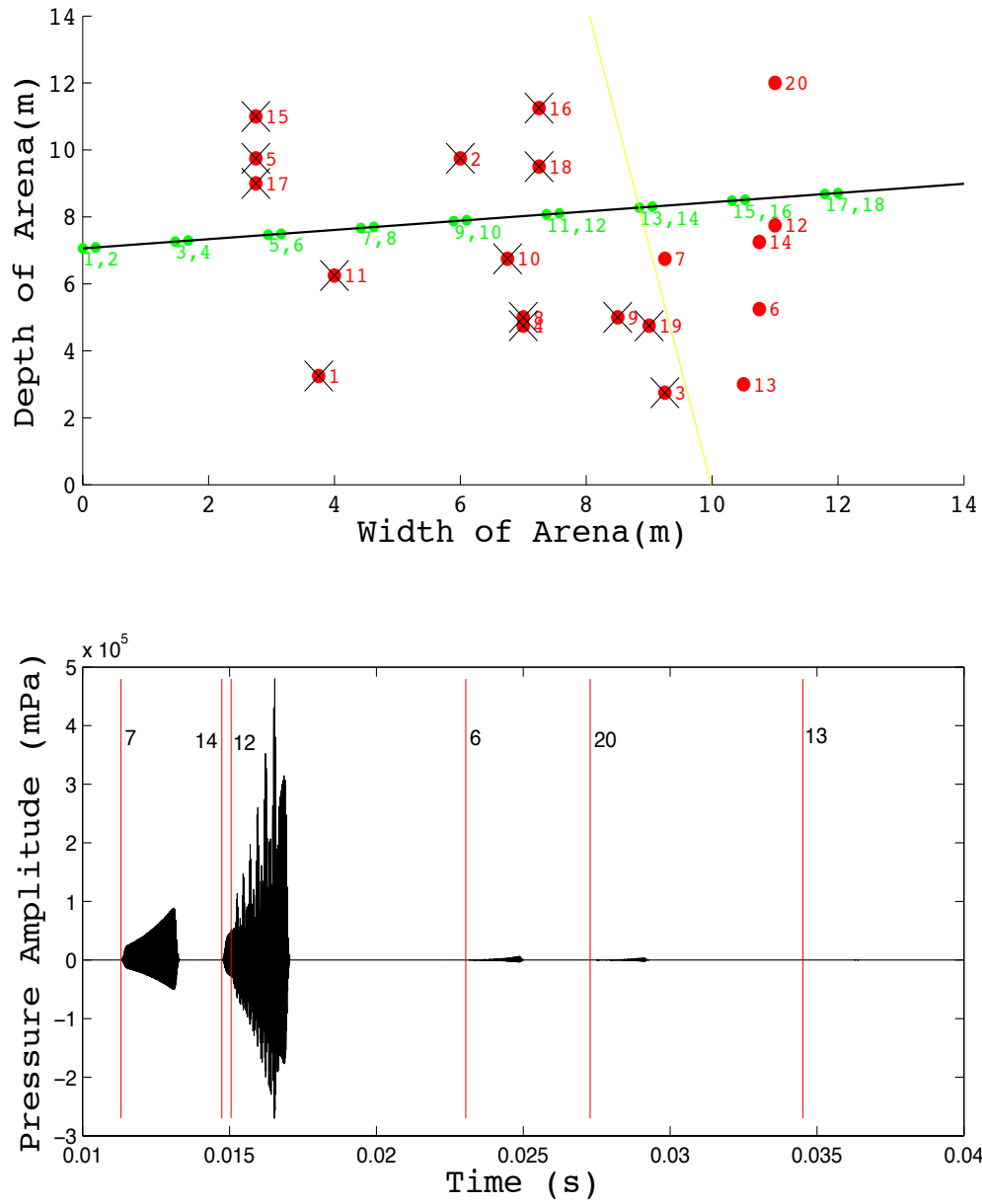


Figure 4.8. Arena, flight path, targets, and position shown in top panel. Echoes from targets received at position 13 shown in bottom panel.

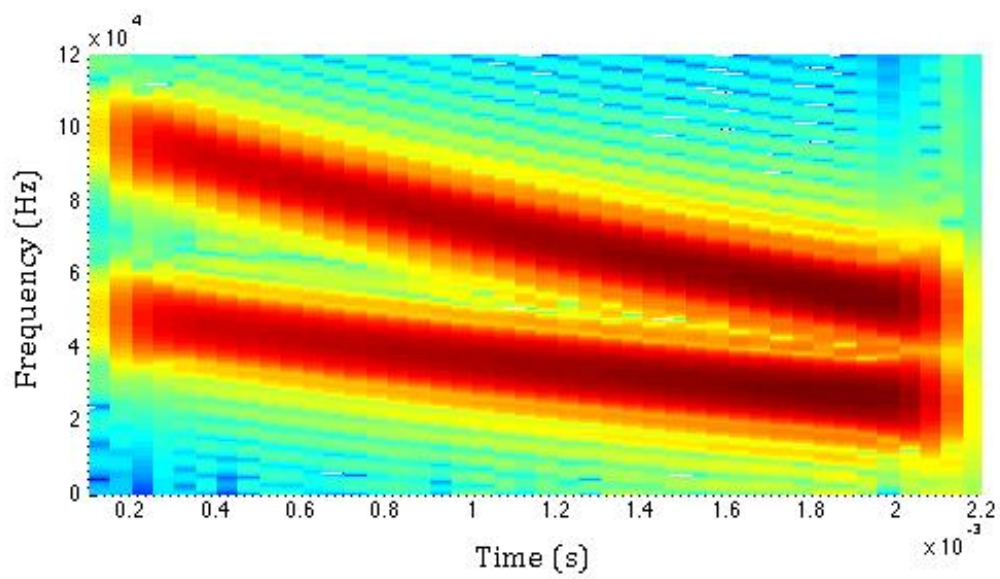
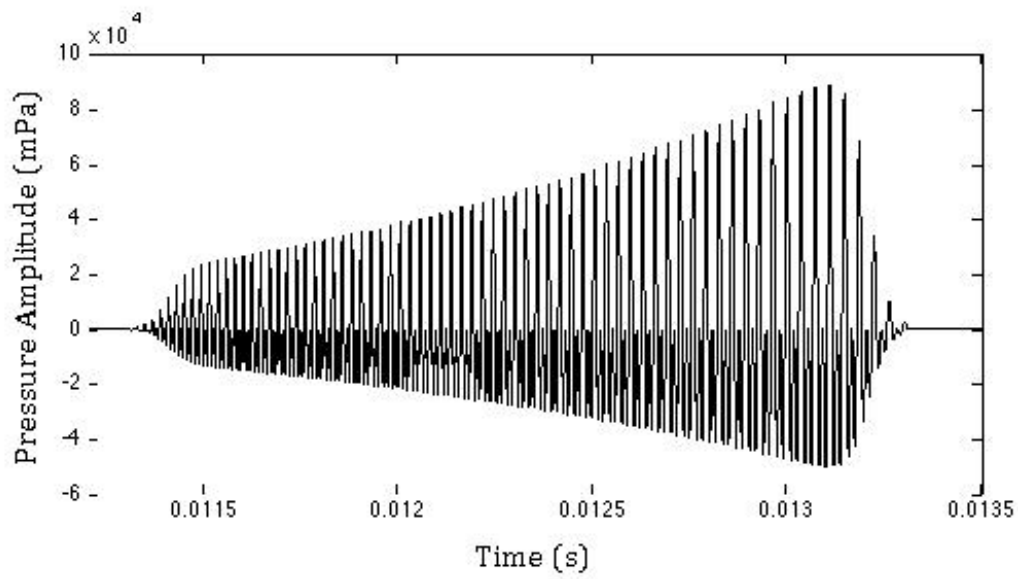


Figure 4.9. Waveform of echo from target 7 in top panel. Spectrogram of target 7 echo in bottom panel.

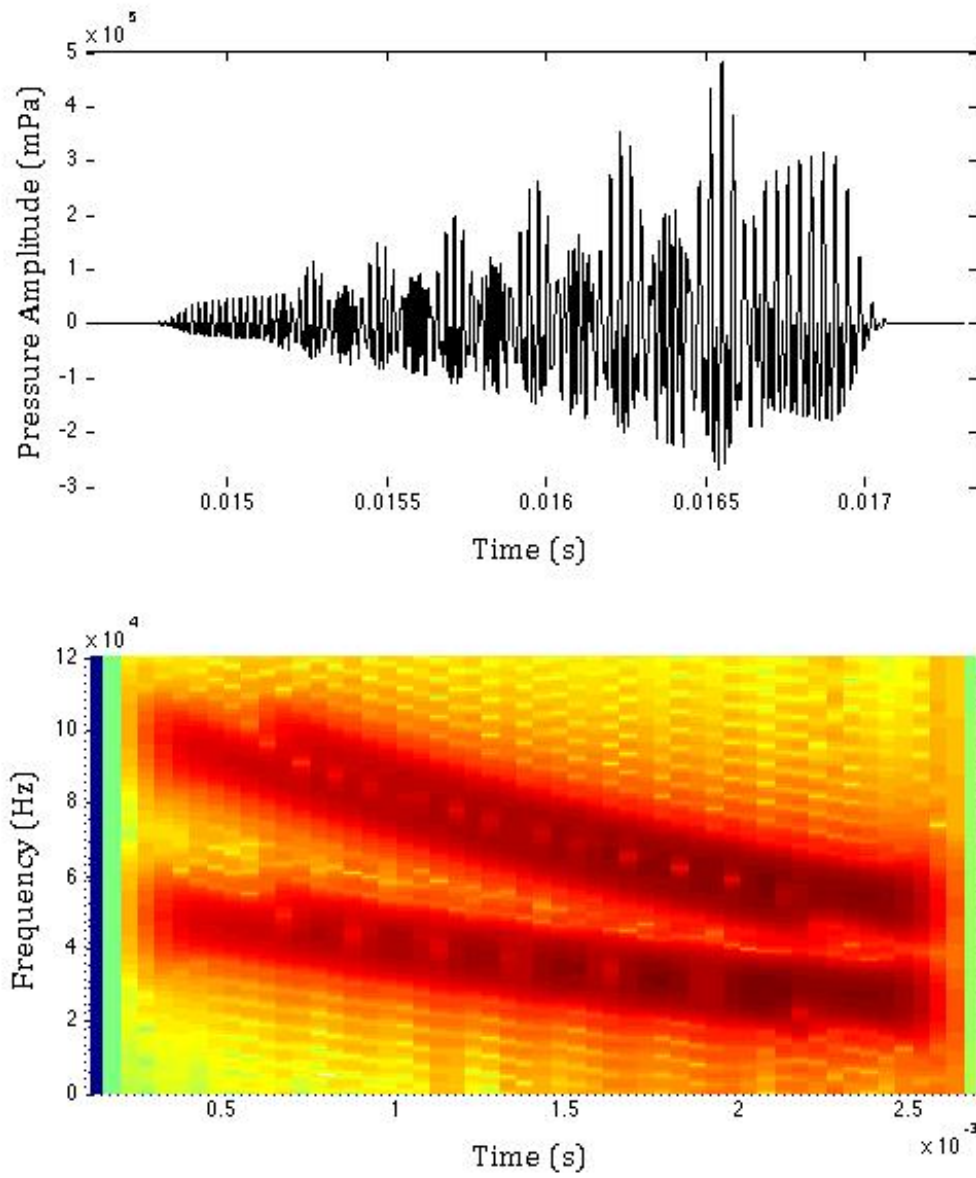


Figure 4.10. Waveform of echo from targets 14 and 12 in top panel.

Spectrogram of resulting 'overlap' echo in bottom panel.

4.7 Discussion

In this study, the scenario model presented provides a picture of the calls generated by flying echolocating bats and what the returning echoes sound like. The output of this model can be used as an input for a neural model. It is important to use physically correct echoes as input to neural models for the most accurate results and insight into the neural coding of these calls and echoes. Scientists studying the behavior of foraging or navigating bats may also use this model. Knowing what the bat hears as it maneuvers in flight and produces calls can help to understand behavior in the field when recording what the bat hears is not possible.

Two key observations about what a bat hears can be made from the analysis of this scenario model. One aspect of bat call generation examined in this model was the idea of calls being emitted in “strobe” groups. If the bat emits calls closely spaced in time, echoes from the first call can arrive after the bat has generated a second call. This can lead to pulse-echo matching difficulties, but as the amplitude of such mismatched calls would likely be greatly reduced due to attenuation and spreading over a greater distance, those echoes may be ignored by the bat, suggesting a method for disambiguating pulse-echo matching. This model can also be used to test strategies for call patterning in a neural model. The second call in a “strobe” group may be used to compare pulse-echo matches made using the first call. Alternatively, the second call could also act as an “off” indicator, focusing a bat’s attention on echoes only arriving before the second call. This would set a specific

distance over which the bat focuses and creates an acoustic picture. This may be useful in cluttered environments where a bat is bombarded by returning echoes.

Another observation made in this study was the generation of “overlap” echoes by targets at similar ranges. The idea of two or more targets creating one “overlap” echo is similar to what has been studied by scientists observing echoes created by flying prey. In the case of a flying insect, echoes bouncing off different parts of the insect or the hitting multiple times due to a beating wing also cause “overlap” echoes. These echoes are referred to as glints and have been extensively studied (70, 71, 5). Glints also have notches in the spectral content. It has been suggested that these notches could act as cues to the bat, informing it about target information such as size or even type. However, as can be seen in the results of this study not only do flying insects create “overlap” echoes, but also targets at similar ranges. Neural mechanisms may exist to detect spectral notches and use notch locations to inform a bat about prey size and type. These same neural mechanisms could potentially also identify an “overlap” echo created by two separate but similarly ranged targets as an insect. This emphasizes the need for additional head-related cues to differentiate trees and foliage from insects.

The scenario model presented in this study is important because scientists studying the behavior of bats in the field can use it to understand what the bat hears. It can also provide an accurate input to scientists creating neural models. The results presented in this study illustrate the importance of call timing and corresponding

echo arrival times, and emphasize the need for further study of echolocation in this area.

5 Peripheral Model

5.1 Introduction

The Scenario Model described in the previous chapter simulated what an echo arriving at the position of a flying bat would sound like. It accounts for the signal frequency content, duration, and interpulse interval. The model also calculates target reflectivity, arrival times of echoes, and attenuation due to spreading and atmospheric absorption. For echoes at sufficient range to arrive separately in time from other echoes, a simple neural network can calculate range using a delay tuned neuron model, where neurons only spike if they receive input from a signal and echo at a specific delay. For the “overlap” echoes described, arising from targets at similar range, a delay tuned neuron will not detect two separate targets. In addition to range, an echolocating bat will need to determine a target’s azimuth and elevation to create a three dimensional acoustic picture. There is not enough information from the Scenario Model alone for a biologically relevant neural model to determine azimuth and elevation and additional sound cues are required.

In order to supply a neural model with an accurate input and provide the cues necessary for three dimensional sound localization, a peripheral auditory model is developed. This model consists of two main parts: the Head Related Transfer Function, and a middle and inner ear model. In order to complete sound localization, more than one receiver is required. Incorporating the Head Related Transfer Function, a calculation of individual echo frequency content and amplitude

at the eardrum is made. This accounts for reflections off the body, head, and neck, as well as the effects of the pinna. A model for the middle and inner ear is then used to acquire an average firing rate at the Auditory Nerve. The main function of the middle and inner ear model is frequency division of the signal and echoes. The result of the scenario model and peripheral model is a biologically accurate input for a neural network. This is an important step in developing a biologically relevant neural model that will take full advantage of sound localization cues.

5.2 Head Related Transfer Function

There are many cues used for sound localization. A sound receiver with two ears (binaural) will acquire two different arrival times for a particular sound source. This is referred to as the interaural time difference (ITD) and can aid in localization. For short sound sources such as a click, onset time differences are used, while phase delays provide information for longer periodic stimuli. Larger head size and lower frequencies, where the large wavelengths can more easily diffract around the head, improve the efficacy of this cue (54, 63, 13, 86). The use of ITD cues for echolocating bats may provide less information given the small head size of the bat and the high frequencies of the calls (16). The use of ITD cues and neural mechanisms for identifying these cues are discussed in the next chapter.

The sound level difference at each ear provides another localization cue. This difference in sound level is called the interaural level difference (ILD). It is a result of the sound having to travel farther, but also results from absorption of the sound

by the head, referred to as head shadow. In order for ILD cues to be significant, the wavelengths of the stimuli should be much smaller than the head size of the receiver (23, 50, 91). The greatest length of the *Eptesicus fuscus* skull is reported to be approximately 0.0172 meters (89). The wavelength of a typical call varies from 0.017 to 0.0034 meters, providing effective ILD cues.

While ITDs and ILDs may provide a receiver with many cues for sound localization, there are several shortcomings. These cues help a listener determine whether the sound is coming from the left or the right, but do not provide enough information to differentiate elevation. It can also be difficult to determine if a sound source is in front or behind if solely using ITD and ILD cues. The “cone of confusion” is a term used to describe a cone shaped area where any points along a cross-section will provide identical ILD and ITD cues (88). Further cues must be used to correctly identify elevation.

When a sound travels to the receiver, it bounces off the head, body (including the shoulders and neck), and pinnae, providing subtle but important spectral azimuth and elevation filtering. This filtering is commonly referred to as the Head Related Transfer Function (HRTF) (7). These cues are most important for elevation localization. In this model, the animat moves in 2 dimensions, so elevation cues are not needed, however the HRTF does provide an additional azimuth cue and is incorporated into the model.

The HRTF is defined as $H(f)=\text{Output}(f)/\text{Input}(f)$. It compares the sound source measured at the eardrum with what would be expected to be measured at the center of the head, were the head not there. HRTF measurements are specific to individual animals, based on their unique anatomy. In the case of a bat, elaborate pinnae cause great diversity in HRTF measurements. An example of an *Eptesicus fuscus* is seen in figure 5.1. The large pinna with ridges and the tragus, which extends up from the base of the ear, create unique spectral cues.



Figure 5.1 *Eptesicus fuscus*.

Credit Matt Reinbold, Flickr Commons, Wikimedia Commons

5.3 *Eptesicus Fuscus* HRTF Measurements

HRTF measurements were made for the *Eptesicus fuscus* and reported on by Aytekin, Grassi, Sahota, Moss (2004). Dr. Cynthia F. Moss provided the data from this experiment and HRTF measurements for bat S1 from that HRTF study were incorporated to this model. Figures 5.2-5.10 show how the HRTF for a particular *Eptesicus fuscus* affect the echoes generated by the scenario model. Measurements were made for four *Eptesicus fuscus* (S1, S2, S3, S4). Microphones were inserted into the bat's ear canal and the bat was placed at the center of a recording apparatus with its head pointing at 0° azimuth and elevation. Sounds were broadcast 84 centimeters from the center of the bat's head from 685 different positions on the frontal hemisphere. Figure 5.2 shows the maximum gain of the HRTF for bat S1 for the right and left ear. The left and right ear HRTF are not symmetrical. It was reported that this might be a result of structure or orientation difference between the bat's ears. For the left ear there is a maximum gain at 65 kHz and the minimum gain occurs at about 50 kHz. The maximum HRTF for the right ear is shifted down in frequency and has lower maximum gains.

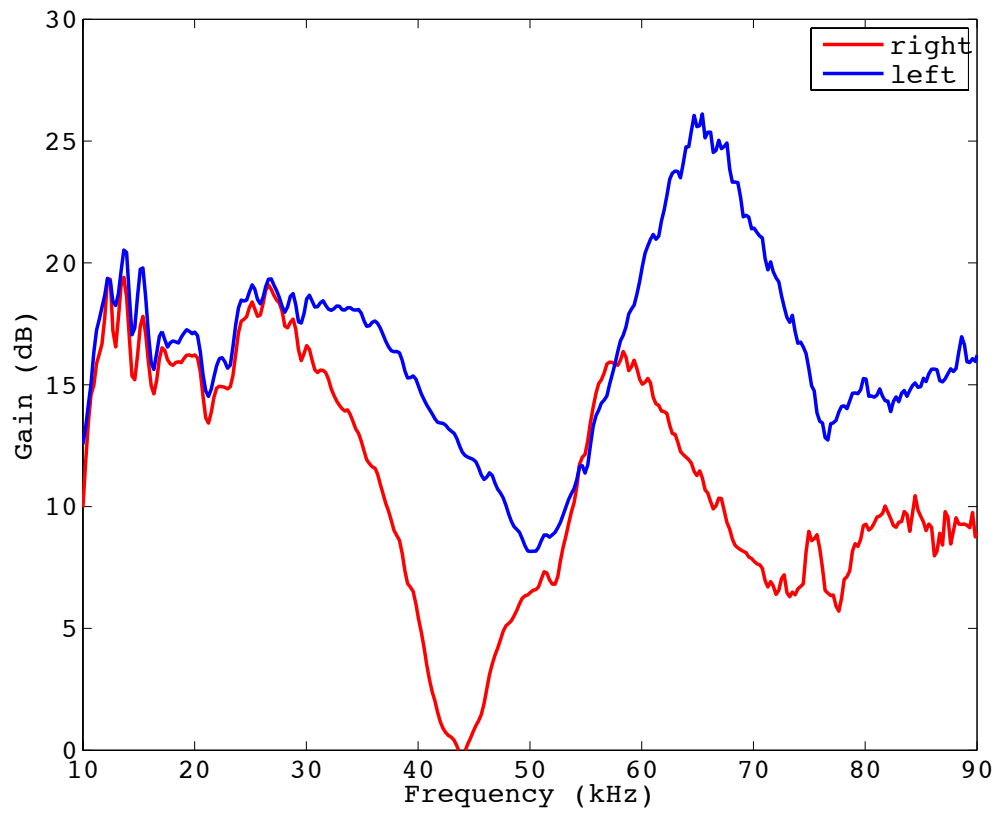


Figure 5.2. Maximum gain of HRTF for the right and left ear.

Convolving the HRTF with the original modeled signal reveals the effect of the HRTF. The signal is convolved with the HRTF corresponding with azimuth 45.36° and 0.18° elevation. Figure 5.3 shows points where all HRTF measurements were made in blue. Measurements were made on the frontal sphere from -90° to 90° left to right of the midline and -90° to 90° above and below the horizon. The green points are where the elevation is closest to 0° , these are the points used in the model. Measurements were made in 5° increments. Figures 5.4-6 show the effects of the HRTF on the signal at 45.36° circled in green in figure 5.3. As expected, the gain from the HRTF is greater in the right ear.

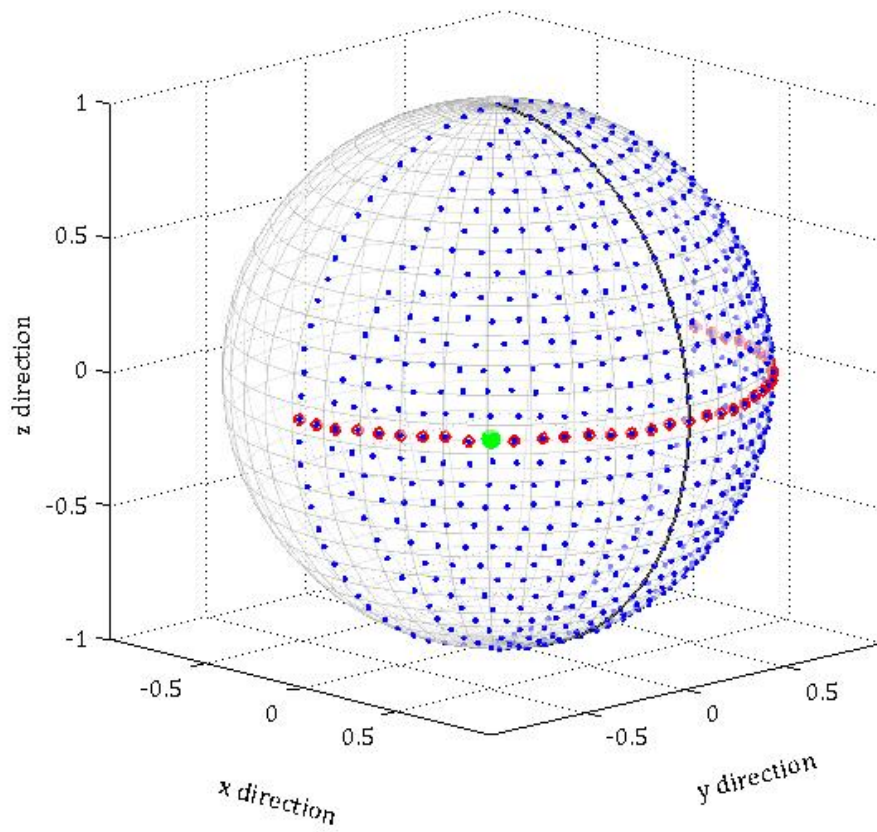


Figure 5.3. Map of HRTF measurement locations. Locations used in model circled in red. Location used in figures 5.4-6 marked with green.

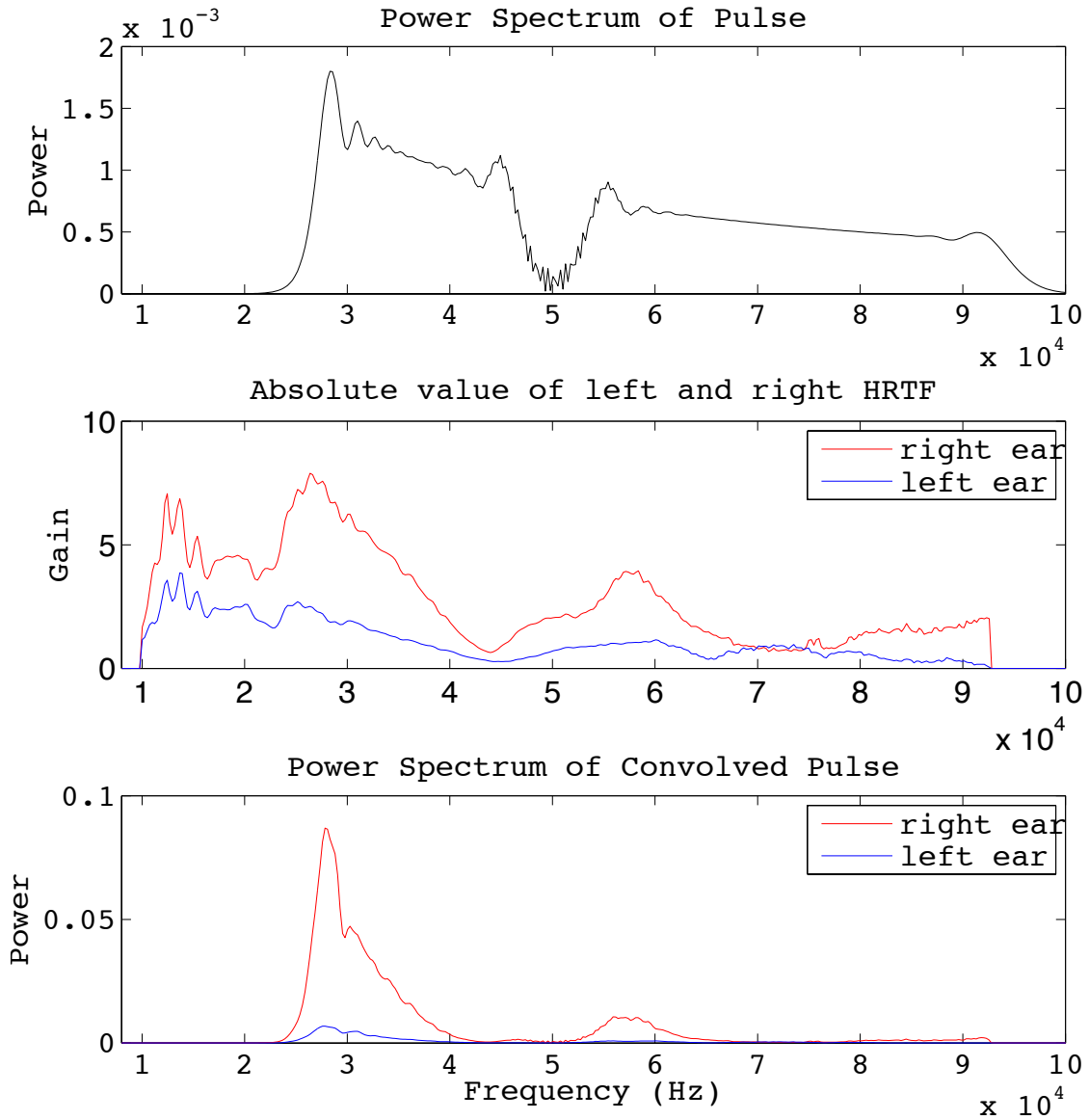


Figure 5.4. Top panel shows power spectrum of original signal. The middle panel is the absolute value of the left and right HRTFs that are convolved with signal. The bottom panel shows the resulting power spectrum of the convolved pulse.

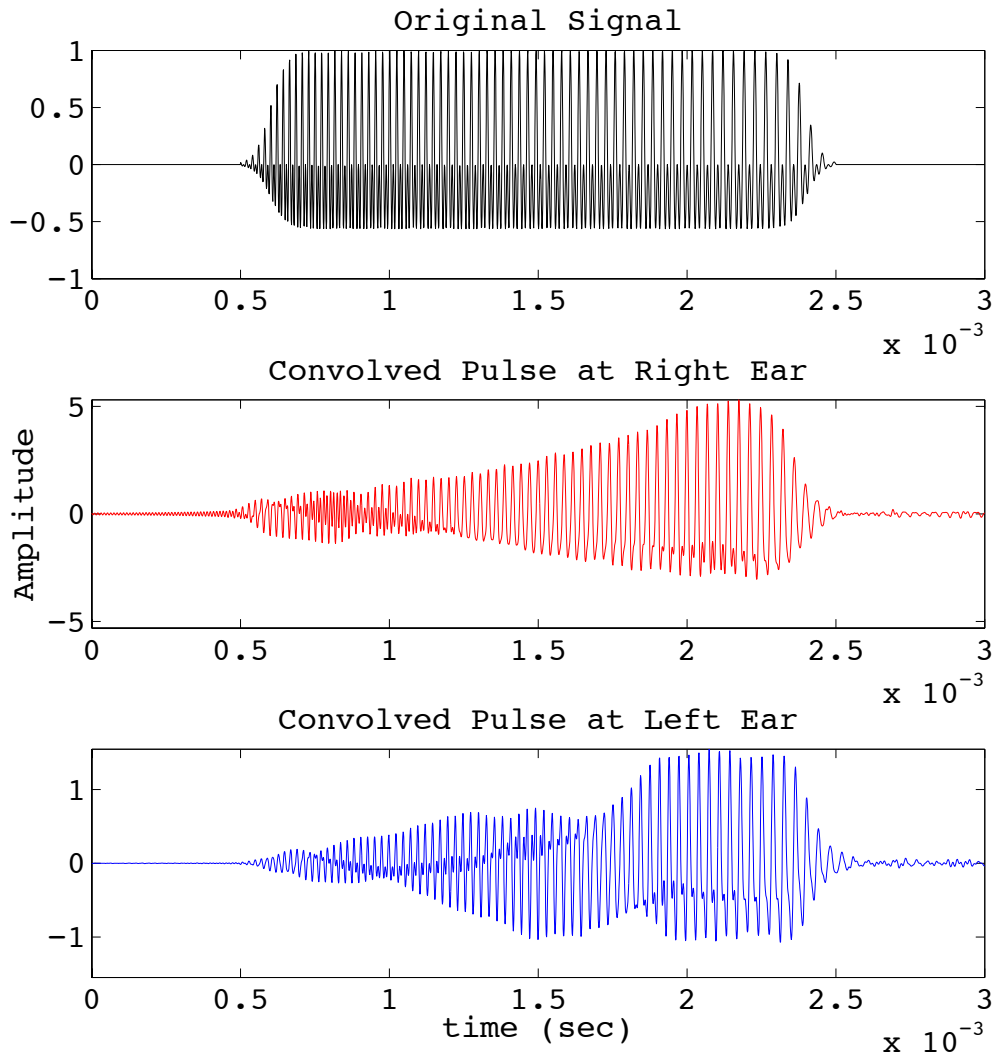


Figure 5.5. Top panel is waveform of animat signal. Middle panel is waveform of signal convolved with right HRTF and the bottom panel is the waveform of the signal convolved with the left HRTF.

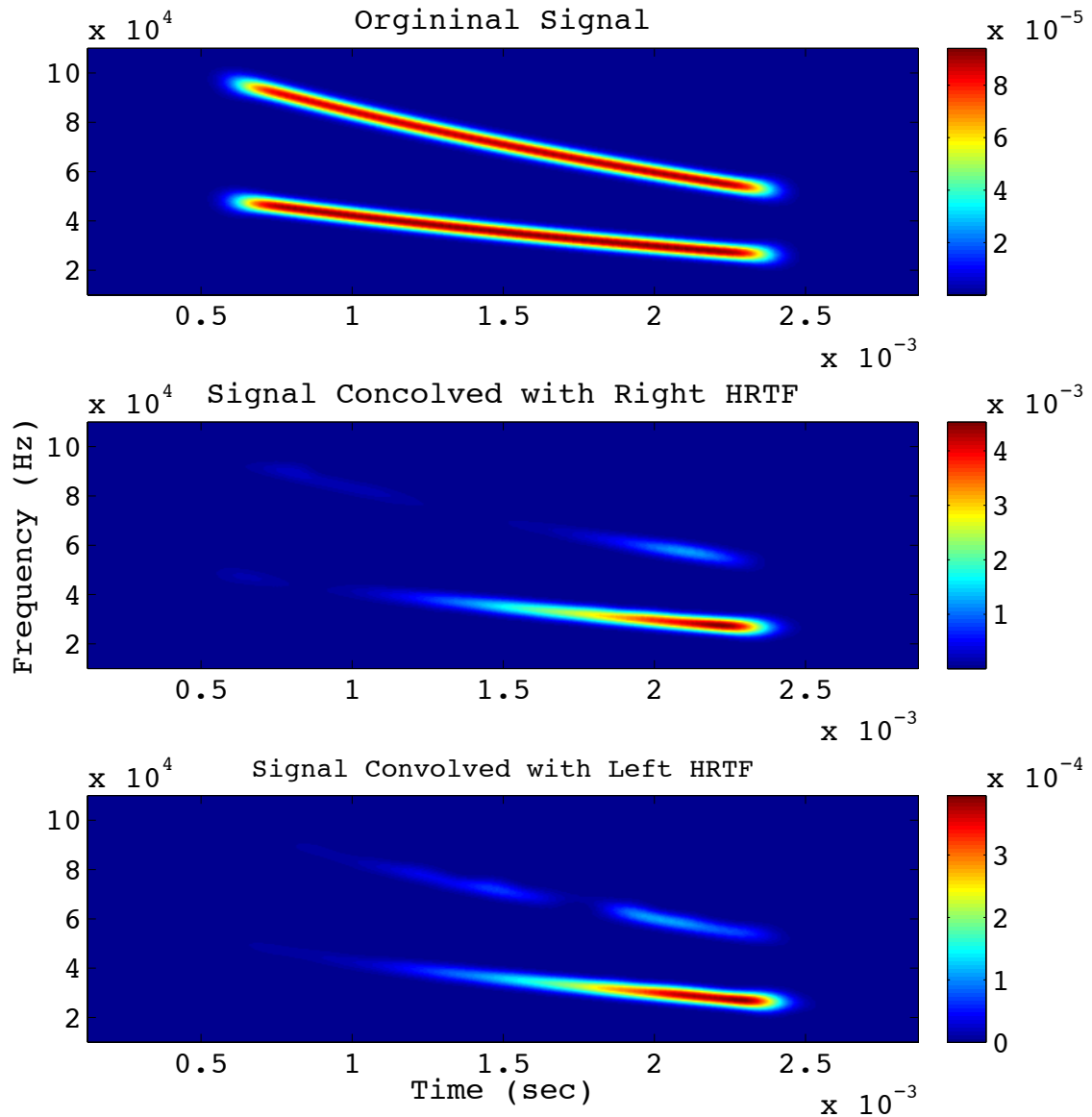


Figure 5.6. Spectrogram of original signal in top panel. Middle and bottom panels show spectrogram of signal convolved with right and left HRTFs.

5.4 HRTF Measurement Implementation

In this model, a nearest neighbor function is used to select which HRTF measurement to convolve returning echoes with. After the echoes are generated in the scenario model, the head-target angle between the animat and each target at each signal generation location is matched to the nearest neighbor HRTF measurement location along the elevation=0° plane. The HTRF's are then convolved with each echo and then the echoes are summed together at the arrival times so that each emitted signal results in one stream of echoes. Echo streams from signals produced in “strobe groups” are summed together as well because certain target arrangements and pulse patterns can result in echoes from a secondary signal arriving during the echo stream duration of a prior signal.

In figures 5.7 and 5.8 the echoes that have been convolved with the corresponding HRTFs are shown for the target arrangement and animat location shown in figure 4.8. Figure 5.7 shows the echo returns from target 7 alone in time, while figure 5.8 shows an “overlap” echo resulting when echoes from targets 14 and 12 return. Each echo in the overlap is convolved with its corresponding HRTF before summing. In figure 5.7 the top panels show the waveform and spectrogram of the returning echo convolved with the right ear and the bottom panels show the convolution at the left ear. The amplitude of the echo at the right ear is greater than at the left as might be expected because target 7 is to the right of the animat's midline. The echo at the right ear has most of its energy in the first harmonic, while the echo at the left ear has strong energy in both harmonics. In figure 5.8 the “overlap” echo is shown

convolved with the corresponding HRTFs separately and then summed together. Again, the top panels show the results at the right ear and the bottom panels at the left ear. The resulting echo does have greater amplitude at the right ear, which is expected since both targets creating the overlap echo are to the right of the animal. The notches in the frequency created by the overlapping echoes are slightly out of phase in the left and right ear.

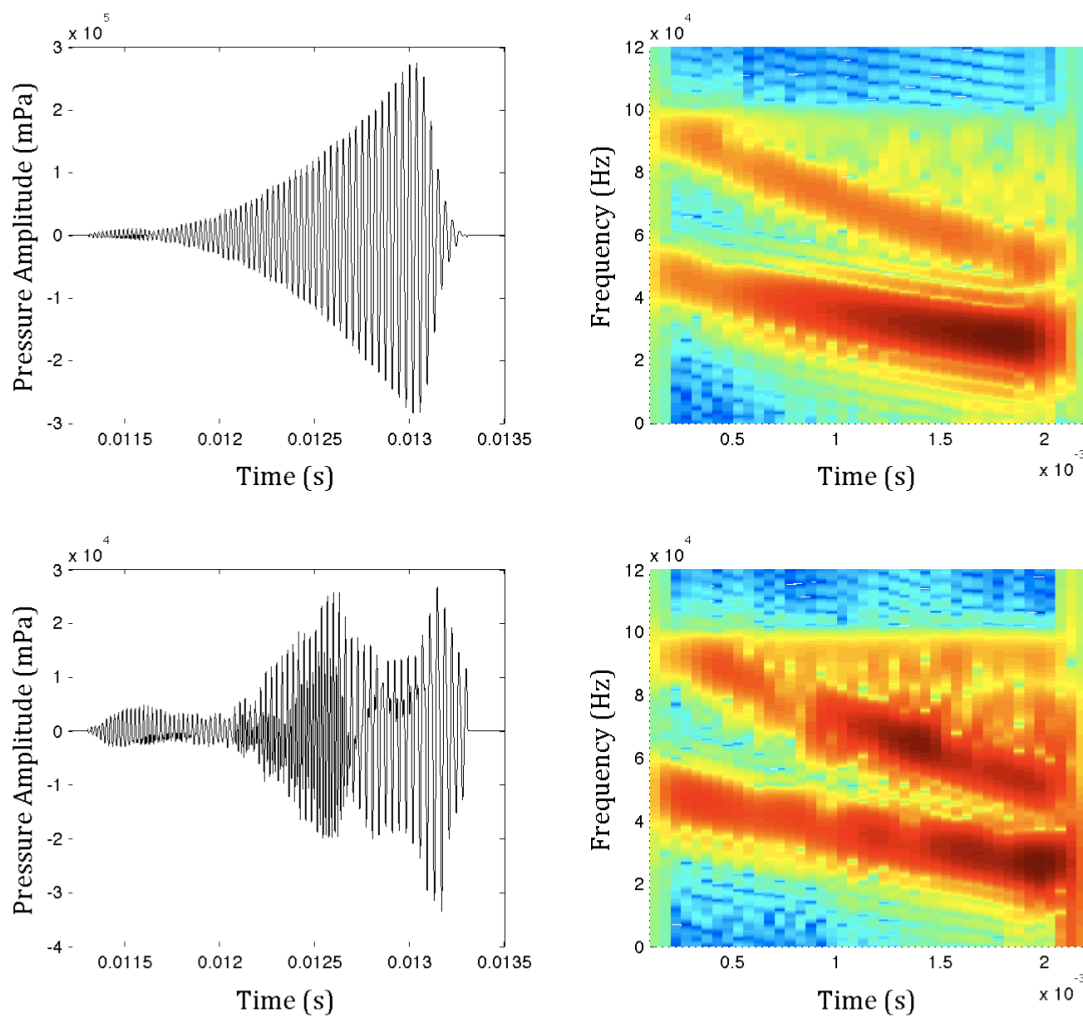


Figure 5.7. Waveform and spectrogram of single echo convolved with nearest neighbor HRTF for right and left ear. Top panels are right ear and bottom panels are left ear.

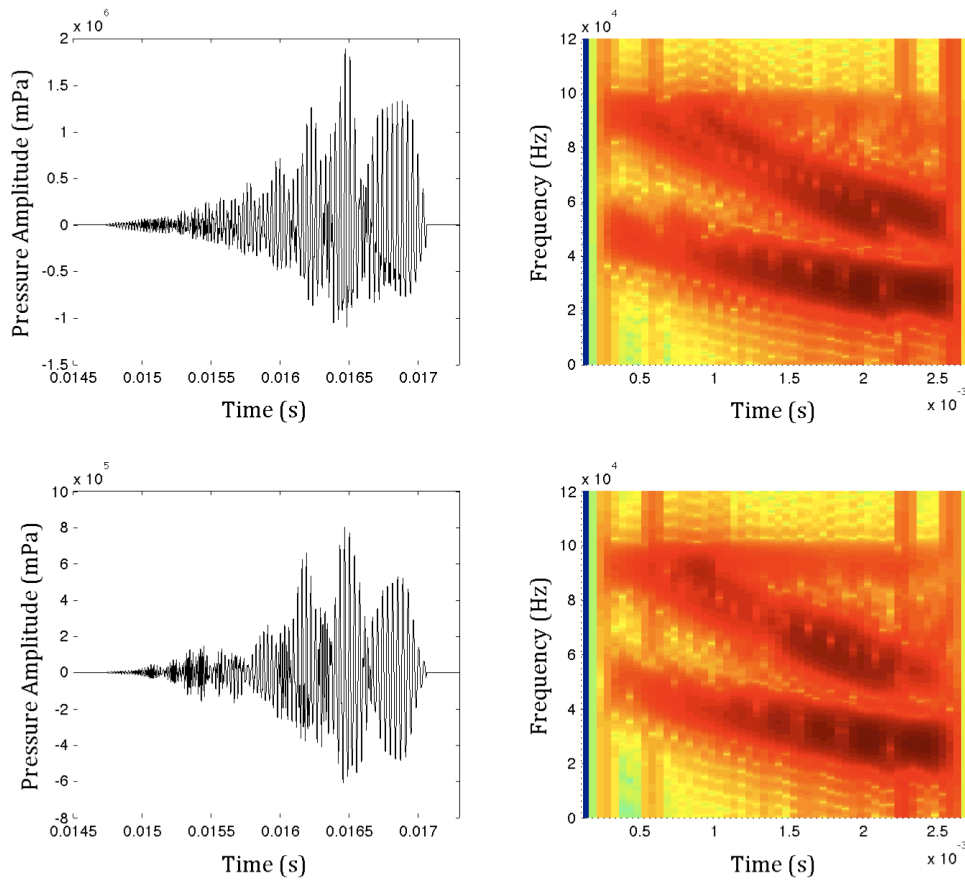


Figure 5.8. Waveform and spectrogram of overlap echo convolved with nearest neighbor HRTF for right and left ear. Top panels are right ear and bottom panels are left ear.

The HRTF is believed to help in localization of targets by creating notches in the frequency spectrum specific to a given elevation and azimuth. Figures 5.9 and 5.19 show how the HRTF changes as you move along the horizontal plane with elevation 0° for each ear starting at 90° (to the right of the bat) and moving in 30° increments to -90° (to the left of the bat). Figure 5.9 shows results at the right ear and figure 5.10 shows results at the left ear. As expected, the gain at 90° is greater than at -90° for the right ear and reversed for the left ear. The dominant feature in the HRTFs for the right ear is a notch that occurs in the 40-45kHz range. The HRTFs for the left ear also display a notch, but the location has more variety and notably 90° and 60° lack the single local minimum a secondary peak occurring around 50kHz. All the HRTFs provide similar gain in the low frequency range. The HRTF notch position changes primarily with elevation, so for this study is not as useful a cue given that the animat is moving in a two dimensional plane. Most significant to localization will be overall differences in gain at the left and right ears.

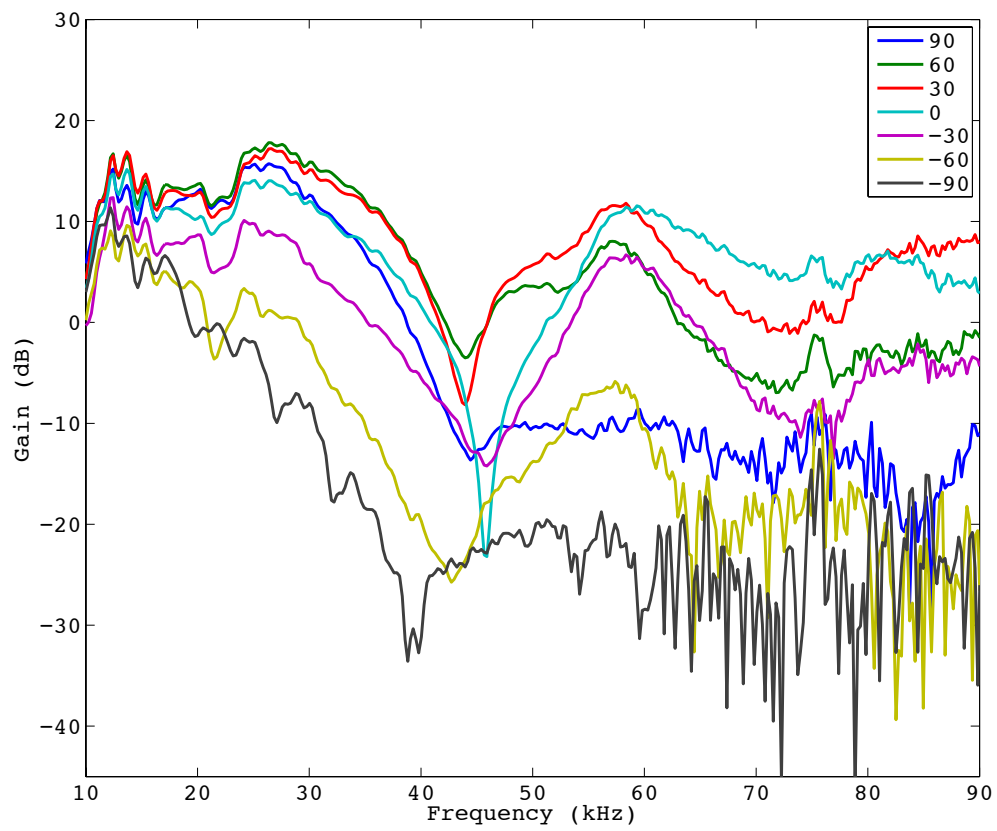


Figure 5.9. HRTFs for right ear at zero elevation at 30° increments.

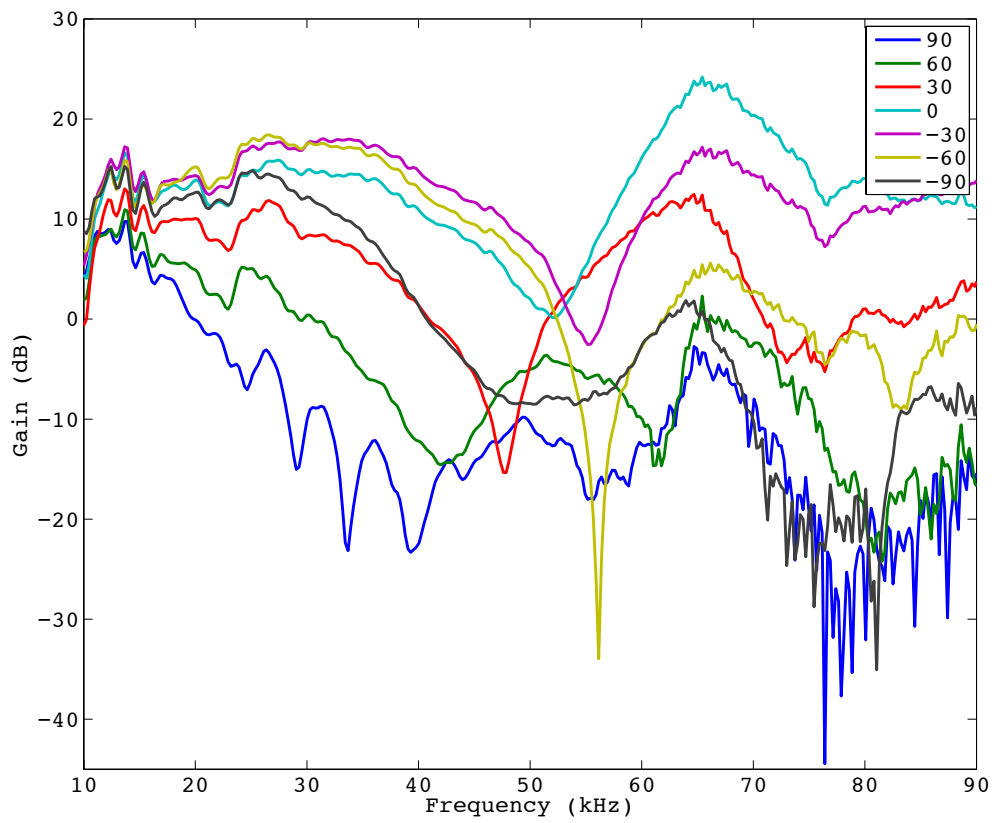


Figure 5.10. HRTFs for left ear at zero elevation at 30° increments.

5.5 Middle and Inner Ear Model

The head related transfer function is used to model echo amplitude and frequency content at the eardrum. To model the effects of the middle and inner ear and find the response of the auditory nerve, the EarLab desktop modeling environment is used in this study, developed by Dr. David Mountain at Boston University. The model encompasses the middle and inner ear. The middle ear consists of the eardrum and three ossicles, malleus, incus, and stapes. The primary function of the middle ear is to amplify the incoming auditory signal. The tiny bones serve as an impedance matcher as the sound wave is moving from one medium (air) to the fluids and membranes of the inner ear. The pressure wave is converted to a mechanical wave as vibrations travel from the malleus, to the incus, and finally the stapes. The footplate of the stapes is connected to the oval window of the cochlea, the beginning of the inner ear. The stapes presses on the oval window causing the fluid in the cochlea to move.

The cochlea is a spiral shaped bone filled with fluid, and the basilar membrane partitions the space of the spiral bone. The basilar membrane is a rigid structure that changes in stiffness from the base to the apex. As a result of this varying flexibility, higher frequencies will result in vibrations at the base of the basilar membrane, while lower frequencies stimulate the apex. In this way, the basilar membrane serves as a frequency divider. A species specific “place-frequency map” is commonly defined along the basilar membrane using the Greenwood function to find the characteristic frequency (CF) at a given location,

$$CF = A(10^{ax/L} - K)$$

where A is a constant controlling the high frequency limit of the map, a is a constant controlling the slope of the map, L is the cochlear length, and K is a constant controlling the lower frequency behavior of the map. When the basilar membrane vibrates, the hair cells located in the Organ of Corti move. The movement of these hair cells results in nerve impulses at the auditory nerve, which are analyzed further in the brain.

In this study, the Earlab Desktop Modeling Environment is used to model the function of the middle and inner ear. The model consists of several modules and species specific parameters. These included the middle ear module, linear basilar membrane module, inner hair cell module, and auditory nerve module. The middle ear module acts as a high-pass filter. The basilar membrane module receives input from the middle ear module produces an output consisting of many channels each representing a specific location along the basilar membrane. The mechanics of the basilar membrane are approximated with linear digital band-pass filters. The inner hair cell module approximates the inner hair cell transduction process. A half-wave rectified receptor current version of the mechanical stimulus is produced. An array of inputs from the basilar membrane module are received by the inner hair cell module, and the model produces an array of outputs representing the receptor potential in a population of inner hair cells. The inner hair cell module output feeds into the auditory nerve module. There is adaptation occurring at the auditory nerve, however since the signals that generate returning echoes are short and sweep in

frequency, the auditory nerve is thought to spike generally once for a particular frequency, so adaptation would not affect the response. There are “sink” modules for the basilar membrane, inner hair cell, and auditory nerve modules, which capture the output frame by frame and write output to be analyzed later.

There are many parameters of the modules that can be adjusted for specific species. Most notable is the Greenwood function used in the basilar membrane module. Figure 5.11 shows the output of the Greenwood function with *Eptesicus fuscus* specific parameters. Here $A=5500\text{Hz}$, $a=1.279$, $L=12\text{mm}$, and $K=0$.

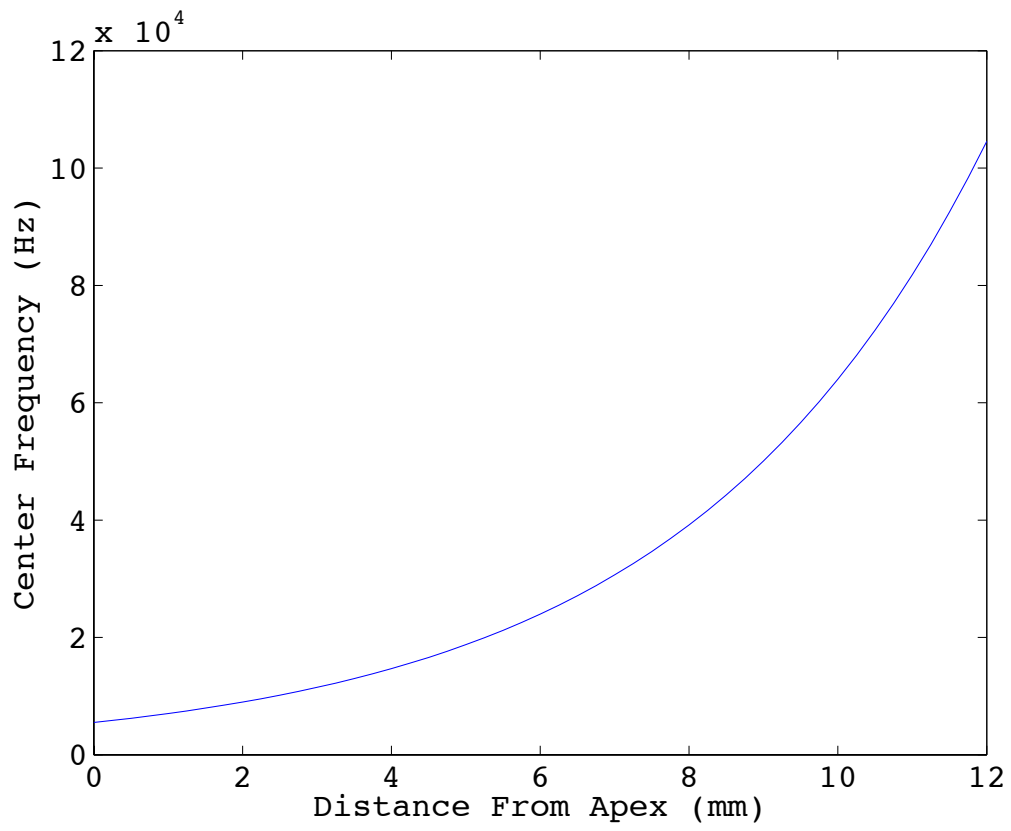


Figure 5.11. Place-Frequency Map with *Eptesicus fuscus* specific parameters.

5.6 Auditory Nerve Response

The final output of the middle and inner ear model created using EarLab, is an instantaneous firing rate at the auditory nerve. Figure 5.12 shows the instantaneous firing rate of the auditory nerve when excited by the animat signal. There are 64 output channels, each with a best frequency, such that the auditory nerve is responding to a particular frequency in the signal. In figure 5.12, a response to both the first and second harmonic is visible. The nerve responds over the 2ms of the signal, with the greatest response at the beginning of the signal. Since the typical *Eptesicus fuscus* call is short in duration, the auditory nerve will likely fire only once or twice for a given signal or echo input.

The response of the auditory nerve to the train of echoes resulting from a call being made at position 13, seen in figure 4.8, is shown at the left ear in figure 5.13 and in the right ear in figure 5.14. The echo from target 7 and the “overlap” echo from targets 14 and 12 cause the auditory nerve to respond at both the right and left ear. All three of those targets are to the right of the animat’s midline, and as is expected the response of the right auditory nerve is greater than the left auditory nerve. The left auditory nerve also shows a response to the echo from target 20 was to the left of midline, and the right auditory nerve responds to target 6 which is to the left of midline.

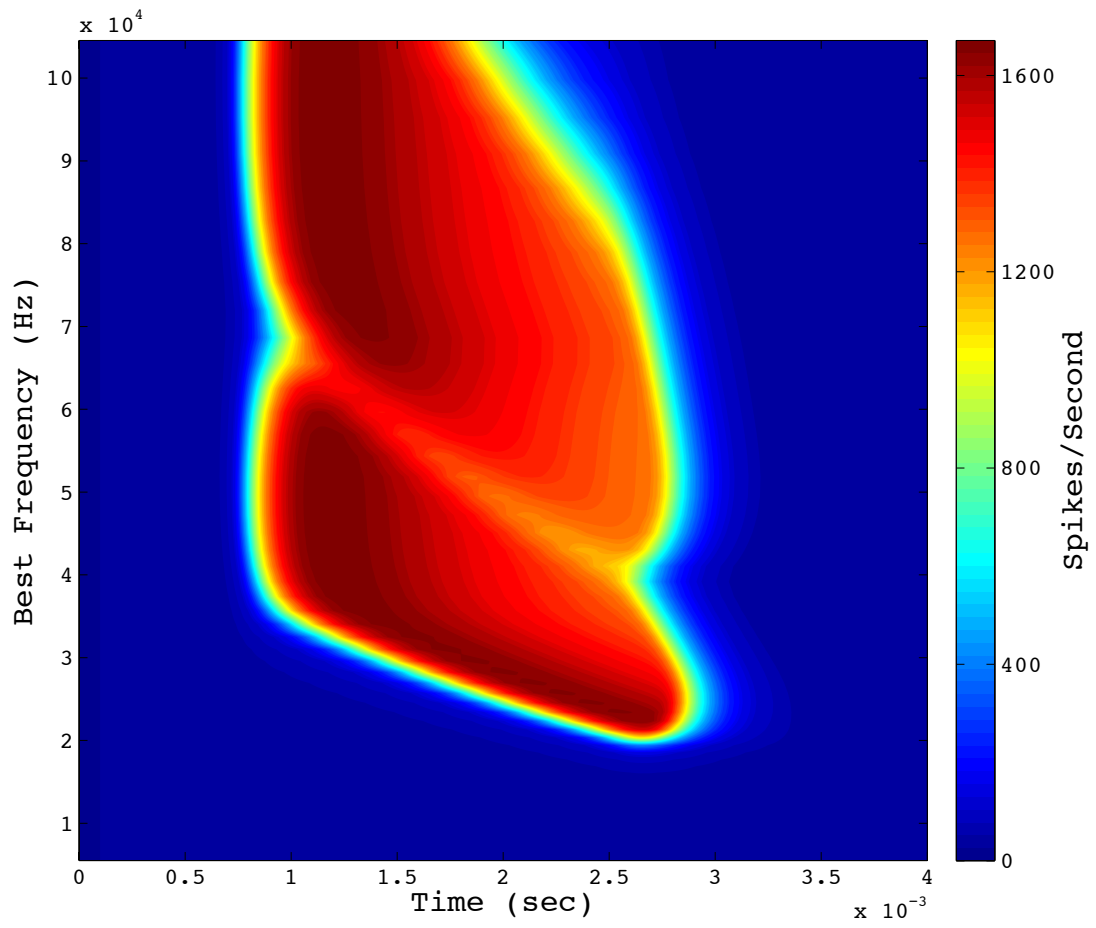


Figure 5.12. The auditory nerve response due to animat signal input.

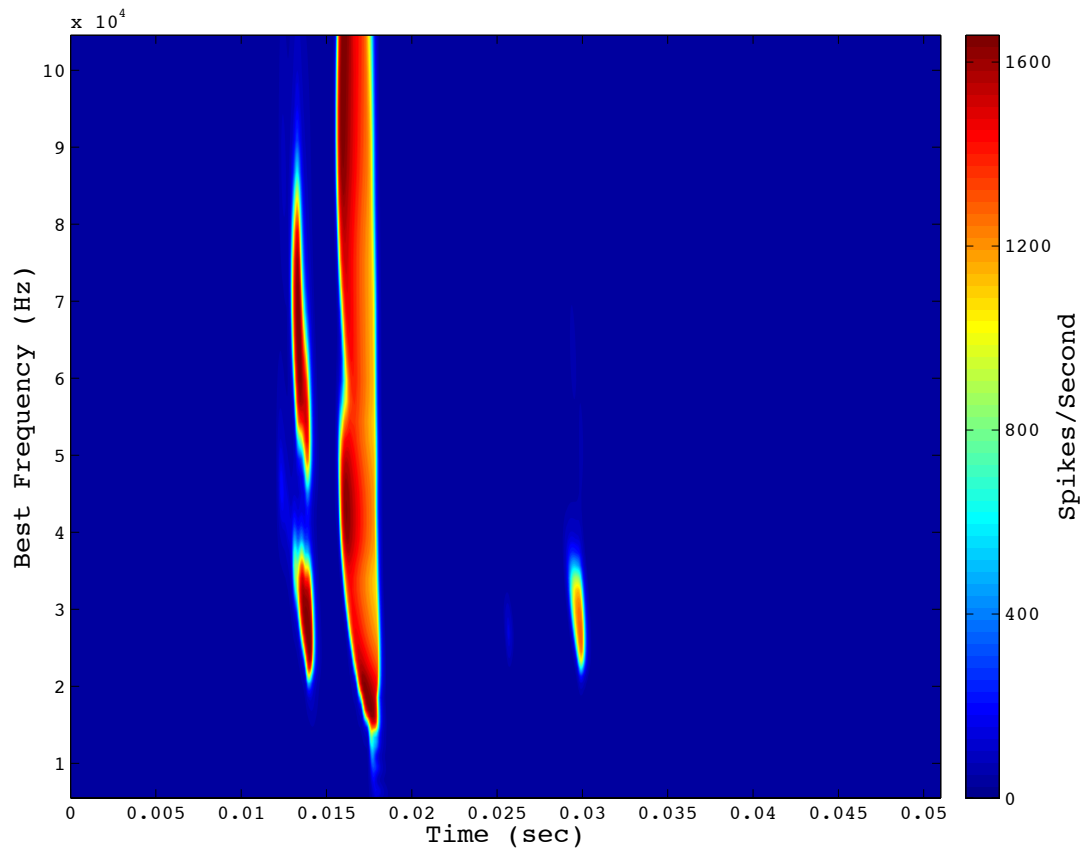


Figure 5.13. The auditory nerve response at the left ear to echoes arriving at position 13 in figure 4.8.

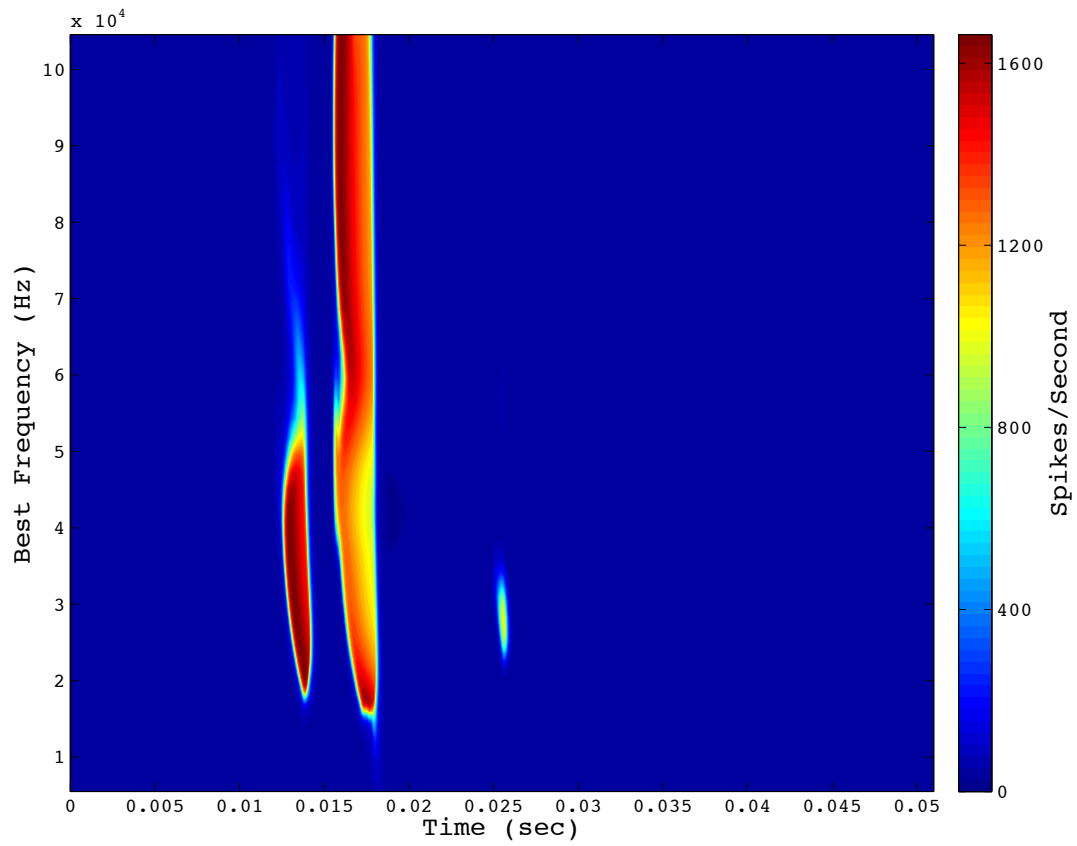


Figure 5.14. The auditory nerve response at the right ear to echoes arriving at position 13 in figure 4.8.

In figure 5.15, the response of the auditory nerve to the “overlap” echo is more closely examined. The top panel shows response at the left auditory nerve and the bottom panel shows the response at the right auditory nerve. The most prominent difference between the two AN responses is that the left AN has a strong response at 40kHz, while the right AN responds weakly at that frequency. The difference in response at the left and right AN is the dominant cue in azimuth localization required for this 2 dimensional model. In order to more closely analyze these differences, the difference of the response at the left ear to the right ear is shown in figure 5.16. Positive values indicate response greater response at the left AN, and negative values indicate greater response at the right AN. Examining the difference in response of the left and right AN to the echo from target 7 highlights that the left AN responds dominantly to the second harmonic of the echo, and the right AN responds dominantly to the first harmonic of the echo. The prominent difference in the response of the AN to the “overlap” echo is that the left AN responds more around 45kHz. The figure also reinforces that the left AN responds to the echo from target 6 and the right AN responds to the echo from target 20. The difference in the response at the left and right AN highlights the importance of these differences for azimuth localization.

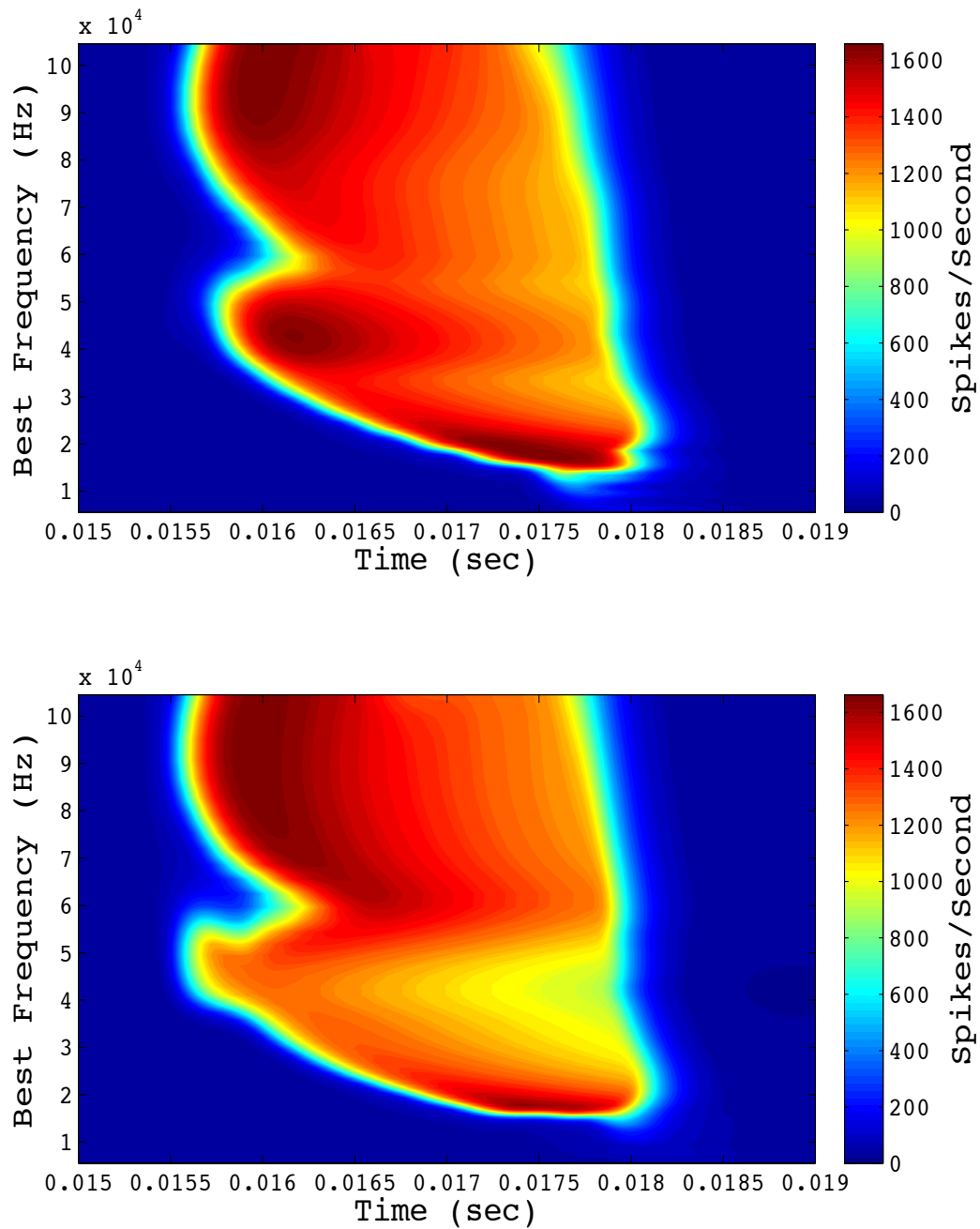


Figure 5.15. Response of auditory nerve to “overlap” echo. The top panel is the left AN response and the bottom panel is the right AN response.

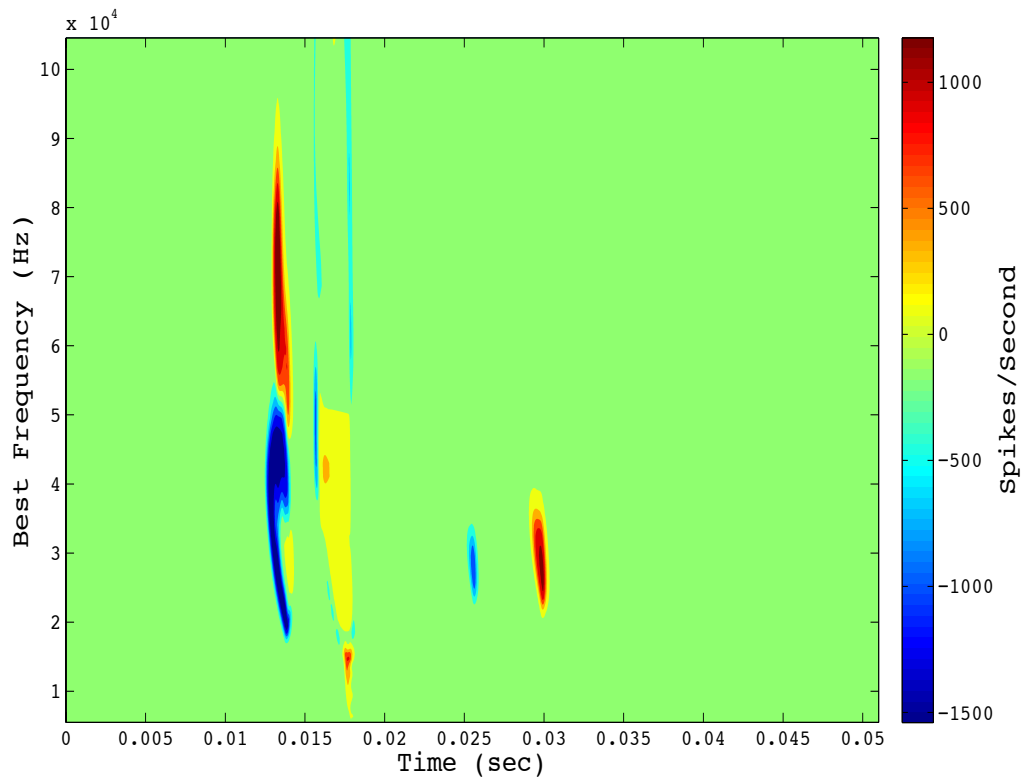


Figure 5.16. Contour of the left AN response minus the right AN response. Positive values indicate dominate left AN response to echoes, and negative values indicate dominate right AN response to echoes.

5.7 Discussion

The results of this model highlight the importance of the HRTF and frequency division at the basilar membrane. These two features come together to show that for certain azimuth, the difference between the right and left AN response can act as a cue for localization. For the echo from target 7, the left AN responds to the second harmonic of the echo and the right AN responds to the first harmonic. The difference between the AN responses for the “overlap” echo are less prominent. Only the right AN registers the echo from target 6, and only the left AN registers the echo from target 20. The peripheral model used in this study is a vital component in an overall model of echolocation, and provides important cues to be used by a biologically relevant neural model.

6 Neural Model

6.1 Introduction

For target localization in two dimensions, range and azimuth must be determined. Several neural models for echolocation have been developed, as previously discussed in the introduction (64, 20, 47, 48, 49, 14, 94, 26). The model developed and presented here builds on previous work to suggest that a combination of binaural and monaural pathways in conjunction with neural adaptation for echolocation, can accurately determine range and azimuth from pulse-echo information. In this study, a neural model is proposed that uses localization cues to create a “picture” of the target field. Input to the neural model comes from the peripheral model described in the previous chapter, and is based on acoustic modeling of echoes received in a cluttered habitat. This neural network uses modeled auditory inputs that take into account spatial information, HRTFs, and cochlear modeling. This is a new “whole” approach to modeling echolocation in the brain. By focusing on the basic neural needs for target localization from pulse emission to neuron spiking, a better picture of echolocation can come into focus.

6.2 Auditory Pathways

The response at the auditory nerve continues through a neural network as subsequent neurons are stimulated along the auditory pathways. There are many ascending and descending pathways from the auditory nerve to the cortex that have been identified. Ascending binaural and monaural pathways, that exhibit both inhibition and excitation, are considered in this study. It has been suggested that

descending pathways are used for feedback to the cochlear nucleus to improve information gathered from acoustic stimuli, or control what stimuli continue forward on ascending pathways. Although descending pathways are likely used by echolocating bats, they are not needed for the purpose of this study and are not considered here (35, 65, 67).

The ascending pathways described in literature (52, 82, 83) begin at the auditory nerve connection to the dorsal cochlear nucleus (DCN) and ventral cochlear nucleus (VCN). The pathway from the posterior VCN (PVCN) has been identified as a potential “what” pathway (42, 84,12), and is therefore not considered in this study as only localization is modeled. The pathway from the anterior VCN (AVCN) is identified as the “where” pathway. The AVCN projects to the contralateral Lateral Superior Olive (LSO) via the medial nucleus of the trapezoid body (MNTB) which provides inhibitory input. The AVCN projects excitatory input directly to the ipsilateral LSO. Studies suggest that interaural level differences (ILDs) are computed at the LSO (57, 81). The AVCN also projects to the ipsilateral and contralateral medial superior olive (MSO) where studies suggest interaural time differences (ITDs) are computed (90, 8, 93). The MSO then projects to the Inferior Colliculus (IC) via the dorsal nucleus of the lateral lemniscus (DNLL) which projects inhibitory input to the IC. The LSO projects directly to ipsilateral and contralateral IC, as well as through the DNLL to the ipsilateral IC. There are also direct projections to the IC from the DCN. A diagram summarizing these pathways is shown in figure 6.1.

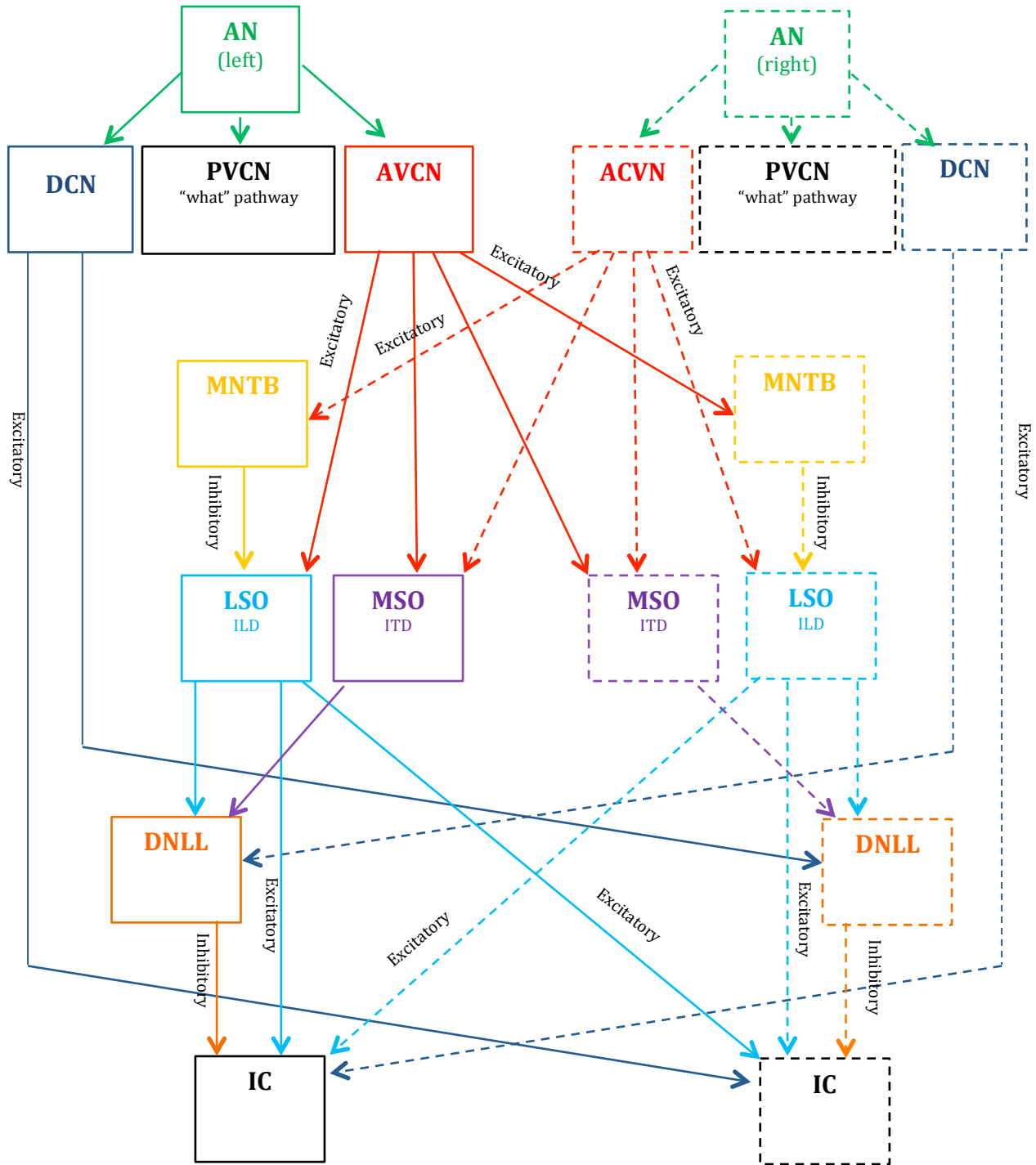


Figure 6.1 Ascending auditory pathways considered in study.

In this model, a pathway from the AN to detect target range, and another to detect azimuth are developed. Information from these two pathways is used to develop a neuronal “picture” of the target field ahead of the animal. The details of the pathways and the neuronal mechanism for range and azimuth detection are discussed in this chapter.

6.3 MSO Function

A large number of echolocating bats have evolved, each employing slightly different methods of echolocation. While much of the auditory mechanisms and pathways for echolocating bats are the same as non-echolocating animals, there are exceptions and adaptations that have been studied, most notably the possible function of the MSO. In many non-echolocating animals with large heads and low frequency hearing, the MSO is large, receives binaural input, and is presumed to function in ITD detection. For animals with smaller heads and high frequency hearing, the MSO is greatly reduced in size, as ITD cues are less viable. It has been found, however, that the MSO of echolocating bats, including the *Eptesicus fuscus*, is large despite the small heads and high frequency hearing. In some studies, echolocating bats employing constant frequency calls were found to have MSO with binaural neurons while bats with frequency modulated calls were found to have predominantly monaural MSO neurons (16).

In a study of the MSO in *Eptesicus fuscus* (33), neurons were found to have best frequencies ranging between 11-79kHz. Half the neurons were monaurally excited by the contralateral ear, while the other half received binaural input. Neurons that received binaural input varied in whether they received inhibitory input or excitatory input and from which ear. The study used a variety of stimuli including pure tone burst, trains of pure tone bursts, and sinusoidal amplitude modulated tones (SAM). The carrier frequency for the SAM tone was the cell's best frequency. Cells were found that phase locked to the envelope of the tone. This suggested that a function of the MSO in *Eptesicus fuscus* could be to filter for specific interpulse intervals.

Echoes with amplitude modulation, or beating, occur when two or more echoes overlap in time. This type of echo is important for bats whose prey, such as moths, have wing beating quickly to produce echoes that overlap in time. These overlapping wing beat echoes are referred to as "glints" (69). Since the frequency of wing beats can be related to the size of the moth or type of insect, "glint" echoes can reveal not only prey localization cues, but also information about the prey itself. This would be primarily useful to bats emitting constant frequency calls. Bats with sharply frequency modulated calls would not produce a single frequency for long enough to produce SAM-like tones.

In this study cluttered target fields are modeled. It was shown that some target arrangements could generate "overlap" echoes, similar to the "glint" echoes created

by wing beats of prey. It is possible that the MSO is also functioning to detect these “overlap” echoes created in cluttered environments as well. The SAM tone experiments found neurons that phase locked with the envelope of the tone were able to do so up to modulation frequencies of 350Hz, or a period of 2.86ms. That is longer than the signal duration used in this model, however this proposed function of the MSO could still be helpful in identifying “overlap” echoes for longer duration calls, which the *Eptesicus fuscus* do produce. Again, since these calls are frequency modulated, this identification procedure is less likely, however the tail end of *Eptesicus fuscus* calls can be more flat at times, opening up the possibility of “overlap” echo detection at the MSO.

Perhaps more important than “overlap” or “glint” echo detection at the MSO, could be identification of two echoes separated in time but created by reflections off the same target when calls are generated in “pulse pairs”. An interpulse interval of 20ms or 50Hz would fall easily below low frequency cutoffs. MSO neurons would respond to two echoes, one as a result of the first call and the next as a result of the second call in the “pulse pair”. Echoes generated from “pulse pairs” could be identified and compared for focusing of target localizations. While this specific type of neuron is not included in the neural model in this study, it could be a valuable avenue to explore.

6.4 Delay Tuned Neurons

In order to detect the range of targets, signal-echo matching must occur. Neurons that respond to specific echo delays can provide range information. Delay tuned neurons have been identified in echolocation bats. Several studies have examined the response of delay tuned neurons in the IC, medial geniculate nucleus (MGB), and the auditory cortex (AC) of the mustached and big brown bat (56, 37, 18, 19, 61).

The sharpness of delay tuned neurons is an important property for target localization coding. Sharply tuned neurons produce more precise delay coding. In one study of the mustached bats, delay tuned neurons in the IC and MGB were found to respond to delay of 1-14ms, for a maximum range detection of 4 meters. The majority of delay tuned neurons responded to delays up to 10ms suggesting that a target range of up to 1.7m may be most functionally relevant to the mustached bat. Some delay tuned neurons were found to respond to a wide variety of delays, which would make simple range detection coding impossible (80). One suggestion for these types of neurons is that they could be used for filtering features of targets within a given block of space. Combinations of information from these targets could be used to analyze the target space.

A study of neurons in the midbrain of the *Eptesicus fuscus* (19) also identified delay tuned neurons. Two groups of delay tuned neurons were identified. One group responded best to delays of 8-17ms, or 1.36-2.89 meter range. These neurons were identified as encoding range during the “approach” phase of flight. Another group of neurons responded best to delays of 17-30ms, or 1.36-5.1 meter range, making

them more suitable for encoding target range during the “search” phase of flight. It is clear that delay tuned neurons play an important role in range detection; a model of a population of delay tuned neurons is incorporated into the neural model of this study.

6.5 Delay Tuned Neuron Model

In this study, delay tuned neurons are modeled for target range detection. Previous studies have suggested use of a postinhibitory-rebound (PIR) model to simulate the behavior of a delay tuned neuron (14). Inhibition from the bat’s call creates a long latency response in the neuron. There is a brief rebound period of depolarization, after the inhibition of the cell, to a potential above resting potential, but not high enough to reach the spike threshold. An echo provides the cell with an excitatory input that on its own would not cause the cell to spike. If the excitatory input of the echo coincides with this brief rebound, the cell will fire. Postinhibitory rebound firing has been widely observed in a variety of cell types and areas of the brain including the IC.

The delay tuned neuron in this study is modeled using MacGregor’s state-variable point model for repetitive firing in neurons (PTNRN10). This model has four state variables: the transmembrane potential (E), the time-varying threshold (TH), the spike variable (S), and the potassium conductance above resting level (GK). The input is a single input function SCN , and the output of the model (P) combines the E

and S to produce a trace like one that would be recorded with an intracellular microelectrode:

$$\frac{dE}{dt} = \frac{-E + \{SCN + GK * (EK - E)\}}{TMEM}$$

$$\frac{dTH}{dt} = \frac{-(TH - THO) + c * E}{TTH}$$

$$S = \begin{cases} 0 & (E < TH) \\ 1 & (E > TH) \end{cases}$$

$$\frac{dGK}{dt} = \frac{-GK + B * S}{TGK}$$

$$P = E + S * (50 - E)$$

THO is the resting threshold of the cell and TMEM is the membrane time constant. The parameters TTH and c describe the rise of the threshold and are used to simulate accommodation in the cell. B and TGK set refractoriness, or the post-firing increase in potassium conductance of the membrane (44).

This point neuron model approximates a neuronal membrane patch and can produce tonic or phasic firing based on the parameters c and TTH. For an excitatory input, the current causes the transmembrane potential E to rise exponentially, the speed of which is determined by the parameter TMEM. When the membrane potential begins to rise, it causes the threshold, TH, to increase in proportionate to c and with time constant TTH. The potential E rises faster than the threshold, and once the potential passes the threshold, a spike is generated and the spike variable S goes from 0 to 1 indicating an action potential has been released.

The conductance to potassium, G_K , increases with proportion to B once an action potential has fired. It then decays back down to 0 with the time constant T_{GK} . It is this increase in the potassium conductance that causes the transmembrane potential to begin to return to the equilibrium potential, E_K . This model does incorporate some accommodation, such that over time, a constantly applied current will no longer cause the cell to spike. This is due to the threshold rising to a point that is higher than the resting potential of a cell with applied current SCN . Figure 6.2 shows the behavior of the point neuron and the state variables for long constant current. The current causes two spikes to be elicited before the threshold rises enough to prevent firing.

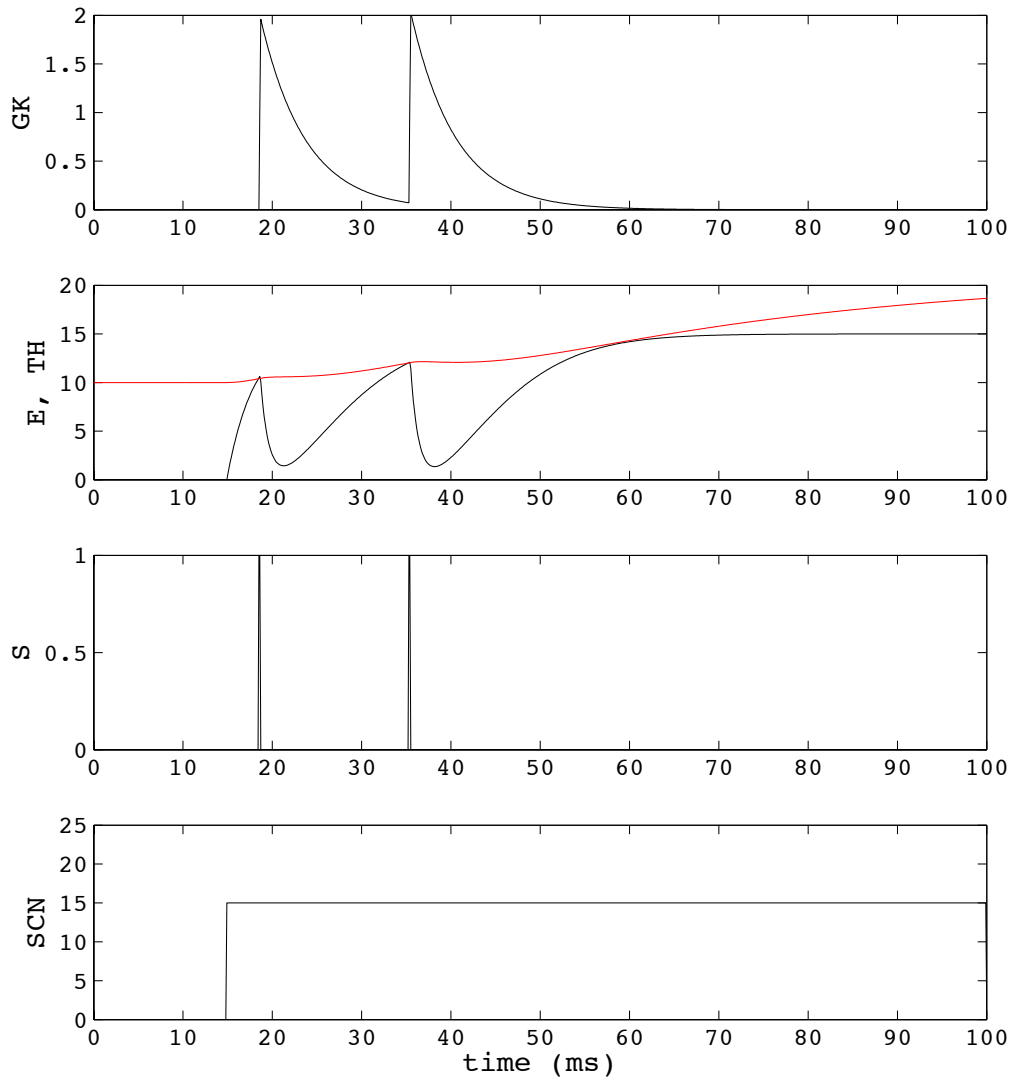


Figure 6.2 Behavior of state variables in MacGregor point neuron model.
 $c=0.75$, $TTH=40\text{ms}$, $B=50$, $TGK=5\text{ms}$, $TH_0=10\text{mV}$, $TMEM=3\text{ms}$, $EK=-10\text{mV}$.

In order to produce a delay tuned neuron using this model, the point neuron was stimulated first with an inhibitory input at the onset of the signal, and then an excitatory input at the onset of the echo. The MacGregor point neuron does not include specific channels to regulate postinhibitory rebound, however its parameters can be adjust to achieve the same results. Each delay tuned neuron has a specific inhibition current stimulation at the time of a generated signal, and exhibition current stimulation at the return time of echo. These current are both 1ms in duration, but vary in magnitude, which could be explained by a different number of cells receiving different numbers of presynaptic input. The time constant for the threshold, TTH, and proportion parameter, c are unique to individual delay tuned neurons. The combination of these four parameters produces neurons that fire only when first inhibited by a signal and then excited by an echo within a specific delay range. Figure 6.3 shows the input and response of a delay tuned neuron tuned to spike for delays of 5-6ms.

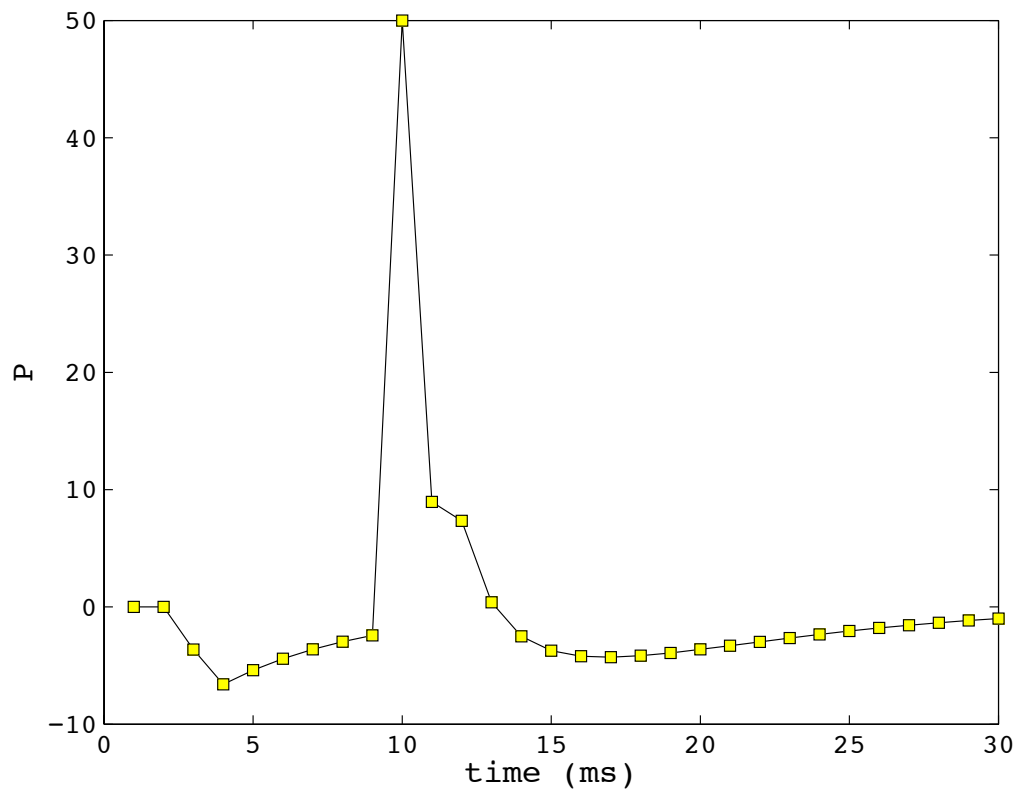
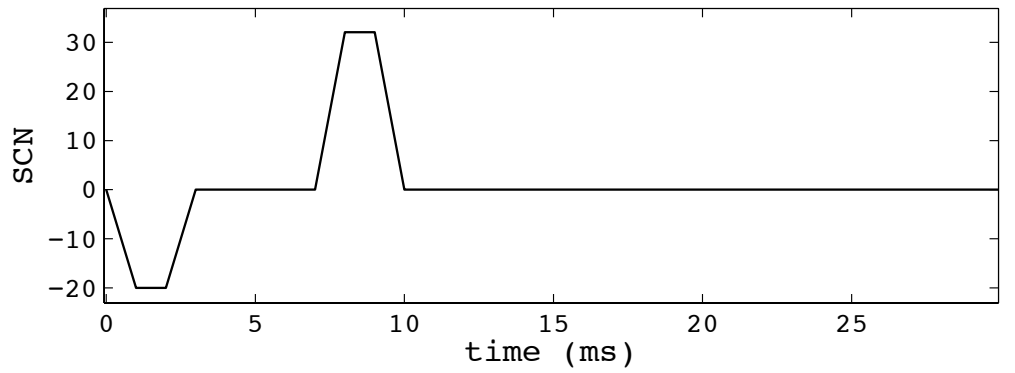


Figure 6.3 Top panel shows delay tuned neuron input (with inhibition from pulse and excitation from echo). Bottom panel is neuron potential showing a spike at the time of the echo.

6.6 Range Detection Pathway

For range detection, a three layer neural network was created. All neurons modeled are based on the MacGregor point neuron model, with parameters tuned to achieve desired spike timing. The firing rate output at the auditory nerve from the peripheral model is used as input to a layer of MacGregor neurons. The firing rate at the auditory nerve is divided into 64 spectral bands. Each input is normalized and scaled to use as a stimulating current for one neuron. One set of neurons fires for the animat signal, another for the echoes at the right ear, and a third for the echoes at the left ear. In figure 6.4, the spike times of each neuron is shown for the auditory nerve output at position 13. The AN response to the signal and echoes at the right and left ear was shown in figures 5.12-5.14. The black markers in figure 6.4 indicate the spike times from the signal, the red markers indicate spike times due to echoes at the right ear, the blue markers indicate spike times due to echoes arriving at the left ear. In general, the neuron will fire once for the signal and once for an echo. The AN response at the left ear was strong, however, and neurons with best frequencies where the two harmonics of the signal meet fire twice. The prominent phase shift of the first echo noted in figure 5.16 can also be seen in the spike times at this first layer of neurons.

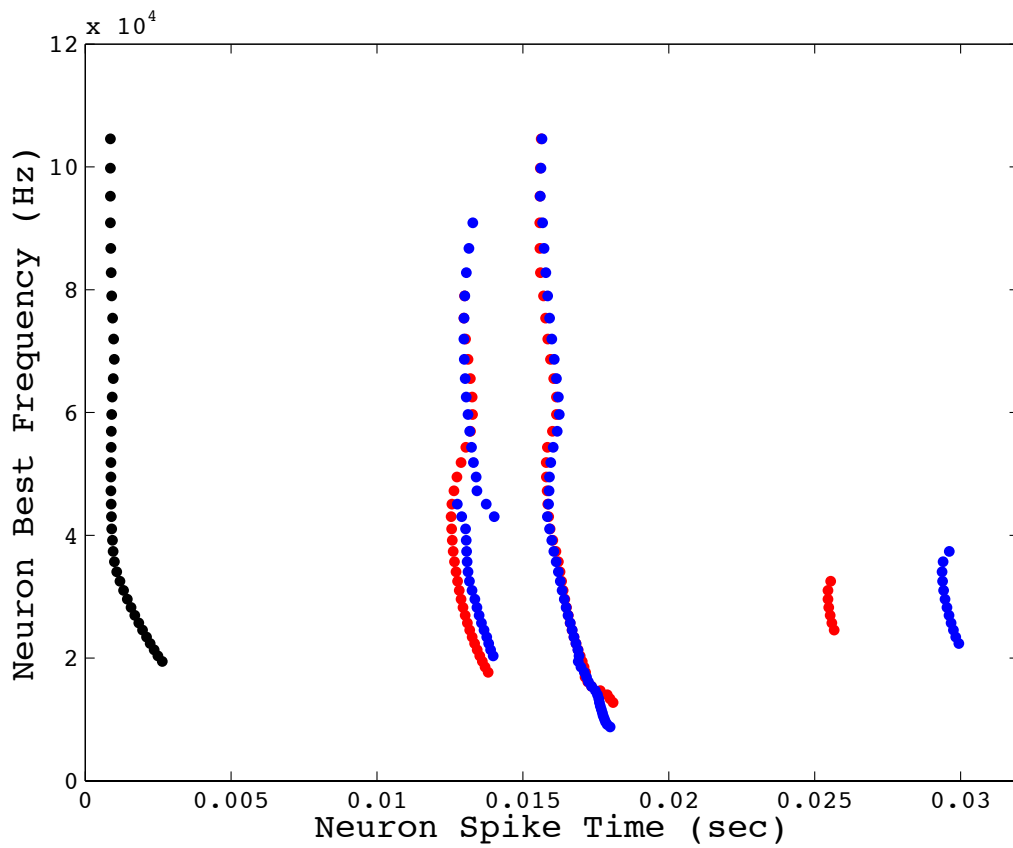


Figure 6.4. Spike times of 64 neurons each with a best frequency. Black markers indicate firing due to the signal, red markers indicate firing from echoes arriving at the right ear, and blue markers indicate firing from echoes arriving at the left ear.

Each neuron in the first layer of MacGregor neurons feeds into 20 different delay tuned neurons, each with a specific delay tune range. Adjusting the threshold time constant and proportionality constant, T_{THO} and c , sets the delay tune range. The inhibition and excitation current can also be adjusted. This accounts for the number of synaptic connections. In figure 6.5 the range of each delay tuned neuron is shown. The millisecond range a delay tuned neuron will fire over varies and the ranges of neurons overlap. This overlap allows for finer range detection. This second layer of neurons detects a spread of target range for a given echo. Comparing spiking neurons across the second layer of the range detection pathways allows a third layer of neurons to more precisely detect target range.

6.7 Discussion

In this chapter, previous neural models for target localization have been discussed as well as the predominant ascending auditory pathways to be considered when developing a neural model. Much more work must be done to fully develop a neural model for range detection. The framework for range detection has been suggested and is in development stages. In this study, it is shown that MacGregor style neurons can be adapted to display postinhibitory rebound behavior. This postinhibitory rebound behavior can be used to model delay tuned neurons that will fire for a range of delays. Layers of these neurons can be used to finely tune for range. More work must be done to develop a model of azimuth detection to be combined with the range detection model suggested here.

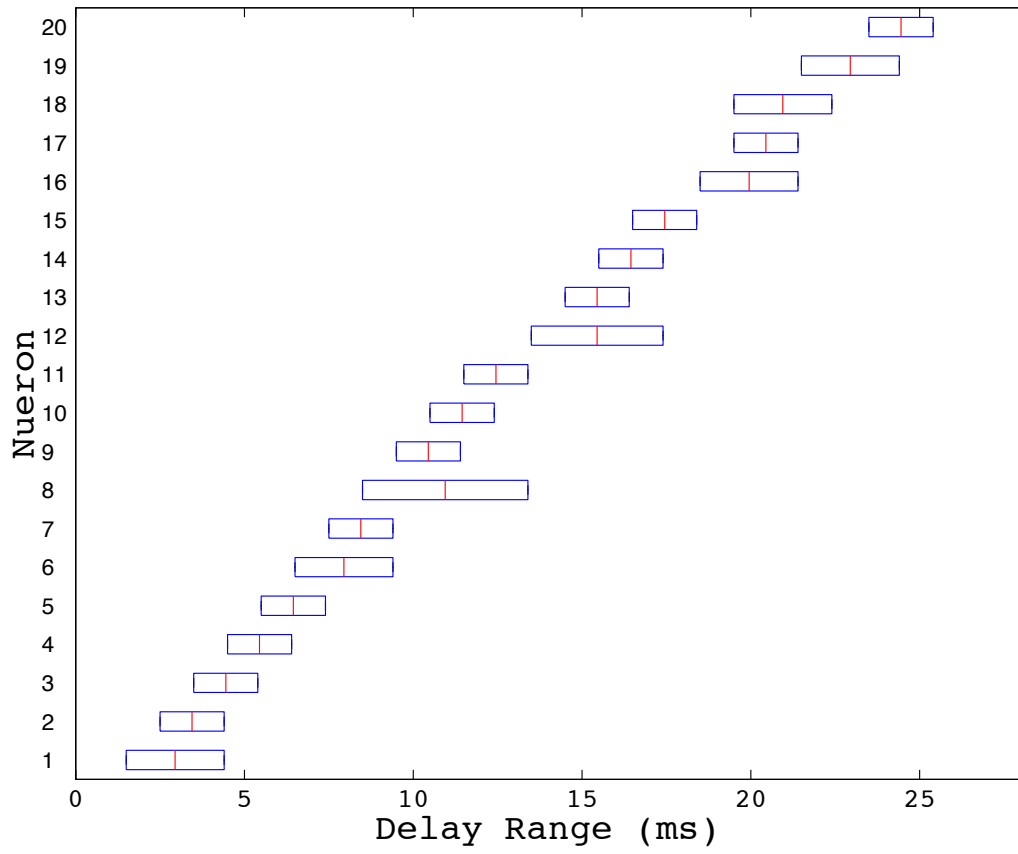


Figure 6.5. Range of each delay tuned neuron.

7 Conclusion

In this thesis, a biologically relevant model of echolocation is described, as well as field recordings of echolocating bats. A field research study was conducted to better understand the echolocation strategies of bats echolocating in cluttered environments. Field recordings of FM bats in the wild revealed differences between laboratory and field behavior, and also identified a correlation between sonar sound groups and levels of clutter. Pulses emitted by bats in “cluttered” environments were more often emitted in sonar sound groups. Field recording analysis also provided more accurate input guidelines for an echolocation models. This field study was unique in that it presented sustained recordings of a bat flying in a cluttered environment over multiple days and years. It showed that despite the perceived challenges a bat may face navigating in such an environment, these locations are utilized not only during navigation, but also feeding. With a more open feeding area only feet away, the bat recorded at the Mashpee Glade continually feed in this cluttered area. Sonar sound groups presented more frequently in the Mashpee Glade

A new, whole systems, biologically relevant approach to echolocation modeling was developed to be used as a tool to probe the importance of timing in echolocation in cluttered environments. The scenario model can stand alone to provide insight into what an echolocating bat “hears” and be used to probe echo timing difficulties that

arise in cluttered environments. The model also showed that overlap echoes can result from a variety of targets at great spatial separations and cause spectral notches that must be separated from the spectral notches created by flying insect prey. The scenario and peripheral model combine to provide a powerful tool for generating acoustically accurate neural model inputs based on habitat and behavioral observations, as well as established models of HRTFs and the middle and inner ear. It was shown that a network of modified MacGregor style neurons can be used to accurately determine target range. Further work must be done to incorporate an additional neural network level for azimuth localization. Combined, range and azimuth information can create an acoustic “picture” of the virtual flight field.

8 Acknowledgments

This dissertation is dedicated to Dr. David Mountain and Dr. Donald Griffin.

I met Dr. Griffin as a high school student, and he introduced me to the fascinating world of bats and echolocation. Many evenings were spent at Trout Pond listening for the buzz of a bat catching its prey. Dr. Griffin taught me to have patience when searching for scientific answers (and when bundling up cords at the end of the night). He also inspired me to strive to fully embrace the inquisitive and unafraid mind necessary to be a great scientist, as he was. I will forever be grateful to him and think fondly to those three summers of nights spent listening in the dark.

Dr. Mountain rescued me from an unfinished PhD, and allowed me to follow my passion without ever asking for or getting much in return. He took me in as a graduate student from another university when I had no place else to go, knowing very little about me. Dr. Mountain's style of teaching forced me to fully take responsibility for my own scientific decisions and insights. He showed me how to take new approaches when solving scientific problems and how to build solutions. He guided me through completing this document despite grave illness, and showed me how to live the fullest of lives: ever embracing science, family, friends, community, and conservation. I will thank him till eternity for his support and guidance, and always think of him when I look upon a historic home.

Many other thanks must be given, in particular to my thesis committee, Dr. Willie Padilla, Dr. Cy Opeil, and Dr. Kris Kempa.

I would also like to thank the Boston College Physics Department for their unwavering support, in particular Dr. Rein Uritam who guided my many years of studies and who I enjoyed working for as a teaching assistant, Dr. Mike Naughton for supporting me in this work, and the ever helpful administrative department.

Thank you to Dr. Cynthia Moss for sharing her HRTF data with me.

Thank you to Aleks Zosuls for his guidance, support, and participation in the field research portion of this work.

Thank you to Dr. Britt Raubenheimer who stepped in and stopped me from leaving my PhD studies, showed me how to have great resilience in all circumstances, and who first forced me to answer questions completely on my own.

Finally, thank you to my family: Mom, Dad, Julie, Mary Elizabeth, and Alistair, for their love and support. In particular, I would like to thank my father for his scientific contributions to this work, for gathering sound recordings with me in the dark, and for being an awesome dad.

9 Works Cited

1. **Agosta, S. J.** (2002) Habitat use, diet, and roost selection by the big brown bat (*Eptesicus fuscus*) in North America: a case for conserving an abundant species. *Mammal. Rev.* 32(2), 179-198.
2. **Aytekin, M., Grassi, E., Sahota, M., Moss, C. F.** (2004) The bat head related transfer function reveals binaural cues for sound localization in azimuth and elevation. *J. Acoust. Soc. Am.* 116(6), 3594-3605.
3. **Barchi, J. R., Knowles, J. M., Simmons, J. A.** (2013) Spatial memory and stereotyping of flight paths by big brown bats in cluttered surroundings. *J. Exp. Biol.* 216, 1053-1063.
4. **Barshan, B., Kuc, R.** (1992) A bat-like sonar system for obstacle localization. *IEEE Trans Syst Man Cybern.* 22(4), 636-646.
5. **Bates, M. E., Simmons, J. A., Zorikov, T. V.** (2001) Bats use echo harmonic structure to distinguish their targets from background clutter. *Science.* 333(6042), 627-630.
6. **Bell, G. P., Fenton, M. B.** (1984) The use of Doppler-shifted echoes as a flutter detection and clutter rejection system: the echolocation and feeding behavior of *Hipposideros ruber* (Chiroptera: Hipposideridae). *Behav. Ecol. Sociobiol.* 15, 109-114.
7. **Blauert, J.** (1997) Spatial hearing: the psychophysics of human sound localization. MIT Press.
8. **Brand, A., Behrend, O., Marquardt, T., McAlpine, D., Grothe, B.** (2002) Precise inhibition is essential for microsecond interaural time difference coding. *Nature.* 417, 543-547.
9. **Brigham, R. M., Cebek, J. E., Hickey, M. B.** (1989) Intraspecific variation in the echolocation calls of two species of insectivorous bats. *J. Mammal.* 7(2), 426-428.
10. **Broders, H., G., Findlay, C. S., Zheng, L.** (2004) Effects of clutter on echolocation call structure of *Myotis septentrionalis* and *M. lucifugus*. *J. Mammal.* 85(2), 273-281.
11. **Brunet-Rossinni, A. K., Austad, S. N.** (2004) Aging studies on bats: review. *Biogerontol.* 5, 211-222.

12. **Canlon, B. Illing, R. B. Walton, J.** (2009) Cell biology and physiology of the aging central auditory pathway. *Springer handbook of Auditory Research*. 34, 39-74.
13. **Carr, C. E., Konishi, M.** (1990) A circuit for detection of interaural time differences in the brain stem of the barn owl. *J. Neuroscience*. 10(10), 3227-3245.
14. **Cheely, M., Horiuchi, T.** (2003) Analog VLSI models of range tuned neurons in the bat echolocation system. *J. App Signal Process*. 7, 649-658.
15. **Christian, J. J.** (1956) The natural history of a summer aggregation of the big brown bat, *Eptesicus fuscus*. *American Midland Naturalist*. 55(1), 66-95.
16. **Covey, E., Casseday, J. H.** (1999) Timing in the auditory system of the bat. *An Rev. Physiol*. 61, 457-476.
17. **Covey.** (2005) Neurobiological specializations in echolocating bats. *The Anatomical Record Part A*. 287, 1103-1106.
18. **Dear, S. P., Simmonds, J. A., Fritz, J.** (1993) A possible neuronal basis for representation of acoustic scenes in auditory cortex of the big brown bat. *Nature*. 364, 620-623.
19. **Dear, S. P., Suga, N.** (1995) Delay-tuned neurons in the midbrain of the big brown bat. *J. Neurophysiol*. 73, 1084-1100.
20. **Dror, I. E., Zagaeski, M. Moss, C. F.** (1994) Three-dimensional target recognition via sonar: a neural network model. *Neural Net*. 8(1), 149-160.
21. **Dzal, Y., McGuire, L. P., Veselka, N., Fenton, B. M.** (2010) Going, going, gone: the impact of white-nose syndrome on the summer activity of the little brown bat (*Myotis lugifugus*). *Biol. Lett.* 7(3), 392-394.
22. **Farney, J., Fleharty, E. D.** (1969) Aspect ration, loading, wing span, and membrane areas of bats. *J. Mammal*. 50(2), 362-367.
23. **Fedderson, W. E., Sandel, T. T., Teas, D. C., Jeffress, L. A.,** (1957) Localization of high-frequency tones. *J. Acoustic. Soc. Am.* 29, 988-991.
24. **Fenton, M. B., Bell, G. P.** (1981) Recognition of species of insectivorous bats by their echolocation calls. *J. Mammal*. 62(2), 233-243.
25. **Firzloff, U. Schuller, G.** (2003) Spectral directionality of the external ear of the lesser spear-nosed bat, *Phyllostomus discolor*. *Hear. Res.* 181, 27-39.

26. **Fontaine, B., Peremans, H.** (2009) Bat echolocation processing using first spike latency coding. *Neural Net.* 22, 1372-1382.
27. **Ghose, K., Moss, C. F.** (2003) The sonar beam pattern of a flying bat as it tracks tethered insects. *J. Acoust. Soc. Am.* 114(2), 1120-1131.
28. **Ghose, K., Moss, C. F., Horiuchi, T. K.** (2007) Flying big brown bats emit a beam with two lobes in the vertical plane. *J. Acoust. Soc. Am.* 122(6), 3717-3724.
29. **Griffin, D. R.** (1940) Notes on the life histories of New England cave bats. *J. Mammal.* 21(2), 181-187.
30. **Griffin, D. R., Galambos, R.** (1941) The sensory basis of obstacle avoidance by flying bats. *J. Exp. Zoo.* 86(3), 481-506.
31. **Griffin, D. R.** (1958) *Listening In The Dark.* New Haven: Yale University Press.
32. **Griffin, D. R., Webster, F. A., Michael, C. K.,** (1960) The echolocation of flying insects by bats. *Animal Behavior.* 8, 141-154.
33. **Grothe, B., Covey, E., Casseday, J. H.** (2001) Medial superior olive of the big brown bat: neural responses to pure tones, amplitude, modulations, and pulse trains. *J. Neurophysiol.* 86(5), 2219-2230.
34. **Hiryu, S., Bates, M. E., Simmons, J. A., Riquimaroux, H.** (2010) FM echolocating bats shift frequencies to avoid broadcast-echo ambiguity in clutter. *PNAS.* 107(15), 7048-7053.
35. **Huffman, R. F., Henson, O. W.** (1990) The descending auditory pathway and acousticomotor systems: connections with the inferior colliculus. *Brain Res.* 15(3), 295-323.
36. **Jakobsen, L., Brinklov, S., Surlykke, A.** (2013) Intensity and directionality of bat echolocation signals. *Front. Physiol.* 4(89), 1-9.
37. **Kawasaki, M., Margoliash, D., Suga, N.** (1988) Delay-tuned combination sensitive neurons in the auditory cortex of the vocalizing mustached bat. *J. Neurophysiol.* 59, 623-635.
38. **Kazail, K. A., Burnet, S. C., Masters, W. M.** (2001) Individual and group variation in echolocation calls of big brown bats, *Eptesicus fuscus* (Chiroptera: Vespertilionidae). *J. Mammal.* 82(2), 339-351.

39. **Kazil, K. A., Masters, W. M.** (2003) Female big brown bats, *Eptesicus fuscus*, recognize sex from a caller's echolocation signals. *Anim. Behav.* 67, 855-863.
40. **Koay, G., Heffner, H. E., Heffner, R. S.** (1997) Audiogram of the big brown bat (*Eptesicus fuscus*). *Hear. Res.* 105, 202-210.
41. **Kothari, N. B., Wohlegemuth, M. J., Holgard, K., Surlykke, A., Moss, C. F.** (2014) Timing matters: sonar call groups facilitate target localization in bats. *Front. Physiol.* 5(168), 1-13.
42. **Kraus, N., Nicol, T.** (2005) Brainstem origins for cortical 'what' and 'where' pathways in the auditory system. *Trends Neuroscience.* 28(4), 176-181.
43. **Kurta, A., Baker, R. H.** (1990) Mammalian Species: *Eptesicus fuscus*. *The American Society of Mammalogists.* 356, 1-10.
44. **MacGregor, R. J.** (1987) Neural and Brain Modeling. San Diego: Academic Press Inc.
45. **Masters, W. M., Jacobs, S. C., Simmons, J. A.** (1991) The structure of echolocation sound used by the big brown bat *Eptesicus fuscus*: Some consequences for echo processing. *J. Acoust. Soc. Am.* 89, 1402-1413.
46. **Masters, W. M., Raver, K. A. S., Kazial, K. A.** (1995) Sonar signals of big brown bats: *Eptesicus fuscus*, contain information about individual identity, age, and family affiliation. *Anim. Behav.* 50, 1243-1260.
47. **Matsuo, I., Tani, J., Yano, M.** (2001) A model of echolocation of multiple targets in 3D space form a single emission. *J. Acoust. Soc. Am.* 110, 607-624.
48. **Matsuo, I., Kunugiyama, K., Yano, M.** (2003) An echolocation model for range discrimination of multiple closely spaced objects: Transformation of spectrogram into the reflected intensity distribution. *J. Acoust. Soc. Am.* 115, 920-928.
49. **Matsuo, I., Yano, M.** (2004) An echolocation model for the restoration of an acoustic image from a single-emission echo. *J. Acoust. Soc. Am.* 116, 3782-3788.
50. **McFadden, D., Pasanen, E. G.** (1976) Lateralization at high frequencies based on interaural time differences. *J. Acoust. Soc. Am.* 59, 634-639.
51. **Metzer, W.** (1989) A possible neuronal basis for Doppler-shift compensation in echo-locating horseshoe bats. *Nature.* 341, 529-532.

52. **Moller, A. R.** (2000) Hearing: its physiology and pathophysiology. Elsevier Science.
53. **Moss, C. F., Bohn, K. Gilkenson, H., Surlykke, A.** (2006) Active listening for spatial orientation in a complex auditory scene. *PloS. Biol.* 4(e79), 615-626.
54. **Moushegian, G., Jeffress, L. A.** (1959) Role of interaural time and intensity differences in the lateralization of low-frequency tones. *J. Acoust. Soc. Am.* 31, 207-219.
55. **Orbist, M. K.** (1995) Flexible bat echolocation: the influence of individual, habitat, and conspecifics on sonar signal design. *Behav. Ecol. Sociobiol.* 36, 207-219.
56. **O'Neil, W. E., Suga, N.** (1979) Target range-sensitive neurons in the auditory cortex of the mustached bat. *Science.* 203(4375), 69-73.
57. **Park, T. J., Monsivais, P., Pollak, G. D.** (1997) Processing of interaural intensity differences in the LSO: role of interaural threshold differences. *J. Neurophysiol.* 77, 2863-2878.
58. **Parson, E. C. M., Dolman, S. J., Wright, A. J., Rose, N. A., Burns, W. C. G.** (2008) Navy sonar and cetaceans: just how much does the gun need to smoke before we act? *Marine Pollution Bull.* 56, 1248-1257.
59. **Petrites, A. E., Eng, O. S., Mowlds, D. S., Simmons, J. A., DeLong, C. M.** (2009) Interpulse interval modulation by echolocating big brown bats (*Eptesicus fuscus*) in different densities of obstacle clutter. *J. Comp. Physiol. A.* 195(6), 603-617.
60. **Popper, A. N., Fay, R. R.** (1995) Hearing by bats. New York: Springer-Verlag.
61. **Portfors, C. V., Wenstrop, J. J.** (1999) Delay-tuned neurons in the inferior colliculus of the mustached bat: implications for analysis of target distance. *J. Neurophysiol.* 82, 1326-1338.
62. **Roitblat, H. L., Au, W. W. L., Nachtigall, P. E., Shizumura, R., Moons, G.** (1995) Sonar recognition of targets embedded in sediment. *Neural Net.* 8, 1263-1273.
63. **Roth, G. L., Ravindra, K. K., Hind, J. E.** (1980) Interaural time differences: implications regarding the neurophysiology of sound localization. *J. Acoust. Soc. Am.* 68, 1643-1651.
64. **Saillant, P. A., Simmons, J. A., Dear, S. P., McMullen, J. A.** (1993) A computational model of echo processing and acoustic imaging in frequency-

- modulated echolocation bats: The spectrogram correlation and transformation receiver. *J. Acoust. Soc. Am.* 94, 2691-2712.
65. **Saldana, E., Feliciano, M., Mugnaini, E.** (1991) Distribution of descending projection from primary auditory neocortex to inferior colliculus mimics the topography of introcollicular projections. *J. Comp. Neurol.* 371(1), 15-40.
 66. **Salomons.** (2001) Computational Atmospheric Acoustics. Kluwer Academic Publishers.
 67. **Scholfield, B. R., Cant, N. B.** (1999) Descending auditory pathways: projections from the inferior colliculus contact superior olivary cells that project bilaterally to the cochlear nuclei. *J. Comp. Neurol.* 409, 210-223.
 68. **Simmons, J. A., Fenton, M. B., O'Farrell, M. J.** (1979) Echolocation and pursuit of prey by bats. *Science.* 203(4375), 16-21.
 69. **Simmons, J. A.** (1980) The processing of sonar echoes by bats. *Animal Sonar Systems.* 28, 695-714.
 70. **Simmons, J. A.** (1989) A view of the world through the bat's ear: the formation of acoustic images in echolocation. *Cognition.* 33, 155-199.
 71. **Simmons, J. A., Moss, C. F., Ferragamo, M.** (1990) Convergence of temporal and spectral information into acoustic images of complex sonar targets perceived by the echolocating bat, *Eptesicus fuscus*. *J. Comp. Physiol. A.* 166, 449-470.
 72. **Simmons, J. A., Saillant, P. A. Wotton, J. M., Haresign, T., Ferragamo, J. M., Moss, C. F.** (1995) Composition of biosonar images for target recognition by echolocating bats. *Neural Net.* 8, 1239-1261.
 73. **Simmons, N. B.** (2005) Order Chiroptera. Mammal species of the world: a taxonomic and geographic reference, third edition, volume 1. Johns Hopkins University Press.
 74. **Suga, N., Simmons, J. A., Jen, P. H.** (1975) Peripheral specialization for fine analysis of Doppler shifted echoes in the auditory system of the "CF-FM" bat *Pteronotus parnelli*. *J. Exp. Biol.* 63, 161-192.
 75. **Suga, N. O'Neill, W. E., Manabe, T.** (1978) Cortical-neurons sensitive to combinations of information-bearing elements of biosonar signals in mustached bat. *Science.* 200, 778-781.

76. **Surlykke, A., Moss, C. F.** (2000) Echolocation behavior of big brown bats, *Eptesicus fuscus*, in the field and the laboratory. *J. Acoust. Soc. Am.* 108(5), 2419-2429.
77. **Surlykke, A., Ghose, K., Moss, C. F.** (2008) Acoustic scanning of natural scenes by echolocation in the big brown bat, *Eptesicus fuscus*. *J. Exp. Biol.* 212, 1011-1020.
78. **Surlykke, A., Pedersen, S. B., Jakobsen, L.** (2009) Echolocating bats emit a highly directional sonar sound beam in the field. *Proc. R. Soc. B.* 276, 853-860.
79. **Thaler, L., Arnott, S. R., Goodale, M. A.** (2011) Neural correlates of natural human echolocation in early and late blind echolocation experts. *PloS. ONE.* 6(5):e20162.
80. **Thomas, J. A., Moss, C. F., Vater, M.** (2002) Echolocation in bats and dolphins. University of Chicago Press.
81. **Tolin, D. J., Yin, T. C. T.** (2005) Interaural phase and level difference sensitivity in low-frequency neurons in the lateral superior olive. *J. Neurosci.* 25(46), 10648-10657.
82. **Vater, M., Kossel, M., Horn, A. K.** (1992) GAD- and GABA- immunoreactivity in the ascending auditory pathway of the horseshoe and mustached bat. *J. Comp. Neurol.* 325(2), 183-206.
83. **Vater, M., Braun, K.** (1994) Parvabumin, calbindin, D-28k, and calretinin immunoreactivity in the ascending auditory pathway of the horseshoe bat. *J. Comp. Neurol.* 341(4), 534-558.
84. **Wang, W. J., Wu, X. H., Li, L.** (2008) The dual-pathway model of auditory signal processing. *Neuroscience Bull.* 24(2), 173-182.
85. **Whitaker, J. O., Gummer, S. L.** (1992) Hibernation of the big brown bat, *Eptesicus fuscus*, in buildings. *J. Mammal.* 73(2), 312-316.
86. **Wightman, F. L., Kistler, D. J.** (1992) The dominant role of low frequency interaural time differences in sound localization. *J. Acoust. Soc. Am.* 91, 1648-1661.
87. **Williams, C. T., Leonard, Ireland, L. C., Williams, J. M.** (1973) High altitude flights of the free-tailed bat, *Tadarida brasiliensis*, observed with radar. *J. Mammal.* 54(4), 807-821.
88. **Woodworth, R. S.** (1938) *Experimental Psychology.* Holt, New York.

89. **Workman, A. A.** (2008) Big brown bat (*Eptesicus fuscus*). Department of Wildlife and Fisheries. Mississippi State University.
90. **Yin, T. C. T., Chan, J. C. K.** (1990) Interaural time sensitivity in medial superior olive of cat. *J. Neurophysiol.* 64(2), 465-488.
91. **Yost, W. A., Dye, R. H.** (1988) Discrimination of interaural differences of level as a function of frequency. *J. Acoust. Soc. Am.* 83, 1846-1851.
92. **Yovel, Y., Franz, M. O., Stilz, P., Schnitzler, H. U.** (2008) Plant classification from bat-like echolocation signals. *PLoS Comp. Biol.* 4(3), 1-13.
93. **Zhou, Y., Carney, L. H., Colburn, H.S.** (2005) A model for interaural time difference sensitivity in the medial superior olive: interaction of excitatory and inhibitory synaptic inputs, channel dynamics, and cellular morphology. *J. Neurosci.* 25(12), 3046-3058.
94. **Ziegrebe, L.** (2008) An autocorrelation model of bat sonar. *Biol. Cybern.* 98, 587-595.